Impact of Filling Processes on Protein Solutions

Inauguraldissertation

zur
Erlangung der Würde eines Doktors der Philosophie
vorgelegt der
Philosophisch-Naturwissenschaftlichen Fakultät
der Universität Basel

von

Ursula Johanna Bausch
aus Ilshofen, Deutschland

Basel, 2008

Genehmigt von der Philosophisch-Naturwissenschaftlichen Fakultät
auf Antrag von

Prof. Dr. H. Leuenberger

Dr. G. Betz

PD Dr. P. van Hoogevest

Basel, den 11. Dezember 2007

<div align="right">

Prof. Dr. H.-P. Hauri
Dekan

</div>

to my parents

Acknowledgements

Table of Contents

Abbreviations:

A	generated friction surface
CHO	Chinese hamster ovary
d	clearance between piston and cylinder in a rotary piston pump
δ	characteristic pump parameter
DV	dosage volume
FS	cumulative friction surface
i.v.	intravenous
LOD	Limit of Detection
LOQ	Limit of Quantification
M	molar
mg	milligram
ml	millilitre
MPa	Mega Pascal
PCS	photon correlation spectroscopy
PEG	polyethylene glycol
PI	polydispersity index
R^2	coefficient of determination
rhGH	recombinant human growth hormone
RPP	rotary piston pump
s	second
SD_{rel}	relative standard deviation, precision
SEC-HPLC	size exclusion high performance liquid chromatography
WMP	Watson Marlow Peristaltic Pump
z ave	z average = mean hydrodynamic diameter

A SUMMARY

During production proteins are exposed to various stresses which can cause protein denaturation and inactivation. The objective of the present study was to investigate the effect of shear forces which can occur during filling operations of pharmaceutical solutions with dosing equipment. Such shear forces possibly have a negative influence on shear sensitive substances and may lower the quality and yield of the final drug product.

In the scope of this work a peristaltic pump and different sizes of rotary piston pumps (RPPs) were compared in respect to induced protein aggregation due to shear damage caused by dosing equipment. The influence of various parameters such as filling speed, dosing volume, friction surface and exposure to air-liquid interfaces and on the intensity of the shear stress was examined. A characteristic rotary piston pump parameter δ was developed and introduced as an indicator describing the potential of a rotary piston pump to cause protein damage. Furthermore, excipients were tested on their ability to protect the model protein against shear-induced damage. 2 model proteins in solution, lactase (β-galactosidase) and rituximab, a recombinant chimeric monoclonal antibody, were used and tested for their suitability as model proteins. No activity loss was seen for the sheared lactase solution, therefore finally rituximab was chosen as a model protein.

The level of protein aggregation in the unsheared and sheared solutions was determined by Photon Correlation Spectroscopy (PCS) and SEC-HPLC. TEM was used to visualise protein aggregation.

It was found that protein aggregation was induced by rotary piston pumps however not by the peristaltic pump. The degree of protein damage was marginally low for large rotary piston pumps such as RPP 3 and 4 and showed a considerable increase with smaller sizes like RPP 1 and 2. A loss of protein monomers of 3.2 % ± 1.8% was found after 3 hours of circulation with RPP 1 in the test system. For RPP 2 a loss of 0.4% ± 0.2% was found. No loss was seen for RPP 3. The different clearance between the piston and the cylinder in the different sizes of pumps was suggested to

be one reason for the large difference in exerted shear stress leading to protein aggregation. Two more factors were suggested to have an influence on the exerted stress caused by a RPP, which are the generated friction surface per dosed ml and the dosage volume. Although an influence of the dosage volume could not be confirmed by the conducted shear experiments. These 3 factors were respected for the calculation of parameter δ. The evaluation of the filling speed showed minor influence with a trend to fast filling speeds being more favourable, whereas the exposure to the air-liquid interface did not show an influence. A slight trend was seen that the combination of 5% trehalose dihydrate and 0.5% polyethylene glycol showed the best protective effect out of the excipients examined.

An evaluation of the analytical methods used in this work revealed that PCS is an extremely sensitive method to detect protein aggregates and was therefore very suitable to monitor the changes in the protein solutions after circulation in the test system. A significant lower sensitivity was observed for SEC-HPLC.

It can be concluded that for filling of shear sensitive pharmaceutical protein solutions, it is critical to choose the appropriate equipment. Large sizes of RPPs such as RPP 3 and 4 or peristaltic pumps should be employed as dosing equipment. Furthermore high speed gives better results than low speed, i.e. machine stops during production should be avoided.

B INTRODUCTION

Peptides and proteins as active pharmaceutical ingredients have gained very much in importance in the recent years. The introduction of the recombinant DNA technology and the hybridoma technology, has led to the development of a large number of protein pharmaceuticals. All leading pharmaceutical companies do research in this area and seek to register new innovative protein pharmaceuticals like vaccines, monoclonal antibodies, polyclonal antibodies, enzyme activators and inhibitors, functional regulators such as hormones and cytokines. An overview of recombinant proteins approved in the European Union till 2004 is given in Table G.1.1 (ISB, 2004) in chapter G.

Protein pharmaceuticals have in comparison to structurally small chemical entities a high specificity and activity at relative low concentrations. This is one reason for their importance in the battle against diseases. The activity of a protein is related to the specific three dimensional structures. Any conformational change may lead to denaturation and aggregation resulting in no or reduced activity. During production operations as stirring, pumping, filtration, centrifugation, sterilization, shaking and shipping, protein aggregation is routinely found due to the presence of physical, chemical and thermal stresses. This is a major concern as it lowers final yield of the product. Furthermore denatured aggregated protein presents a clinical danger when i.v. administered (Demeule et al., 2006).

Due to technical advances in analytical separation and purification, biotechnologically manufactured proteins can be obtained at a very high level of purity. However, achieving a stable protein formulation which maintains the integrity of the protein pharmaceutical during manufacturing and during an acceptable shelf-live is still a major challenge in development.

Further, optimization of the manufacturing process and understanding potential risks during the various production steps can as well contribute to increase final yield. The present study concentrates on examining shear forces which may occur during dosing operations with respective equipment and to possibly optimize the filling

process. Excipients are tested for their suitability to protect proteins from degradation during the filling process.

C THEORETICAL BACKGROUND

C.1 Protein Stability

C.1.1   Protein Structure

Proteins consist of a defined sequence of amino acids, which is referred to as the primary structure. The amino acid chain folds up to a precisely determined three-dimensional structure. It is the three-dimensional structure on which the activity of a protein depends. The chain contains local regions of regular structure, α-helices, β-strands and β-turns. The local ordered regions constitute the secondary structure and are separated by segments of random coil. The whole chain is folded into a three-dimensional tightly packed globular structure, the tertiary structure. If a protein consists of more than one amino acid chain, the defined position of the chains to each other is referred to as the quaternary structure (Doonan, 2002).

C.1.2   Protein Folding

The formation of secondary structure elements are based on hydrogen bonds. α-helices are stabilized by internal hydrogen bonds. The hydrogen bonding is between amino acids close to each other in the sequence. β-strands do generally not occur singly in proteins as they cannot form internal hydrogen bonds. This is why they occur in sheets. Two or more strands are located alongside one another and are stabilized by forming hydrogen bonding networks between the strands. The strands forming the sheet can be located far away from each other in the amino acid sequence.

Various forces contribute to the overall folding of the protein into the tertiary structure. The formation of β-sheets, which brings together remote regions of the amino acid chain, but as well each amino acid residue contributes via it's interactions with other amino acid residues. There are various types of interactions: hydrogen bonds which are formed between the side chains of polar residues or with peptide bonds; ionic interactions formed between amino acids with ionized acidic or basic residues;

electrostatic interactions formed between the peptide bond which has dipole character and other dipoles or charged residues (van der Waals' forces). Individually all of these interactions are relatively weak but the total of the entire interactions make a large contribution to the shape and stability of the protein. The repellent forces between non-polar domains of the protein and water are responsible for hydrophobic interactions (Wang, 1999).

C.1.3 Protein degradation

Due to the complex folded three-dimensional structure, proteins are highly susceptible to degradation (Manning et al., 1989). Degradation is often categorized in two different classes: chemical and physical. Chemical degradation refers to any process that involves modification of the molecule via covalent bond formation or cleavage. Resulting is a new chemical entity. Physical degradation involves changes in the secondary, tertiary and quaternary structure. However, chemical and physical degradation do not occur completely independent of one another (Randolph et al., 2002). Chemical degradation can induce further physical degradation as for example reduction of disulfide bonds can lead to loss of the protein native conformation and vice versa, e.g. denaturation can cause oxidation to amino acid residues that have been buried inside before (Kendrick et al., 2002). On the other hand chemical changes may not always have an influence on the protein conformation or activity. It depends on the location of the amino acid (Wang, 1999).

C.1.3.1 Chemical degradation

Proteins can undergo chemical changes through several pathways like

- hydrolysis
- deamidation
- oxidation
- beta elimination
- disulfide exchange
- racemization

A large number of possible chemical reactions have been determined as decomposition pathways of polypeptides. They have been summarized in a review article by Manning et al. (1989). Out of all of the reactions, hydrolysis and oxidation reactions are of major concern as a source of chemical instability. Following a brief description of the pathways is given.

Hydrolytic cleavage can occur at the peptide bond (RNH-CO-R), known as proteolysis, and more likely at the ester linkage (R-O-CO-R). Peptide bonds are considered to be stable unless hydrolysis is supported by a neighbouring group. The amino acids serine, threonine and first of all aspartic acid form peptide bonds which have been identified as the weak link of the chain. It has been found that the hydrolysis of peptide bonds of aspartic acid in dilute acid is 100 times faster than that of peptide bonds of other amino acids. Particularly prone to proteolysis is the bond between aspartic acid and proline or glycine (Wang, 1999). The hydrolytic rate is mostly influenced by solution pH and temperature; it is increased by extreme pH and high temperature. Often, hydrolysis is a continuation after deamidation of asparagine residues.

The nucleophilic addition of water to the side chain amide of either asparagine or glutamine under removal of ammonia refers to the deamidation reaction. This is a most common degradation reaction in aqueous solution which is catalysed by both acid and base. It has been found that in general asparagine is much more labile than glutamine. Asparagine is most stable between pH 2 – 5 in proteins. The deamidation reaction at pH 5 – 12 proceeds rapidly and entirely and passes through a cyclic imide (succinimide) where the side chain carbonyl group attaches to the nitrogen atom on the peptide backbone. Depending on which bond in the cyclic imide breaks the des-amido peptide, the isopeptide or D-isomers result. In acidic media (pH 1 - 2) it is a slow reaction which seems to skip the succinimide intermediate (Daniel et al., 1996). The peptides deamidate by direct hydrolysis. Cross et al. (1991) showed that the deamidation rate of asparagine in neutral and alkaline media is significantly influenced by the neighbouring amino acid on the carboxyl side. Increasing size and branching of this residue decreased the rate of deamidation compared to that of the asparagine-glycine sequence which is most labile. Furthermore secondary and tertiary structures can have a stabilizing effect on asparagine residues, as they are

buried inside and therefore inaccessible. It has been found that α-helical as well as β-turn structures have a tendency to protect asparagine against deamidation. Therefore certain proteins are only deamidated if they have undergone denaturation first. Besides acidic and alkaline pH, the deamidation rate is increased by high temperature. Ionic strength and the choice of a suitable buffer are important as the anion can have a catalytic effect.

Along with deamidation, oxidation is the most common form of chemical degradation of peptide pharmaceuticals (Cleland et al, 1993). Oxidation can occur at cysteine and methionine residues, or at the heterocyclic aromatic side chains of histidine and tryptophan. The thio groups of cysteine and methionine are most prone to oxidation. Methionine residues are sensitive to oxidation by atmospheric oxygen, like human growth hormone in a container with only 0.4 % oxygen (Wang, 1999). The thio group of cysteine is oxidized to form disulfide linkages; methionine is at a first stage reversibly oxidized to sulfoxide which can be further oxidized irreversibly to sulfone. The heterocyclic aromatic side chains of histidine and tryptophan form N-oxides. Several types of oxidants are known to cause specific mechanisms of oxidation. The different oxidants react at specific sites in the protein and set free specific decomposition products. Organic peroxides represent a reactive species which oxidize methionine to sulfoxide through a nucleophilic substitution reaction. Sources of organic peroxides are stoppers and silicone tubing as well as excipients like polysorbates. Furthermore singlet oxygen, which is generated through excitation by light, is a potential oxidant. Another source of reactive oxygen is redox-active metals like Fe(III) and Cu(II) which occur in traces as contaminants of buffer salts and sugars (Meyer, 2002). The rate of oxidation is influenced by the solution pH. In general it is increased in neutral to slightly alkaline media.

β-elimination is a frequent decomposition pathway of proteins, where cystine, cysteine, serine, phenylalanine, lysine and threonine residues can be involved. Often β-elimination contributes to further physical degradation and leads to inactivation of the protein. The rate of β-elimination is increased by alkaline pH, high temperature and the presence of metal ions (Manning et al., 1989).

The cleavage of disulfide bonds and formation of new bonds with another sulfhydryl group, i.e. exchange of disulfide bond, is a possible degradation mechanism. As disulfide bonds are often critical for the stability of the three-dimensional structure, interchange of disulfide bonds induce loss of activity. In neutral and alkaline pH the reaction is a nucleophilic attack of an ionized thiol group (thiolate anion) and therefore catalyzed by thiols. The reaction can be inhibited by thiol scavengers (Manning et al., 1989). Disulfide exchange in acidic media follows a different mechanism.

As all amino acids except glycine dispose of a chiral C-atom and hence a protein is composed of multiple chiral centres, the racemization reaction results in the formation of diastereomers. In alkaline media the reaction is considered to proceed through elimination of the α-proton to form a negatively charged planar carbanion. By addition of a proton to this intermediate a mixture of D- and L-enantiomers for the individual amino acid results. The rate of racemization is particularly high for aspartic acid residues in proteins, which is 10^5-fold higher than for the free amino acid, in comparison to a 2- to 4-fold increase for all other amino acids, as the mechanism involves the formation of a cyclic imide (Manning et al., 1989).

C.1.3.2   Physical degradation

Proteins possess a specific conformational structure, which minimizes the exposure of hydrophobic groups. This unique globular structure is a requirement for the proteins physiological and pharmacological activity. Physical degradation is the change of the native secondary or higher order folded structure. For proteins in dilute solutions (< 1 mg/ml) unfolding is often reversible, which means that the protein refolds to its native globular structure if the favourable solution conditions are restored. However, at concentrations above 2 mg/ml, which is often encountered for pharmaceutical protein solutions, the two-state thermodynamic model is not applicable (Kendrick et al., 2002). Intermolecular interactions are likely to induce reversible and irreversible aggregation and precipitation. Possible irreversible physical degradation reactions which follow denaturation are:

- non native aggregation

- precipitation

- adsorption to surfaces and interfaces

The mechanisms of non-native protein aggregation are not yet fully understood. Arakawa et al. (2006a) suggested pathways for the formation of non-native aggregates according to Figure C.1.1, where mechanism A1 starts from the presence of a contaminant. This contaminant, which could be damaged protein, host cell proteins, or even nonprotein material, may lead to the formation of soluble oligomers and subsequently could serve as a nucleus, which induces assembly of further native protein.
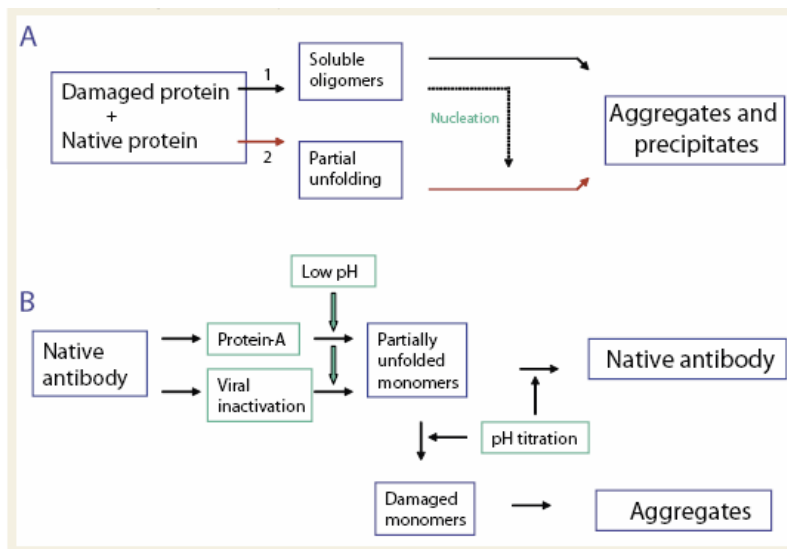
Figure C.1.1: Pathways of protein aggregation (Arakawa et al., 2006a)

In the second mechanism (Figure C.1.1, A2) proteins aggregate from a partially unfolded state which was described as a transiently expanded conformational species within the native state ensemble (Kendrick et al., 1998b; Kim et al., 2001). The structure of proteins has to be considered as not too rigid and thus, the native conformational state fluctuates between a folded and a more expanded form. Kendrick et al., (1998b, 2002) suggested the scheme shown in Figure C.1.2 for the formation of aggregates of recombinant human interferon-γ. Non-native protein aggregation has been identified as a reversible modification of the native structure followed by an irreversible aggregation step.

$$N \rightleftharpoons N^* \longrightarrow A; \quad (a)$$

$$A + A_{n-1} \longrightarrow A_n; \quad (b)$$
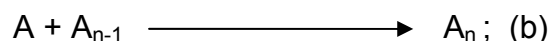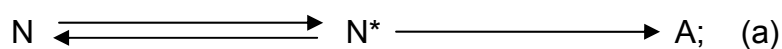
Figure C.1.2: Recombinant human interferon-γ aggregation mechanism

In Figure C.1.2, N^* is a transiently expanded conformation in equilibrium with N. A is an aggregation-competent conformation. The transformation of N^* to A is an irreversible reaction. A is a partially unfolded conformation, also called molten globule or acid-denatured. Hydrophobic parts, which are buried inside the protein structure in native state, are exposed on the surface. A is prone to aggregation to minimize the exposed hydrophobic surface and therefore undergoes assembly reactions to form larger aggregates.

Non-native aggregates are characterized by an increased level of non-native intermolecular β-sheet structures and a loss in α-helical structures (Kendrick et al., 1998a + b). Aggregation is most critical as it regularly occurs during routine production steps like refolding, purification, sterilization, shipping and storage (Manning et al., 1989). In some cases the cause for protein aggregation is very difficult to be identified as the impairment of the protein happens at a different process step than the formation of the aggregates. An example for this is the recombinant manufacturing of monoclonal antibodies, where the protein is exposed to low pH, but formation of aggregates is induced upon pH increase as shown in Figure C.1.1, B. Even under favourable solution conditions and in absence of any applied stresses protein aggregation can be observed.

Aggregation leads to higher-order structures which may be soluble but with increasing size the aggregates become insoluble and precipitation occurs.

With increasing hydrophobicity of the protein, whether it is in native or unfolded conformation, adsorption to surfaces and interfaces can be observed. Adsorption to glass or plastic surfaces as in vials or infusion bags and adsorption to filters regularly pose problems in production.

C.1.4   Physical stability of proteins in aqueous solution

Physical stability of proteins in solution is controlled by conformational and colloidal stability of the protein under the solution conditions. The role of conformational and colloidal stability was summarized by Chi et al. (2003b) in a review article.

Conformational stability depends on the thermodynamic equilibrium of the native and the partially unfolded state and is characterized by ΔG_{unf}, the free energy of unfolding. With increasing ΔG_{unf} values the thermodynamic equilibrium is pushed towards the more compact native protein conformation. It was shown for recombinant human interferon-γ that increasing ΔG_{unf} resulted in a decreased aggregation rate (Kendrick et al, 1998a). The difference in free energy which stabilizes the native conformation is only approximately 5 – 20 kcal/mol compared to unfolded, denatured and biologically inactive conformations. This small conformational stability is the result of large stabilizing and large destabilizing forces. The native state seems to be predominantly stabilized by hydrophobic interactions (Dill, 1990).

Colloidal stability is reflected by the B_{22} value, the osmotic second virial coefficient. The B_{22} value is a measure for overall protein-protein interactions, like Coulombic, van der Waals, and all other short range interactions. It quantifies intermolecular interactions. Positive B_{22} values show that protein-solvent interactions are favoured over protein-protein interactions and therefore repulsive forces between protein molecules are dominant. Negative B_{22} values indicate that protein-protein interactions are dominant, i.e. proteins are colloidally unstable and assembly to aggregates is favoured (Chi et al., 2003a, 2003b).

Thus to achieve a physically stable protein solution the aggregation process, which consists of at least 2 steps, structural changes followed by an assembly step, has to be controlled by increasing conformational and colloidal stability. It has been shown for recombinant human granulocyte colony stimulating factor that either of the 2 steps can be rate limiting depending on the solution conditions (Chi et al., 2003a).

C.1.5   Physical factors affecting protein stability

Protein degradation may be affected by a variety of physical factors, such as temperature, pH, agitation, exposure to interfaces and surfaces, pressure, shearing, etc.. Wang (1999) has discussed these influencing factors on the stability in a review article. These factors easily perturb the fragile balance between stabilizing and destabilizing factors.

Temperature: Increasing temperature usually leads to physical denaturation. Whereas electrostatic interactions are practically not affected by rising temperature, hydrogen bonding is diminished, and hydrophobic interactions are up to a certain limit enhanced. Denaturation may in some cases be reversible depending on experimental conditions. High temperature accelerates as well chemical degradation reactions, such as hydrolysis and deamidation. Usually the thermodynamic stability of proteins, characterized by ΔG_{unf}, the free energy of unfolding, is positive within a temperature range; outside this range, at temperatures higher or lower, ΔG_{unf} becomes negative and proteins are destabilized.

Proteins are often stable within a narrow pH range. pH may strongly influence physical and chemical stability. Formulation pH defines the overall charge on the protein and its distribution, which influences electrostatic effects. If protein molecules are highly charged, the repulsive forces between the molecules stabilize proteins in solutions colloidally and prevent aggregation and denaturation. On the other hand when a protein is highly charged, e.g. at pH far from the isoelectric point (pI), the density of charged groups on the molecule is high and may lead to an increased intramolecular charge repulsion which destabilizes the protein conformation. In addition specific electrostatic forces, such as salt bridges and ion pairing are affected and can have an influence on protein stability (Wang, 1999; Chi et al., 2003b).

During exposure to interfaces and surfaces proteins can suffer damage to their native structure. Due to their amphiphilic character, proteins tend to accumulate at hydrophobic surfaces and interfaces. They are aligned in a way to expose the hydrophobic residues to air and / or surface and unfold to maximize the exposed hydrophobic parts. Additionally a subsequent process of continuous adsorption and release of structurally perturbed protein molecules into the solution can occur and

cause further protein aggregation and denaturation (Randolph et al., 2002). This can lead to very high percentages of loss of native protein molecules. Depending on the extent of the surface active property, the degree of hydrophobicity of the protein molecule and flexibility of the protein structure, a protein is more or less sensitive to the exposure to surfaces and interfaces. The same applies to agitation and shearing, where new air / water or solid / water interfaces are continuously created and hydrophobic areas of proteins are exposed, initiating denaturation. Agitation and exposure to denaturing interfaces is one of the most common physical stresses as it occurs routinely during shipping and handling, as well as during processing operations, such as mixing, pumping and centrifugation of protein solutions. Maa and Hsu (1997) showed that recombinant human growth hormone formed noncovalent aggregates in the presence of high shear and air-liquid interface. Harrison et al. (1998) found that the binding activity of single-chain Fv antibody fragments decreased in a stirred vessel in the presence of air-liquid interfaces.

There is evidence in literature that high pressure of a few hundred MPa can cause denaturation. The impact of pressure on protein molecules should be considered in certain manufacturing processes and in certain drug delivery devices. The volume of unfolded protein in solvent is smaller and therefore unfolded proteins are more compressible. It has been suggested that intrusion of water into the hydrophobic parts of the protein takes place under pressure. The protein is destabilized and as a result denatured (Kendrick et al., 2002).

C.1.6 Stabilization of proteins

Stabilization of protein molecules aims to protect sensitive functional groups in the native molecule from covalent degradation reactions, as well as protecting the folded native structure by intensifying the rigidity of the molecule and thus make it less sensitive to unfold due to destabilizing effects. There are generally two possible approaches of stabilization of proteins: internal and external stabilization (Wang, 1999). Internal stabilization refers to any structural modifications to the protein molecule. External protein stabilization applies to stabilization by changing the properties of the solvent in contact with the molecule.

A search of literature reveals that a wide range of possibilities to improve stability of protein therapeutics exists (Wang, 1999; Capelle et al., 2007). They can be divided in 3 groups: Stabilizing excipients, site-directed mutagenesis, and chemical modification.

1. Stabilizing excipients:

   The most common way to stabilize protein therapeutics is the addition of excipients to the formulation. The types of protein stabilizing excipients include sugars and polyols, salts, detergents, amino acids, amins, polymers and metal ions, see Table C.1.1 with a list of commonly used excipients in protein formulations (Capelle et al., 2007).

   Polyalcohols, such as glycerol and sugars, stabilize proteins by the preferential interaction mechanism (Gekko et al., 1981a; Gekko et al., 1981b; Xie et al., 1997). One of the most studied excipients of this type is sucrose (Kim et al., 2003; Kendrick et al., 1998b; Lee and Timasheff, 1981). Sucrose is preferentially excluded form the protein's surface due to repulsion from the protein backbone, which is thermodynamically unfavorable. Proportionally to the proteins' exposed surface, this interaction results in an increase of the chemical potential of the protein. By the LeChatelier principle, the system will aim to minimize this thermodynamically unfavorable effect and therefore the protein is driven to the most compact conformation with the smallest surface area. Thus, the presence of sucrose shifts the equilibrium shown in Figure C.1.2 towards the more compact native state. The structurally expanded species, which precedes protein aggregation, is disfavored. Therefore sucrose makes proteins more resistant against any stress that leads to a more expanded state of the protein. Preferentially excluded excipients may also reduce chemical degradation as the accessibility of buried inside side chains is reduced. The Wyman linkage function was applied by Timasheff et al. (e.g. Timasheff, 1998) to protein conformational stability and can be used to explain the mechanism of preferential exclusion. Excipients that are preferentially excluded are also known as cosolutes or cosolvents and include as well salts and amino acids. Preferential interaction was measured for various cosolutes added to protein solutions and it was found that this mechanism can explain

the impact of cosolutes on protein solubility and stability (Lee et al., 1974; 1981; Gekko et al., 1981a; Arakawa et al., 1982; 1983; 1984a; 1984b; 1985; 1990; Kita et al., 1994).

Salts and buffers have complex effects on protein stability, where the influence of buffers is not limited to having the appropriate pK_a for the formulation. Depending on the type and concentration of the salt, the charged groups of the protein and the type of ionic interactions between them, salts may have a stabilizing, a destabilizing or no effect. At high concentrations salts can stabilize proteins through the preferential exclusion mechanism. The effect correlates with the Hofmeister series for anions (Kendrick et al., 2002):

$citrate^{3-}$ / $citrate^{2-}$ > PO_4^{3-} ≈ HPO_4^{2-} ≈ SO_4^{2-} > OAc^-, F^- > Cl^- > Br^- > I^- > ClO_4^-. Salts at low concentrations predominantly influence stability of proteins in solution by non-specific electrostatic shielding (Debye screening). Electrostatic interactions between charged groups are reduced, which can stabilize the protein. Furthermore specific ion binding to a protein can occur and may also lead to a stabilization of the protein. However, if ions bind more strongly to the nonnative protein conformation, destabilization of the native state results (Chi et al., 2003).

Detergents are often added to protein formulations to inhibit aggregation and adsorption to surfaces and interfaces. Both, protein and detergents are surface active molecules. At interfaces and surfaces they orient in a way to minimize exposure of hydrophobic parts to the aqueous solution, which for proteins can lead to damage of the native conformation. The addition of surfactants lowers the surface tension of the solution and reduces the number of protein molecules adsorbed to surfaces and interfaces and therefore has a stabilizing effect on protein solutions. Nonionic surfactants, such as polysorbates are routinely used. Randolph et al. (2002) give an overview of surfactant-protein interactions. Arakawa et al. (2003) have shown that Tween 20 protects effectively ciliary neutrotrophic factor from aggregation caused by agitation. Bam et al. (1998) found that Tween 20 used in molar ratios > 4 inhibits aggregation of human growth hormone during agitation. Vidanovic et al. (2003) observed that Tween 80 and Cremophor EL employed close to the

critical micelle concentration destabilized IgG in solution and stabilized it in the presence of glycine.

Polymers stabilize proteins by one or more of the following properties: preferential exclusion, surface activity, steric hindrance of protein-protein interactions, increased viscosity leading to limitation of structural movement (Wang, 1999).

Some proteins can be stabilized by metal ions like zinc, calcium and magnesium. They bind to the protein and intensify the rigidity of the whole structure resulting in an overall more stable and resistant state of the protein. In literature many examples can be found for this mechanism, e.g. it has been shown that insulin is stabilized by calcium or zinc ions (Wang, 1999).

Hydrophilic cyclodextrins may also protect proteins from aggregation. This has been shown for recombinant human growth hormone using hydrophilic β-cyclodextrins (Tavornvipas et al., 2004), suggesting that hydrophilic β-cyclodextrins are potentially useful excipients for parenteral preparation. Furthermore Tavornvipas et al. (2006) found that the use of the appropriate cyclodextrin is also dependent on the type of the denaturing stress on the protein.

2. Site-directed mutagenesis

   Protein stability can be influenced by modifying amino acids through site-directed mutagenesis. To enhance stability of proteins by change of amino acids, labile amino acids can by exchanged, hydrogen and disulfide bond can be increased, internal hydrophobicity can be increased and surface hyrophobicity lowered, flexibility and charge density can be decreased. However, the overall protein conformation has to be preserved.

3. Chemical Modification

   The introduction of charge groups or water soluble polymers as polyethylene glycol and glycosylation results in a more hydrophilic surface of the protein which as well fortifies the intramolecular interaction. This can stabilize proteins

and is referred to chemical modification. A further possibility to make the protein structure more rigid is to introduce inter-and intramolecular cross linking using bifunctional reagents (Halbeisen, 1993).

C.1.7 Protein formulations

Typically proteins are formulated as solution for injection or infusion. If for stability reasons a liquid preparation is not possible, usually a lyophilisate is developed. For a stable liquid preparation control of pH and ionic strength is imperative. In Table C.1.1 an overview of commonly used excipients in protein formulations is given (Capelle et al., 2007). A typical formulation contains:

- buffer salt as citrate or phosphate
- pH adaptation to physiological pH or as close as possible, if not stable
- a surfactant is added to prevent adsorption to container surfaces

Table C.1.1: List of commonly used excipients in protein solutions

Excipient	Examples
Salts	Ammonium sulfate, calcium chloride, magnesium sulfate, magnesium chloride, potassium chloride, sodium chloride, sodium gluconate, sodium sulfate, zinc chloride
Buffers	Acetate, carbonate, citrate, citrate-phosphate, glycine, HEPES, histidine, maleate, phosphate, succinate, tartrate, triethanolamine (Tris)
Sugars and polyols	Cyclodextrins, fructose, glucose, glycerol, inositol, lactose, maltose, mannitol, sorbitol, sucrose, trehalose
Amino acids	Alanine, arginine, aspartic acid, glycine, lysine, proline
Surfactants	Poloxamer 188/407, polysorbate 20/40/80, sodium lauryl sulfate
Antioxidants and preservatives	Ascorbic acid, benzyl alcohol, benzoic acid, citric acid, chlorobutanol, m-cresol, glutathione, methionine, methylparaben, phenol, propylparaben, sodium sulfite
Polymers	Dextran, polyethylene glycol
Other	Albumin, dimethyl sulfoxide, EDTA, ethanol, thioglycolic acid

The included excipients are FDA approved for parenteral administration and part of the inactive ingredients list or part of FDA approved biopharmaceuticals (Nayar et Manning, 2002; Parkins et al., 2000; Cleland et al., 1993; Gupta et al., 2003; Arakawa et al., 2001; Powell et al., 1998).

As cryo-protectants for freeze-dried forms, non-reducing sugars such as sucrose and trehalose are used. It was found that trehalose is involved in stabilizing membranes and proteins in animals surviving in dry environment and in anhydrobiotic organisms

and was first introduced as excipient by Genentech for Herceptin® (Capelle et al., 2007).

A great challenge is the development of highly concentrated preparations above 100 mg/ml, which are needed for subcutaneous administration (Harris et al., 2004).

C.1.8　Methods for characterization of proteins

C.1.8.1　Analytical techniques in protein characterization

A wide range of chemical and physical analytical methods including their principles for the characterization of proteins and monitoring of instabilities is available in literature. For each protein product a number of analytical methods should be selected and customized to accomplish its specific needs. Biological assays to determine the biological activity of a protein are as essential as the determination of structural properties as the biological activity is dependent on the structure. Table C.1.2 gives an overview of commonly used analytical methods including their major applications (Wang, 1999).

Table C.1.2: Analytical methods used in protein characterization

Analytical techniques	Major applications
Analytical centrifugation	Protein aggregation
CE	Protein degradation, Determination of T_m
CD	Estimation of secondary structure, Determination of T_m, Probing protein conformation, Determination of multimers
DSC	Determination of T_g, Determination of T_m, Protein unfolding
Electron paramagnetic resonance (EPR)	Ligand-protein interactions
Fluorescence	Protein unfolding/interaction, Determination of T_m, Probing protein conformation
HPLC-ion exchange	Protein degradation and aggregation
HPLC-reversed phase	Protein degradation and aggregation, Estimation of contamination
HPLC-size exclusion	Protein degradation and aggregation, Estimation of contamination
IR	Estimation of secondary structures, Determination of T_m, Probing protein conformation
Karl Fischer	Water determination
Light scattering	Protein aggregation
MS	Determination of molecular weight, degradation products and contaminants
NMR	Determination of 3-D and secondary structures, Protein relaxation and softening, Protein unfolding
Raman spectroscopy	Determination of secondary structures
Refractometry	Ligand-protein interactions
UV/visible spectroscopy	Determination of T_m, Protein aggregation, Estimation of contamination, Probing protein conformation

Further methods which have successfully been used in quantification of protein aggregation are assymetrical flow field flow fractionation and sedimentation velocity analytical ultracentrifugation (SV-AUC) (Gabrielson et al., 2007).

However, there is still a lack of analytical methods which can be used to directly examine protein structure and stability at high concentrations without prior dilution or concentration changes during the measurement process (Harn et al., 2007).

Following the methods used for this work are described in more detail.

C.1.8.2   *Photon Correlation Spectroscopy (PCS)*

Photon correlation spectroscopy (PCS) is a method based on time-dependent or dynamic light scattering, which can be used for particle sizing of particles in the range of a few microns that are suspended in a liquid (Weiner, 1984). Determination of the size and size distributions is a common application of PCS (Janmey, 1993). Particles with diameters in the range from 1 to 5000 nm, dependent on sample considerations and the available laser power can be measured (Zetasizer 1000/2000/3000, 1996; Müller et al., 1997). Protein aggregates resulting from protein degradation can be detected by measuring the particle size and particle size distributions of proteins in solution. The size of aggregates can be determined by dynamic light scattering, however for measuring the exact composition of multimodal distributions and the percentage of aggregated protein in solution a prior separation step by e.g. SEC-HPLC or asymmetrical flow field-flow fractionation is necessary (Demeule et al., 2007).

C.1.8.2.1 *Principle*

The Brownian motion of suspended particles in solution causes time dependent intensity fluctuations of light scattered from the particles. The changes in intensity with time are dependent on the size of particles, as small particles move more rapidly than large particles. These changes can be detected with suitable optics and a photomultiplier. The rate of fluctuations of the scattered light is higher for small particles. The scattered light is detected usually at an angle of 90° of the laser beam.

20

A correlator calculates from the measured time dependent variations in intensity of scattered light an autocorrelation function. A theoretical correlation function according to Equation C.1.1 is adapted to the measured autocorrelation function:

$$g(\tau) = e^{-2 \cdot D \cdot K^2 \cdot \tau}$$
Equation C.1.1

where

$$K = \frac{4 \cdot \pi \cdot n}{\lambda} \cdot \sin\left(\frac{\theta}{2}\right)$$
Equation C.1.2

where т is the correlation time, D is the diffusion coefficient and K is the scattering vector (dependent on refractive index of solvent n, wavelength of laser source λ and detection angle θ). D is the only variable factor in Equation C.1.1 and can be related to hydrodynamic particle radius R_h using the Stokes-Einstein equation:

$$R_h = \frac{k \cdot T}{6 \cdot \pi \cdot \eta \cdot D}$$
Equation C.1.3

Where k is Boltzmann's constant, T is absolute temperature and η is solvent viscosity.

C.1.8.2.2 Data analysis

For the characterization of the protein solutions the following parameters are used:

Cumulants Analysis: The analysis of the autocorrelation function can be performed with the cumulants analysis, where the normalized and logarithmized autocorrelation function is equated with the quadratic term: $a + b\tau + c\tau^2$. The logarithmized theoretical correlation function (see Equation C.1.1) is a straight line, as is the logarithmized autocorrelation function of a monodisperse distribution. b is the slope of the straight line and related to the z average mean. c reflects the deviation of the autocorrelation function from the theoretical correlation function and is related to the polydispersity. The deviation increases with increasing polydispersity.

Z average mean: Mean hydrodynamic diameter obtained from the cumulants analysis.

Polydispersity index (PI): PI is calculated with the constants b and c and describes the width of the particle size distribution. It is obtained from the cumulants analysis. A differentiation between a broad distribution and a bimodal distribution is not possible using the cumulants analysis.

Contin analysis: The contin-algorithm is a complex mathematical calculation operation to determine a particle size distribution from the autocorrelation function. During this mathematical operation 12 possible distributions are calculated and the best fit result is displayed. As the contin analysis is good at determining smooth distributions and finding contaminants it is suitable to detect protein agglomerations in very low concentrations. However the resolution of this analysis is low.

C.1.8.3   Size-Exclusion HPLC

SEC-HPLC is an important method for the characterization of highly molecular substances as proteins or polymers. It is the basic method in aggregation analysis to determine and quantify aggregation levels for protein pharmaceuticals and practically always required for regulatory approval (Arakawa et al., 2006a).

Principle:
Molecules are separated due to their difference in size and shape of the solutes, i.e. their hydrodynamic volume. The principal of this method is shown in Figure C.1.3. The stationary phase consists of a porous material of a defined pore size diameter. Molecules with a larger diameter that cannot permeate into the pores pass the column with the mobile phase and elute first. Small molecules that permeate freely into the pores are retarded and take the longest time to pass the column. Molecules of an intermediate size between the two extremes are partially excluded and separated due to their size and occasionally as well due to their shape. They are detected at different retention volumes. The retention volume is calculated from the retention time according to Equation C.1.4.

$$V_R = t_R \cdot V_{flowrate}$$ **Equation C.1.4**

where V_R is the retention volume which describes the retention behavior, t_R is the retention time and $V_{flowrate}$ is the flow rate of the mobile phase.
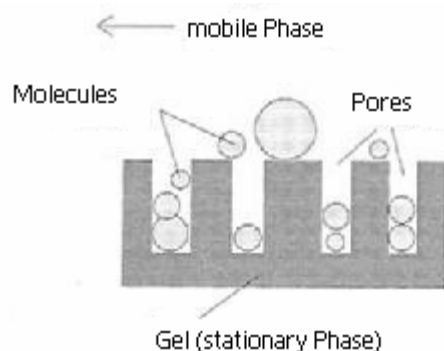
Figure C.1.3: Principal of SEC-HPLC (Otto, M., 2000)

Stationary phase: Routinely, columns with chemically modified polar phases like hydrophilic silica gel of a particle size around 5 to 10 µm and constant distributions of pore size diameter are used. The distribution of pore sizes should be as narrow as possible. The ratio of the total pore volume to the void volume should be as high as possible to improve the peak capacity. The separation efficiency can be increased by using small, regular stationary phase particles and by a narrow, long and densely packed column (Stulik et al., 2003). Furthermore it can be enhanced by injecting small sample volumes and reducing the flow rate. The limit of exclusion from a column corresponds to the molecular size in Dalton above which no retention can be observed anymore. It is dependent on the pore size of the material of the stationary phase and the hydrodynamic volume of the molecule.

Mobile phase: The choice of the mobile phase depends on the solubility of the material to be analyzed. For water soluble material aqueous elution media containing a buffer for pH control are used. For poorly water-soluble substances apolar organic solvents in combination with hydrophobic packing materials are used.

Electrostatic and hydrophobic interactions of the solutes with the stationary phase compromise the pure size exclusion mechanism and should as far as possible be suppressed by modifying the stationary and mobile phase accordingly. Literature

gives evidence that proteins tend to bind to columns during SEC-HPLC (Arakawa et al., 2006a; Stulik et al., 2003; Gabrielson et al., 2007), leading to abnormal chromatograms, protein loss, column damage and inaccurate protein molecular weight data (Ejima et al., 2005). This is especially true for soluble aggregates. In Figure C.1.4 possible mechanisms of protein binding to the stationary phase are shown, where in SEC-HPLC proteins tend to bind according to step C (Tsumoto et al., 2007). For recombinant human platelet-activating factor acteylhydrolase it has been found that it reversibly binds to silica surface (step A) followed by an irreversible conformation modification (step B) which leads to the formation of aggregates (Chi et al., 2005).
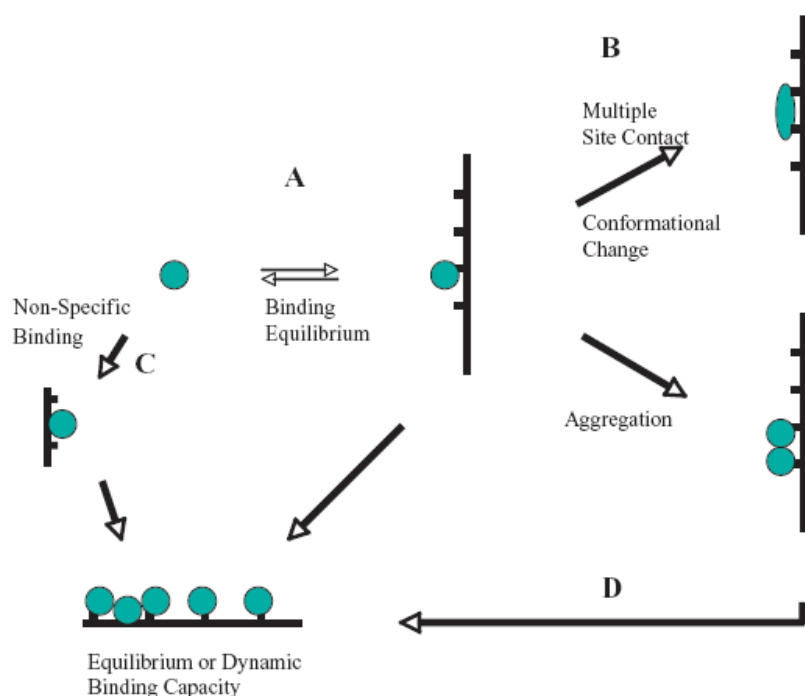
Figure C.1.4: Schematic illustration of protein binding to column resin (Tsumoto et al., 2007)

To decrease these interactions e.g. the active surface silanol groups of silica-based columns can be masked with dextran or agarose. The mobile phase can be adapted in terms of pH, ionic strength and the content of organic modifier in order to suppress hydrophobic and electrostatic interactions (Stulik et al., 2003). Tsumoto et al. give in a review article (2007) an overview of salt effects on protein-surface interactions applied to column chromatography. Salts can have nonspecific charge shielding effects on proteins and column chromatography due to their ionic properties and specific effects which refer to salting-in and salting-out effects of certain salts at

identical concentrations. In SEC-HPLC relatively low concentrations of salts are often sufficient to prevent nonspecific binding (Tsumoto et al., 2007).

For arginine hydrochloride it was demonstrated to be very efficient in suppressing nonspecific binding of proteins as well as their aggregates to the stationary phase when added to the mobile phase in concentrations of 0.2 to 0.75 M (Ejima et al., 2005; Arakawa et al., 2006a+b). Recovery and peak separation were enhanced by arginine hydrochloride. Arakawa et al. (2007) discussed in a review article various mechanisms of how arginine influences proteins and suggested that it acts via interacting favorably with amino acid side chains and limited binding on the proteins' surface, which inhibits aggregation but does not destabilize the protein.

C.2 Regulatory Background

C.2.1   Manufacturing conditions

Protein instability is one of the reasons why protein pharmaceuticals are formulated for parenteral administration and not e.g. for oral administration (Wang, 1999). Furthermore, most protein pharmaceuticals are sensitive to heat and therefore cannot be finally sterilized by steam sterilization. For sterile preparation without sterilization in the final container, the GMP guideline demands a preparation under aseptic conditions (PIC-Leitfaden einer Guten Herstellungspraxis für pharmazeutische Produkte, 2004a). The objective of aseptic processing is to maintain the sterility of a product that is assembled from components, each of which has been sterilized by steam, dry heat, ionizing radiation, gas or filtration.

Sterility of a product cannot be guaranteed by testing. Aseptic production processes have to be validated by 3 consecutive successful process simulation tests using microbial growth media (media fill tests) and re-validated regularly (PIC-Leitfaden einer Guten Herstellungspraxis für pharmazeutische Produkte, 2004b). The aseptic manufacturing process has to be controlled by measures as:

- bioburden of the solution before filtration
- filter integrity tests after use

- microbiological controls during production: personnel, surface contact plates, air sampling, sedimentation plates
- online particle monitoring
- sterility testing of the product in the final container

C.2.2   Requirements on parenteral preparations

The European Pharmacopoeia (2006a) specifies in the monograph parenteral preparations, the requirements for sterile solutions administered by injection like protein solutions. Solutions for injection must be clear and practically free from particles. They have to comply with the test for sterility, the test for particulate contamination: sub-visible particles, test for uniformity of content and the test for bacterial endotoxins or pyrogens. As protein degradation often results in aggregation and precipitation, particles in the solution present besides other points a critical aspect.

C.2.2.1   Test for visible particles

The test for visible particles according to the European Pharmacopoeia (2006b) describes a simple procedure for a visual inspection of parenteral solutions. The aim is to assess the quality of the solution in respect to particulate contamination consisting of mobile undissolved particles other than gas bubbles. The visual inspection is performed with the help of a viewing station consisting of a matt black and a non-glare white panel in vertical position next to each other and a suitable white-light source. Non-labeled containers that are clean and dry on the outside are inspected for particles by gently swirling and observing 5 sec in front of the white panel and in front of the black panel. As it is a non-destructive method a 100% control can be performed.

C.2.2.2   Test for sub-visible particles

The test for sub-visible particles according to the European Pharmacopoeia (2006c), which has to be performed for solutions for injection, is conducted using the light obscuration particle count test. The method allows a determination of a size

distribution using the principle of light blockage. A suitable instrument calibrated with spherical particles of known size between 10 µm and 25 µm is used to examine a statistically relevant number of test specimens after sample preparation. Solutions for injection with a nominal volume of equal or less than 100 ml comply with the test if the average number of particles in the tested units does not exceed 6000 per container equal to or grater than 10 µm and 600 per container equal to or greater than 25 µm. Solutions with a nominal volume of more than 100 ml comply with the test if the average number of particles in the tested samples does not exceed 25 per ml equal to or grater than 10 µm and 3 per ml equal to or grater than 25 µm. The microscopic particle count test is available as a second back-up method in the European Pharmacopoeia (2006c).

C.3 Manufacturing of Protein Pharmaceuticals

Large scale manufacturing of protein pharmaceuticals, e.g. recombinant monoclonal antibodies is well established in industry and range from 10 liter to 10 000 liter volumes. In Figure C.3.1, as an example, the schematic production flow of manufacturing a recombinant antibody is shown (Harris et al, 2004). The production process can generally be divided into two processing parts. The first one concerns the manufacturing of the active pharmaceutical ingredient, i.e. the protein drug substance. In the second part the drug substance is formulated to manufacture the drug product in the final dosage form. Following the two parts are briefly described.

```
   Cell culture expansion (seed strain to production)
                        ↓
  Harvest (centrifugation, tangential and / or normal flow filtration)
                        ↓
       Purification (chromatography, and/or membrane steps)
                        ↓
                   Formulation
                        ↓
                  Final vial filling
```
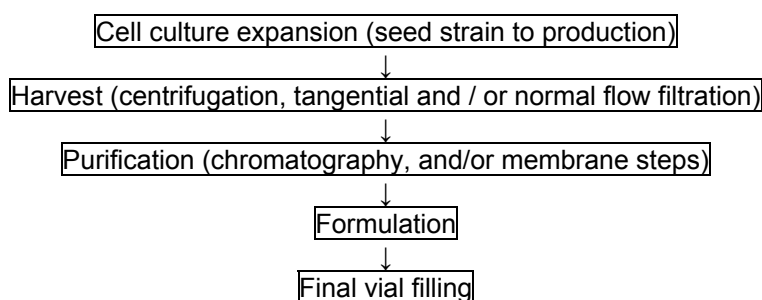
Figure C.3.1: Recombinant antibody production process flow

C.3.1 Biotechnological Part – Manufacturing of protein drug substance

The capability for producing large amounts of high quality proteins is based on the availability of two biotechnologies. Recombinant DNA is utilized to produce the desired protein in the first one. The gene which is responsible for the generation of a certain amino acid sequence of a protein is isolated, modified and subsequently recombined with a plasmid DNA, an extrachromosomal, independently replicating small circular DNA molecule. Restriction enzymes cut DNA at specific places and ligase connects the DNA fragment with the plasmid. The modified plasmid is then introduced into a host cell where it is replicated and transcribed to produce the specific protein. For example Escherichia coli are used for the production of insulin, human growth hormone, interleukin-2 and interferon. Another production technique for insulin utilizes Saccharomyces cerevisiae. CHO (Chinese Hamster Ovary) cell lines are used for the expression of tissue plasminogen activator, coagulation factor VIII and erythropoietin (Schmid, 2002). In the case of Escherichia coli, proteins are expressed in the cytoplasm at high concentrations and result in insoluble inclusion bodies and/or soluble proteins. To release the expressed protein, usually the cells need to be destructed chemically or mechanically. Usually water is used to lyse the cells; however buffers may be used to improve the recovery rate in the supernatant. The further purification steps are depending if soluble folded proteins, soluble misfolded proteins or insoluble inclusion bodies are concerned. Different washing and purification steps are involved. For example in the case of insoluble inclusion bodies a solubilisation, purification and refolding is required to obtain the protein. An overview of the different possibilities for washing and purification methods is given by Arakawa et al. (2002).

The second technology is the hybridoma technique, which is following exemplified by describing the production of monoclonal antibodies. A specific antigen is injected into a test animal. The immune response is initiated and the production of antibodies by B-lymphocytes starts. The antibody-producing B-lymphocytes are isolated from the spleen of the test animal and are in the presence of polyethylene glycol in vitro fused with cells of a lymphocyte tumour (myeloma cells) to form hybridoma cells (Römpp-Lexikon, 1999). Hybridoma cells can be held in culture and indefinitely divided due to their tumour like attributes. The hybridoma cells expressing the desired antibody are selected using immunoassays and cell cloning. The best clones can be preserved for

many years by deep-freezing them. The hybridoma cells are cultured in bioreactors in complex culture media containing besides glucose, fetal bovine serum as nutrient. Supply of oxygen and CO_2 is necessary. In industrial scale they are preferably grown in suspension as batch or continuous production process. A fed batch process, where the production phase in the bioreactor is prolonged by addition of nutrient medium, is preferred as the yield can be increased to several grams antibody per litre. Contrary to micro-organisms, no lysis is necessary for animal cells as the product is secreted. Subsequently a purification protocol is followed. Typically a concentration by ultrafiltration is performed, followed by a pre-purification by binding to protein A. Then the monoclonal antibody is further purified by ion-exchange chromatography and by elimination of aggregated antibodies by gel chromatography (Schmid, 2002). The purification as well includes a treatment for viral inactivation; most effective for that purpose is an exposure to acid (Ejima et al., 2006).

C.3.2 Pharmaceutical part – Manufacturing of the final dosage form

The formulation step transforms the purified bulk protein drug substance into the final solution composed of a defined concentration of protein and excipients. Methods used for the formulation step include large-scale size exclusion chromatography and ultrafiltration. For the preparation of high-concentration formulations, which are desirable for example for subcutaneous administration, ultrafiltration is the preferred method (Harris et al., 2004).

A standard production process for an aseptically manufactured product includes the following steps:

The solution is prepared in a clean room Class C under laminar air flow class A using the protein to be formulated, excipients and water for injection or as mentioned above. The solution is filtered through a sterile filter of pore size 0.2 µm into the class A of a cleanroom class A/B. The filtered solution is then filled into previously depyrogenated and sterilized glass vials or ampoules of hydrolytic class I using a suitable filling and dosing machine or device. Complete filling lines are used for high performance output (starting from 24000 vials / hour) consisting of a washing machine for glass containers, a sterilizing/ depyrogenation tunnel, filling and stoppering machine and crimping machine. The solution is filtered inline through a

sterile filter 0.2 µm. Filled vials are closed with previously sterilized stoppers followed by crimping; ampoules are closed by sealing with heat. Cleanroom conditions class A in B are imperative for all steps where open product or primary packaging components are handled.

Different dosing systems are available for the filling operation, as for example:

- rotary piston pumps: the principle is based on volumetric displacement; see Figure C.3.2.
- peristaltic pumps: a forward flow of solution in an elastic tubing is driven by peristaltic movement.
- time-pressure dosing system: the dosing vessel is kept at constant pressure; pressure differences are compensated with gas (usually nitrogen); dosing via valves, that are opened for a fixed time; the whole process is controlled via a programmable logic controller (PLC) or microprocessor.
- weight-dosing system: dosing valves open till the desired fill weight is achieved; the weight is constantly measured with weighing cells during the dosing process; the process is controlled via PLC.
- sensor dosing system: is based on a principal to fill a container and stop at a given level of product inside the container. A sensor is used to monitor the liquid level. This system is often used for containers which have to be filled 100% without leaving an air bubble in the container as for example dental cartridges. Another advantage is that no product retraction is necessary at the end of filling due to the tolerance of the container, which minimizes the loss of product.

1. Aspiration of bulk solution	2. Piston rotation	3. Filling	4. Piston rotation
The groove of the piston is directed to the bulk solution container. The piston is moving upwards and aspirates the solution into the pump.	The piston makes a 180° rotation. The groove of the piston is directed to the filling needle.	The piston is moving downwards. The solution is ejected and dosed into the final container.	The piston makes a 180° rotation. The groove of the piston is directed to the bulk solution container.

Figure C.3.2: Functional principle of rotary piston pumps (Bausch Advanced Technology Group, 2007).

Rotary piston pumps are solid precision machine parts, without valves and seals, which are easy and fast to clean. Further advantages of this dosing system are that they have a minimal dead quantity and are very flexible in terms of different dosing quantities. Advantages of the time-pressure system and the weight-dosing system are that there are few product contacting parts and a broad processing spectrum as they are as well suitable to fill suspensions and abrasive media. The time-pressure system is suitable for high-performance processing.

Aspects, which should be considered when choosing a dosing system, are that it is easy to clean and sterilize, preferable a CIP/SIP system is available, that it has a high dosing precision and the physical stress for the product is low if the product is sensitive to this. Furthermore the format change should be easy and quick.

C.4 Shear forces during filling and dosing

During processing of pharmaceutical solutions the latter are subjected to various stresses. There is a lot of evidence in literature that particularly proteins are prone to suffer under physical stress like for example high temperature, hydrodynamic shear stress (Elias et al., 1998), exposure to surfaces and interfaces during shaking and

foaming combined with high shear (Maa et al., 1996, 1997). The exerted physical stress can lead to protein degradation, agglomeration and precipitation.

Rotary piston pumps have often been questioned for filling sensitive compounds as for example proteins, due to the potential risk of damage through shear forces that could occur, when passing through the pump. In this work the notions shear and shear forces are used in the sense of physical stress caused by filling systems. This includes the following stresses and their combinations but is not limited to these:

- shear stress in the gap between the cylinder and the piston in a rotary piston pump caused by the movements of the piston
- hydrodynamic shear stress caused by fluid motion
- physical stress due to exposure to surfaces and interfaces

The shear stress τ is defined according to Equation C.4.1.

$$\tau = \mu \cdot \gamma \qquad\qquad \textbf{Equation C.4.1}$$

where γ is shear rate and μ is solution viscosity.

The conditions in a rotary piston pump in respect to the average shear rate for the rotational movement is comparable to the conditions in a concentric cylinder shear device where the solution is introduced into the gap between two cylinders with the inner cylinder rotating. The radii of the cylinders are given by R_o for the outer and κR_o for the inner cylinder. Maa et al. (1996) derived and calculated the average shear rate $\langle\gamma\rangle$ as follows:

$$\langle\gamma\rangle = \frac{4 \cdot \kappa^2 \cdot \omega \cdot \ln\left(\frac{1}{\kappa}\right)}{\left(1 - \kappa^2\right)^2} \qquad\qquad \textbf{Equation C.4.2}$$

where κ is the ratio between the radii of the inner and outer cylinder and ω is the rotating rate of the inner cylinder in radians/second.

The maximum shear rate occurs at the surface of the inner cylinder. An increase in the shear rate can be achieved by values for κ close to 1, which means to diminish the distance between inner and outer cylinder.

The average shear can be calculated by multiplying the shear rate γ with the time spent in the shear field (Maa et al., 1996). Charm and Wong (1970) investigated shear damage for three enzymes when flowing through a capillary tube and found that the degree of inactivation was dependent on the shear rate and the time of exposure and was represented by the product of the two parameters.

The hydrodynamic shear stress τ in a cylindrical tube for a laminar uni-directional flow is zero at the centre of the tube an increases towards the inner surface of the tube, where it is maximal. The calculation of the shear stress results from Equation C.4.3 (Elias et al., 1998).

$$\tau = \frac{r \cdot \delta P}{2 \cdot L}$$

Equation C.4.3

where r is the radial distance from the tube axis, δP is the pressure drop between two points situated at distance L.

C.5 Aim of the work

It is well known that during manufacturing pharmaceutical solutions are subjected to various stresses, e.g. during stirring, sterilization. However not so much is known about physical stress which might occur during filling and dosing operations. In the scope of this study, the impact of physical stress caused by dosing equipment is examined. By circulating a model solution in a suitable test system the impact of shear forces on the model solution is to be evaluated. As dosing equipment a peristaltic pump and rotary piston pumps are examined, compared and evaluated. Influencing parameters of the dosing operation like the dosing equipment itself, filling volume, speed, exposed surface during the operation shall be investigated. The objective is to better understand the filling and dosing process and to evaluate where the potential shear stress originates from. The obtained conclusions shall be utilized

to optimize the process as well as the equipment and to establish rules which shall be respected for filling shear sensitive products.

As small chemical entities are unlikely to show an effect, the focus for a model substance concentrates on protein solutions. Literature gives evidence that proteins are sensitive to physical stress and can suffer damage from it. A protein which is sensitive enough to shear stress as it might occur in the present study has to be searched and evaluated in combination with the experimental test system and an analytical method which can monitor the impact on the protein.

Subsequently excipients and their combinations are evaluated for their protective effect for the kind of physical stress encountered in the respective dosing equipment.

As protein pharmaceuticals are administered as parenteral dosage forms, all considerations for the present study have to be made in respect of sterile manufacturing.

C.6 Model Substances

The search for a model protein from various protein groups like hormones, vaccines, cytokines and enzymes concentrated at first on the group of enzymes. The reason for this choice was that many enzymes are commercially available and the availability of simple enzymatic assays to determine the activity.

β-galactosidase from *Aspergillus oryzae* was used for shear tests in this work because of its molecular weight of about 105 kDa (Tanaka et al., 1975). This corresponds to an average molecular weight for enzymes. Furthermore it is very stable, and an easy to handle enzyme activity test which delivers reliable results is available.

After the first shear tests it became obvious that for β-galactosidase no degradation following exposure to shear stress could be detected. To examine different parameters concerning dosing operations a second model protein was searched which is highly sensitive to shear forces as they occur in the shear model used in this

study. Immunoglobulins in general are known to denature under various conditions including among others temperature change and shear (Wang et al., 2007). Rituximab was selected for this purpose.

The following chapters give a short overview of the character and properties of β-galactosidase and rituximab.

C.6.1 β-Galactosidase

β-galactosidase is as widely distributed in nature as its substrates, oligo- and polysaccharides containing D-galactose joined through a β-glycosidic bond (Wallenfels and Weil, 1972). The universal occurrence on the one hand and the simple enzymatic assay and the great number of substrates on the other hand led to a lot of research done on structure and behaviour of β-galactosidase, which varies depending on the organism source.

C.6.1.1 Structure and catalytic reaction

Structure analysis done by Tanaka et al. (1975) and Akasaki et al. (1976) showed that β-galactosidase from *Aspergillus oryzae* has unlike the molecule from *Escherichia coli*, which is a tetramer, no subunit structure and a molecular weight of 105 kDa. The molecular weight corresponds more or less to the size of one monomer from *Escherichia coli*. Therefore it is supposed that the structure of β-galactosidase from *Aspergillus oryzae* is similar to that of the monomer of *Escherichia coli*.
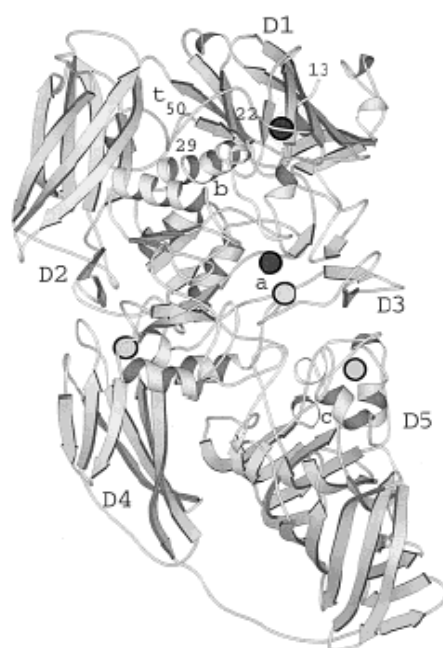
Figure C.6.1: Structure of a monomer of β-galactosidase from *E. coli*. D1-D5 indicate the five domains, a indicates the active site (Juers et al., 2000). ◯ depict Na$^+$ ions, ● Mg^{++} ions.

Juers et al. (2000) examined the structure of β-galactosidase from *E. coli.* The monomer (116 kDa) consists of five structural domains and an active site, which is located at the C-terminal end of the central core of domain 3 and includes also parts of loops from domain 1, 2 and 5. Magnesium ions are present in the active site.

Table C.6.1 shows the amino acid composition of β-galactosidase from *Aspergillus oryzae* (Tanaka et al., 1975).

Table C.6.1: Amino acid composition of β-galactosidase from *Aspergillus oryzae*

Amino acid	Amino acid (M/10^5 g Protein)	Weight %
Alanine	58.1	5.2
Arginine	23.3	4.1
Aspartic acid	89.2	11.9
Cysteine	2.1	0.3
Glutamic acid	70.0	10.3
Glycine	82.2	6.2
Histidine	12.8	2.0
Isoleucine	29.8	3.9
Leucine	69.7	9.1
Lysine	34.5	5.0
Methionine	7.3	1.1
Phenylalanine	39.9	6.6
Proline	60.6	7.0
Serine	60.9	6.4
Threonine	53.9	6.4
Tryptophan	10.5	2.1
Tyrosine	42.6	7.7
Valine	41.3	4.8

The β-galactosidase catalytic reaction involves 3 steps:

$$E + S \; \overset{K_s}{\rightleftharpoons} \; ES \; \overset{k_2}{\longrightarrow} \; ES' + P_1 \; \overset{k_3}{\longrightarrow} \; E + P_1 + P_2$$
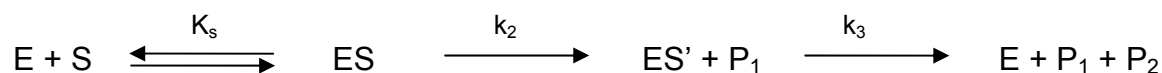
The enzyme E binds rapidly substrate S and forms the Michaelis complex ES. This is followed by the formation of the intermediary complex ES' with simultaneous elimination of the aglyconic leaving group P_1. The ES' complex is hydrolysed to yield free galactose P_2 and the enzyme E (Wallenfels and Weil, 1972).
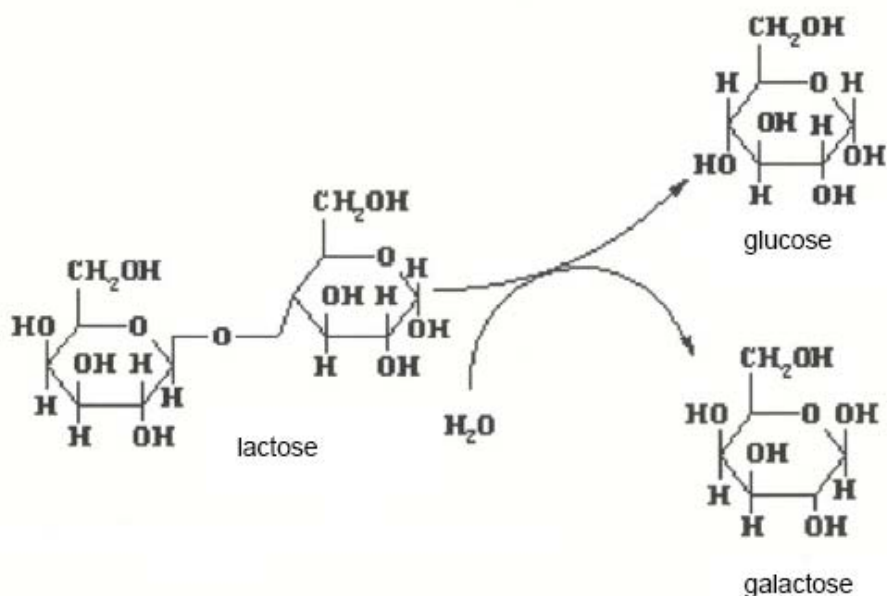
Figure C.6.2: Reaction mechanism of β-galactosidase

β-galactosidase catalyses a β-galactosidic cleavage between the anomeric C-atom and the ether-oxygen atom of di- and oligosaccharides from the galactose side. The galactose part of the galactose-enzyme complex is hydrolysed releasing the enzyme (Stellmach, 1988).

C.6.1.2 *Physicochemical properties and stability*

Tanaka et al. (1975) investigated the properties of β-galactosidase from Aspergillus oryzae and found that the enzyme showed pH optima of 4.5 with OPNG-1 as a substrate and 4.8 with lactose as a substrate. Furthermore a stable pH range from 4.0 to 9.0 was detected. The optimum temperature was found to be 46 °C.

C.6.2 Rituximab

Rituximab is a therapeutic monoclonal antibody for intravenous injection which has been licensed by the US Food and Drug Administration (FDA) in 1997 to treat Non-Hodgkin's lymphoma. Following a short overview on the properties, structure and mechanism of action and of rituximab and monoclonal antibodies in general is given.

C.6.2.1   Monoclonal Antibodies

Monoclonal antibodies are genetically engineered antibodies using mammalian cell lines. Hybridoma cells, which result from a fusion of immune cells with tumor cells, have the ability to produce a specific antibody and at the same time grow in cultures. This was achieved by Milstein and Köhler, who received the Nobel price for their research. The monoclonal antibody is then purified and concentrated.

Rituximab is manufactured using Chinese Hamster Ovary cell suspension in a nutrient medium. The subsequent purification is done by affinity and ion exchange chromatography. A specific viral inactivation and removal procedure is performed (Patient Information Leaflet Rituxan®, 2002).

C.6.2.2   Structure of Rituximab

Rituximab is a chimeric murine / human monoclonal antibody. It is a type IgG_1kappa immunoglobulin, which consists of two heavy chains of 451 amino acids and two light chains of 213 amino acids (Patient Information Leaflet Rituxan®, 2002). The molecular weight is approximately 145 kD, which is a typical molecular weight for monoclonal antibodies (Wang et al., 2007). The light and heavy chains show murine variable region sequences and human constant region sequences, as shown in Figure C.6.3. The variable regions are marked with V; constant regions with C.
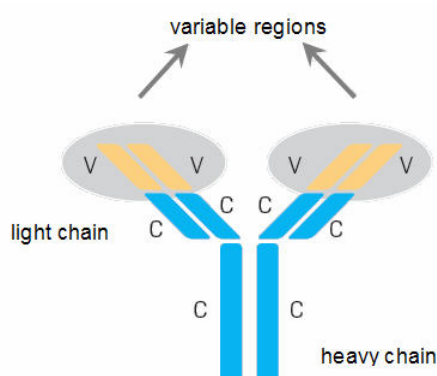
Figure C.6.3: Chimeric monoclonal antibody (Brüggemeier, M., 2005)

The target of rituximab is the CD20 transmembrane antigen on the surface of normal and malignant B lymphocytes. Rituximab molecules bind specifically to the CD20

antigen with a binding affinity of approximately 8.0 nM. An immunological response induces the lysis of the B lymphocytes. Generally there are 2 known pathways for the cell lysis, the complement dependent cytotoxicity (CDC) mechanism and the antibody-dependant cell-mediated cytotoxicity (ADCC) mechanism (Arzneimittelkompendium der Schweiz, 2001). Research in this field is on-going to gain more understanding of the cell-killing mechanisms of anti-tumor antibodies such as rituximab, e.g. (Idusogie et al., 2000).

C.6.2.3   *Physicochemical properties and stability*

Rituximab is stable as a liquid formulation. The concentrated solution of 10 mg /ml, as commercially available on the market, in a citrate buffer solution at a pH of 6.5 has a shelf life of 48 months. It is stable when stored at 2 – 8 °C and it should be protected from direct sunlight. Wang et al. (2007) give an overview in their review article of the stability of monoclonal antibodies in general.

D MATERIALS AND METHODS

D.1 Model Substances

D.1.1 β-Galactosidase

D.1.1.1 Formulation

For the shear experiments an enzyme solution containing β-galactosidase from Aspergillus oryzae (Fluka Chemie GmbH, Buchs, Switzerland) with a molecular weight of 105 kD was prepared by dissolving 1 mg/ml of the enzyme powder in phosphate buffer solution. The phosphate buffer solution pH 4.5 contained 17.8 mg/ml disodium hydrogenphosphate (Merck AG, Darmstadt, Germany) and 12.4 mg/ml citric acid (Hänseler AG, Herisau, Switzerland) in distilled water. The enzyme solution was diluted 1:10 with phosphate buffer solution to obtain a solution containing approximately 0.1 mg/ml β-galactosidase enzyme powder.

D.1.2 Rituximab

D.1.2.1 Formulation

The monoclonal antibody rituximab with a molecular weight of 145 kD was used. It was supplied by Roche, Basel as a sterile, clear, colourless and preservative-free solution at a concentration of 10 mg/ml formulated in 9 mg/ml sodium chloride, 7.35 mg/ml sodium citrate dihydrate, 0.7 mg/ml polysorbate 80, and Water for Injection. The solution pH was 6.5. It was obtained in 10 ml and 50 ml vials.

D.1.3 Excipients

A fundamental condition for the choice of excipients for the stabilization of rituximab against shear stress was the compatibility for the use in parenteral dosage forms. The properties of the selected excipients for evaluation of their protective effect are briefly described in this chapter.

D.1.3.1 Description

Trehalose dihydrate (Georg Breuer GmbH, Königstein, Germany)

chemical formula see Figure D.1.1
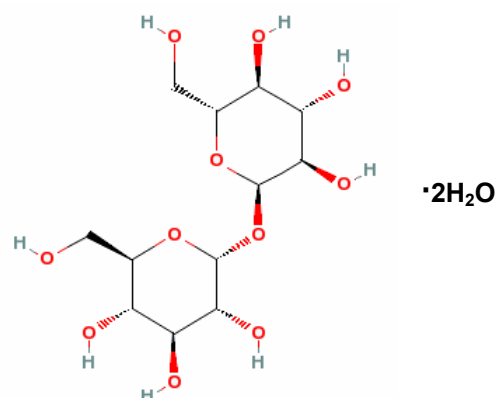
$\cdot 2H_2O$

Figure D.1.1: chemical formula of trehalose dihydrate

empirical formula:	$C_{12}H_{22}O_{11} \cdot 2H_2O$
appearance:	virtually odorless, white or almost white crystals of sweet taste
molecular weight:	378.33 g/mol
solubility:	soluble in water, very slightly soluble in ethanol
technological use:	stabilizes proteins in solution; it prevents protein aggregation by the preferential exclusion mechanism

Polyglycol 6000 (Clariant GmbH, Gendorf, Germany)

chemical formula see Figure D.1.2.

Figure D.1.2: chemical formula of polyethylene glycol

empirical formula:	$HO(CH_2CH_2O)_nCH_2OH$
appearance:	white flakes of characteristic odor
molecular weight:	6000 g/mol (average)
solubility:	soluble in water

technological use: 220 – 262 mPa s viscosity; increases viscosity which leads to steric hindrance and limits structural movements of molecules

Tween 80 (Hänseler AG, Herisau, Switzerland)

chemical formula see Figure D.1.3.
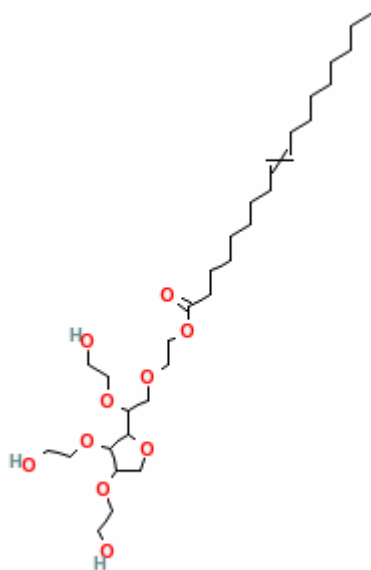
Figure D.1.3: chemical formula of Tween 80

empirical formula: $C_{32}H_{60}O_{10}$

appearance: yellow to amber viscous liquid of characteristic odor

molecular weight: 604.82 g/mol

solubility: soluble in water

technological use: nonionic surfactant; in protein solutions it is used to prevent adsorption of protein molecules at surfaces and air/water interfaces.

D.1.3.2 Formulation

The excipients were added to the formulated rituximab solution described in chapter D. 1.2.1. In total 5 different formulations with excipients were prepared:

- original solution + 0.1% Polyglycol 6000 + 1% Trehalose dihydrate

- original solution + 0.5% Polyglycol 6000 + 5% Trehalose dihydrate

- original solution + 5% Trehalose dihydrate

- original solution + 0.5% Polyglycol 6000

- original solution + 1.24% Tween 80. As 0.07 % Tween 80 is already in the original solution a total concentration of Tween 80 of 1.31 % results.

The excipients were weighed on an analytical balance type AG204 Delta Range (Mettler Toledo Schweiz GmbH, Greifensee, Switzerland) and dissolved in approximately 80 ml original rituximab solution in a volumetric flask (Brand, Germany). Original solution was added to 100.0 ml.

D.2 Shear Experiment

The shear experiments were performed under a laminar flow bench class 100 with a horizontal air flow (Type B-72-30, Skan AG, Basel) to avoid particulate contamination of the tested solution. All parts of the test system as well as all glassware and disposable material in direct contact with the test solution was cleaned with drinking water, finally rinsed three times with freshly distilled water and left for drying under the laminar flow bench. In Table D.2.1 these items are listed.

Table D.2.1: Materials in direct contact with the test solution

Type	Part	Material made of
test system	holding recipient	borosilicate glass
	tubing (inner Ø 5.0 mm; wall 3.0 mm)	silicone
	filling needle	stainless steel AISI 316L
	rotary piston pumps	stainless steel AISI 316L
	platinum cured silicone tubing (inner Ø 3.2 mm; wall 1.6 mm)	platinum cured silicone
laboratory glassware	pipettes (10.0 ml, 20.0 ml, 3.0 ml, 2.0 ml, 1.0 ml)	borosilicate glass
	volumetric flasks (50.0 ml, 100.0 ml)	borosilicate glass
	Erlenmeyer flask	borosilicate glass
	beakers	borosilicate glass
disposable material	tips for pipettes -1000µl blue Treff AG®	polypropylene
	sample tube 1.5 ml Treff AG®	polypropylene

The test solution with the model protein was circulated at a defined displacement speed of the piston, which resulted in a pumping or dosing speed, in the test system. The test system consisted of a holding recipient and a filling needle both connected to the dosing system via silicone tubing as schematically shown in Figure D.2.1. As dosing systems a peristaltic pump or a rotary piston pump were used.
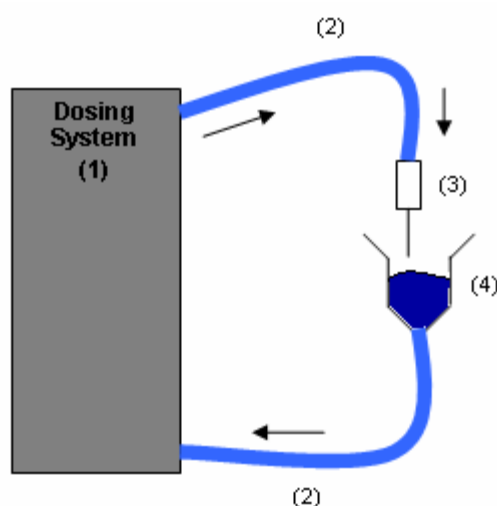
Schematic design of the test system in which the test solution was circulated during shear experiments:

(1) Dosing System:
     Rotary Piston Pump
     or Peristaltic Pump

(2) Silicone Tubing

(3) Filling Needle

(4) Holding Recipient

Figure D.2.1: Schematic design of the test system

Description of the test cycles:

The defined starting volume of the test solution is exactly introduced with a glass pipette into the holding recipient. As many pumping movements as necessary are applied so that the test solution is directly in front of the pump / pump head. The first sample P0 of exactly 1.0 ml was drawn with an Eppendorf micro-pipette 500 µl in a polypropylene sample tube 1.5 ml (Treff AG, Degersheim, Switzerland). The test solution was then circulated in the test system by continuously dosing with the dosing system at a defined speed. After a fixed number of cycles, further samples P1, P2 and P3 were drawn as described above. The volumes of the samples taken were not replaced. One cycle corresponds to the number of strokes needed to pass the total volume in the system once. In the case of the long term experiment the samples were taken after fixed lapses of time.

D.2.1 Dosing System for Rotary Piston Pumps

The dosing system for rotary piston pumps consisted of a dosing machine (Type EDM 3295, Bausch + Stroebel, Germany). The system was equipped with one or two valveless rotary piston pumps as dosing units.

The adjustment of the dosing volume was made mechanically by fixing the piston stroke with a setting spindle. The position is shown in a digital display. The position for minimal filling volume was chosen 180, for the maximal filling volume 300. 180 corresponds to a piston stroke of 18.0 mm; 300 to 39.0 mm, respectively.

The dosing speed was continuously adjustable with a potentiometric control via a turning knob. The values can be set between 0.5 up to a maximal speed of 9.25 indicated according to the position of the turning knob. These values correspond to displacement speeds of the piston between 10 sec/stroke up to 1.8 sec/stroke. The full speed range was covered by the shear test runs.

Rotary Piston Pumps:

The rotary piston pumps (RPP) used for the present shear experiment were valveless and made of stainless steel AISI 316L, as shown in Figure D.2.2. 4 different sizes of rotary piston pumps (RPP 1-4) of 2 different suppliers were used. The different parameters of the 4 pumps are given in Table D.2.2.

Figure D.2.2: Valveless rotary piston pump consisting of a cylinder (top) and a piston (bottom) (Bausch Advanced Technology Group, 2007)

Table D.2.2: Parameters of rotary piston pumps

	RPP 1	RPP 2	RPP 3	RPP 4
Size	size 1	size 2	size 3	size 4
Dosing range (ml)	0.15-1.1	0.7-5.5	1.6-12.5	3.6-28.0
Ø Piston (mm)	6.0	13.0	20.0	30.0
Clearance between Piston and Cylinder (µm)	13.0	17.0	22.0	22.0
Dosing Volume (Dosage 180) (ml)	0.52	2.35	5.55	12.50
Dosing Volume (Dosage 300) (ml)	1.12	5.22	12.28	n/a
Friction surface/ stroke (Dosage 180)* (mm^2)	1280.83	2775.12	4269.42	6029.97
Friction surface/ stroke (Dosage 300)* (mm^2)	1676.67	3632.78	5588.89	8009.18
average shear rate <γ> at 1.8 sec/stroke** (sec^{-1})	2607.11	4321.48	5137.96	7708.35
Supplier	B+S	B+S	B+S	BaseEurope

The length of the piston and the concentricity are the same for all pumps.

*) Calculations see below
**) Calculation see Annex G.9

Calculation of the generated surface of friction:

The generated surface of friction is the area where the piston and the cylinder are in touch with each other at a distance corresponding to the clearance. The friction surface increases with larger dosing volumes and higher strokes within the same size of a rotary piston pump.
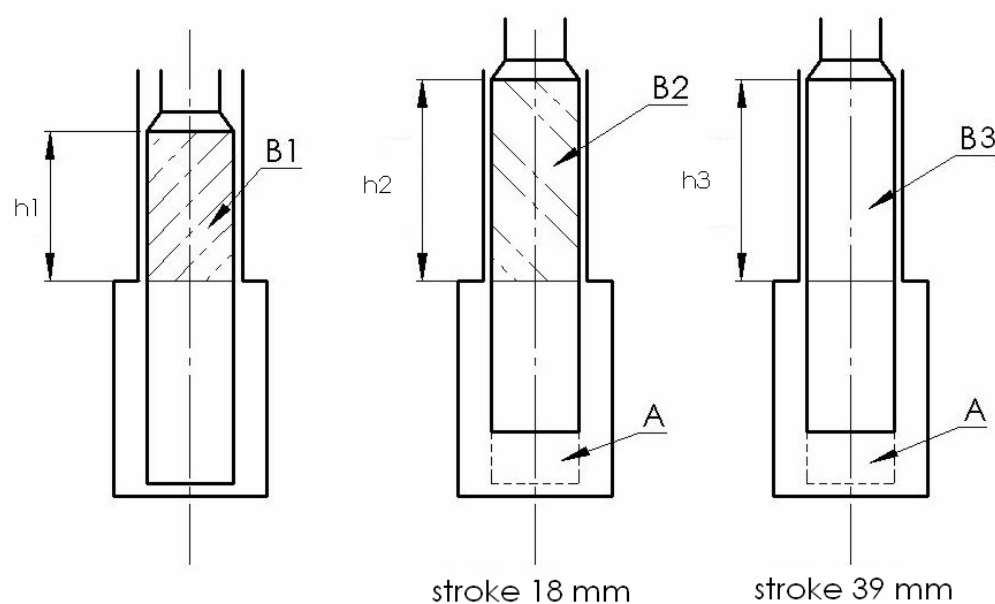
Figure D.2.3: Layout for the calculation of the generated surfaces of friction

Table D.2.3: Calculated surfaces of friction

Pump	d_{piston} [mm]	clearance [mm]	h1 [mm]	h2 [mm]	h3 [mm]	B1 [mm²]	B2 [mm²]	B3 [mm²]
RPP1	6	0.013	49.95	67.95	88.95	941.54	1280.83	1676.67
RPP2	13	0.017	49.95	67.95	88.95	2039.99	2775.12	3632.78
RPP3	20	0.022	49.95	67.95	88.95	3138.45	4269.42	5588.89
RPP4	30	0.022	45.98	63.98	84.98	4333.51	6029.97	8009.18

The generated surface of friction A is calculated according to Equation D.2.1:

$$Ax = Bx - B1 \qquad \textbf{Equation D.2.1}$$

where Ax is the generated surface of friction for a piston stroke of 18 mm (x=2) and a stroke of 39 mm (x=3); Bx is calculated with Equation D.2.2. Results are listed in Table D.2.4.

$$Bx = \pi \cdot d_{piston} \cdot hx \qquad \textbf{Equation D.2.2}$$

where d_{piston} is the diameter of the piston; x (=1,2 or 3) is the index for respective height and friction surface according to Figure D.2.3. h1 corresponds to the lowest position of the piston during one stroke. h2 corresponds to h1 + 18 mm and h3 to h1 + 39 mm. Results are displayed in Table D.2.3. The groove in the piston was neglected for these calculations.

Calculation of cumulative friction surface:

The cumulative friction surface is the integrated area of friction over the displacement of the piston. The displacement during one stroke has a vertical and a horizontal direction, as the piston makes an upward and downward movement and a rotary movement. The cumulative friction surface was calculated for 1 stroke with a rotary piston pump. The cumulative friction surface serves as a measure for the cumulative area on which the protein solution is subjected to shear stress. This is the area during 1 stroke where piston and cylinder are at a distance of the clearance from each other.

The cumulative friction surface was calculated for 1 stroke according to Equation D.2.3 up to Equation D.2.5.

$$FS = FS_{vertical} + FS_{rotary}$$ **Equation D.2.3**

$$FS_{vertical} = (B1(hx - h1)) \cdot 2 + (Bx - B1) \cdot (hx - h1)$$ **Equation D.2.4**

$$FS_{rotary} = B1 \cdot \frac{d_{piston} \cdot \pi}{2} + Bx \cdot \frac{d_{piston} \cdot \pi}{2}$$ **Equation D.2.5**

where FS is the cumulative friction surface, $FS_{vertical}$ is the cumulative friction surface of the vertical movement of the piston, FS_{rotary} is the cumulative friction surface of the rotary movement, x is the index indicating the stroke (2 for 18 mm stroke; 3 for 39 mm stroke) according to Figure D.2.3 and Table D.2.3; B1 and h1 according to Figure D.2.3 and Table D.2.3. The calculated FS is shown in Table D.2.4. The groove of the piston was neglected for this calculation.

Table D.2.4: Cumulative friction surface FS and generated friction surface A per stroke

Pump – dosage volume	FS (mm$^2 \cdot$ mm)	A (mm^2)
RPP 1 – DV 180	60937.39	339.29
RPP 1 – DV 300	126773.73	735.13
RPP 2 – DV 180	184948.38	735.13
RPP 2 – DV 300	337019.27	1592.79
RPP 3 – DV 180	365948.78	1130.97
RPP 3 – DV 300	614404.74	2450.44
RPP 4 – DV 180	674662.55	1696.46
RPP 4 – DV 300	1062705.22	3675.66

D.2.2 Peristaltic Pump

The peristaltic pump employed for the shear experiment was a Watson-Marlow Bredel type 323U/D (WMP) consisting of:

- 1 drive unit 323U
- 1 pumphead 313D (3 roller)

The pump has a speed range of minimal 3 up to maximal 400 rpm. A medium speed of 200 rpm was applied and the pump was used in MemoDose-mode for a controlled dispensing to assure a precise dosing throughout the test runs. The pump has a dosing range of 1 ml up to 50 ml. For the present work a dosing volume of 4.36 ml has been used. The pumphead was loaded with a platinum cured silicone tubing (Ø 3.2 mm; wall 1.6 mm) which resulted in a flow rate of approximately 200 ml/min considering above mentioned operational speed.

D.2.3 Test conditions

Each experiment was performed three times with the same parameters. Three types of shear experiments with their corresponding test conditions can be differentiated: (overview of the performed shear tests see chapter G.2)

I. Test conditions for shear experiment with:

a) a following PCS analysis (rituximab solution)

The shear tests were performed with RPP size 1-4 and with the WMP. Variable parameters for the test runs have been applied:

- Total volume in the system: is shown in Table D.2.5

Table D.2.5: Volumes in the systems used for different pumps

Pump	Total volume
RPP 1	20.0 ml
RPP 2	23.0 ml
RPP 3	20.0 ml / 30.0 ml
RPP 4	35.0 ml
WMP	23.0 ml

- dosing volumes: for RPPs the dosage was 180 or 300 (see Table C.2.2 for corresponding volumes in ml); for WMP the DV= 4.3 ml
- Pumps used: RPP 1-4, WMP
- applied pumping speeds: for RPPs see Table D.2.6.

Table D.2.6: Applied pumping speeds for RPPs

Indication on turn knob	0.5	2	3	5.5	8	9.25
corresponding speed (sec/stroke)	10	5.7	4.3	2.7	2.2	1.8

for WMP: 200 rpm corresponding to 200 ml/min

- Positions of the filling needle:

(1) above the liquid level:

(2) below the liquid level:

- Sampling was performed as follows:

RPP 1: at 0, 2, 4, 6 cycles

RPP 2: at 0, 6, 10, 20 cycles

RPP 3: at 0, 16, 28, 38 cycles

RPP 4: at 0, 16, 27, 38 cycles

WMP: at 0, 24, 48 cycles

Analytics of the samples taken were performed on the same day.

b) a following enzyme assay analysis (β-galactosidase solution)

- Total volume in the system: 20.0 ml
- dosing volume: 300
- Pump used: RPP 1
- applied pumping speed: 9.00
- position of the filling needle: above the liquid level
- Sampling was performed as follows: after 90 and 180 strokes

Samples were analyzed by enzyme assay on the same day immediately after termination of the shear tests.

II. **Test conditions for shear experiment for the evaluation of excipients**

These test conditions were chosen on the basis of the results obtained from the test runs under test conditions I.

- Total volume in the system: 20.0 ml
- dosing volume: 180
- Pump used: RPP 1
- applied pumping speed: 9.25
- position of the filling needle: above the liquid level
- Sampling was performed as follows: at 0, 2, 4 cycles

Samples were analyzed by PCS on the same day immediately after termination of the shear tests.

III. Test conditions for long-term shear experiment over 3 hours

Samples drawn during the Long-term shear test were analyzed by SEC-HPLC to quantify the loss of protein monomers.

- Total volume in the system: is shown in Table D.2.7.

Table D.2.7: Volumes in the systems used for different pumps

Pump	Total volume
RPP 1	23.0 ml
RPP 2	23.0 ml
RPP 3	30.0 ml

- dosing volume: 180
- Pump used: RPP 1 - 4
- applied pumping speed: 9.0
- position of the filling needle: above the liquid level
- Sampling after 0, 60, 120 and 180 min

D.3 Analytical Methods

D.3.1   Enzyme assay

Principle:

The enzymatic activity of β-galactosidase was determined to detect an eventual activity loss after shearing the protein solution. The enzyme assay was performed according to the method of extract chemie, modified by Amano (Stellmach, 1988). o-nitrophenyl-β-D-galactopyranosid abbreviated ONPG is used as a synthetic substrate. β-galactosidase splits ONPG into o-nitrophenol (ONP) and galactose. ONP, colourless in acidic medium, but yellow coloured in alkaline medium can be quantified spectrophotometrically at a wavelength of 420 nm and is a measure for the enzyme activity.

Procedure:

The samples taken were diluted 1:10 by diluting 30 µl sample solution to 300 µl with phosphate buffer solution (17.8 mg/ml disodium hydrogenphosphate (Merck AG, Darmstadt, Germany), 12.4 mg/ml citric acid (Hänseler AG, Herisau, Switzerland); pH 4.5) to obtain a concentration of approximately 0.01 mg/ml β-galactosidase. Substrate solution consisting of 0.172 mg/ml ONPG (Fluka Chemie GmbH, Buchs, Switzerland) in phosphate buffer solution was tempered in a water bath (WB7, Memmert GmbH + Co KG, Schwabach, Germany) at 30°C. 2100 µl substrate solution was added to the 300 µl diluted sample solution in a glass test tube (VWR, Switzerland). Then, the mixture was incubated at 30°C for exactly 10 min. in the water bath. After stopping the reaction by adding 600 µl sodium carbonate solution containing 106 mg/ml Na_2CO_3 (Riedel-de Häen, Seelze, Germany) the absorbance was measured at 420 nm with a spectrophotometer (UV mc^2, Safas, Monaco) in a 10.00-mm-precision-cell type 100-QS (Hellma, Müllheim, Germany) against the blank solution. A blank was prepared in the same way but taking 300 µl phosphate buffer solution instead of diluted sample solution. All weighing was done with an analytical balance (CP3245, Sartorius, Dietikon, Schweiz). Pipetting was done with 2 micropipettes Biohit type m200, 20-200 µl and type m1000, 100-1000 µl (Biohit, Germany). The enzyme activity Ac (units/mg) was calculated according to Equation D.3.1.

$$Ac = \frac{A_{420} \cdot 3}{4.45 \cdot 10 \cdot m}$$ **Equation D.3.1**

where A_{420} is the absorbance at 420 nm, 3 is the total volume of the reaction mixture in ml, 4.45 is the absorbance of 1 µmol ONP per ml at 420 nm, 10 is the reaction time in min and m is the weight of enzyme in mg per 0.1 ml diluted enzyme solution.

One β-galactosidase unit is defined as the quantity of enzyme that sets free 1 µmol ONP per min under above mentioned experimental conditions.

D.3.2　　Selection of analytical methods for rituximab

As no methods for the determinations of rituximab and the detection of eventual changes of the properties of rituximab after being subjected to shear stress in the

shear experiment were available, different analytical methods were evaluated for their suitability in a first step. A selection of the methods was performed. The selected methods were then developed and optimized further to correspond to the needs of this work.

UV-Spectrophotometry:

The original solution as delivered and the sheared solution (30 min.) were analysed spectrophotometrically. A UV-spectrophotometric scan with a DU530 Beckman spectrophotometer (Beckman Coulter, USA) was performed. A maximum absorption of the original and the sheared solution, both diluted 1:20 with distilled water, was detected at 280 nm. No bathochromic or hypsochromic shift of the maximum was seen due to the presence of aggregated protein. Therefore UV-spectrophotometry was not a suitable method to evaluate differently sheared solutions. However, it was confirmed that UV detection at 280 nm could possibly be used in combination with a separation method like SEC-HPLC for quantification.

SEC-HPLC:

The original and a sheared rituximab solution were evaluated by size SEC-HPLC. The rituximab monomer peak was detected for both solutions. The chromatograms allowed a quantification of the rituximab monomer with the peak area. SEC-HPLC was found to be the method of choice for the quantification of rituximab monomer loss.

TEM:

Transmission electron microscopy is an electron microscopic imaging method. The original and the sheared solution were analysed. The original rituximab solution showed with an 11000x magnification a homogenous solution where the single monoclonal antibodies could not be identified. Few undefined particles which could represent oil drops or dust particles could as well be detected. In the sheared solution unstructured formations of different shape and size could be detected. These agglomerations were formed due to the application of shear stress and represent protein aggregates.

TEM was found to be a useful method for the characterization of rituximab original solution. Furthermore it could be used for the qualitative evaluation of the sheared solution. However, the method was not found to be suitable for the evaluation of differently sheared solutions, as a quantitative detection of agglomerations was not feasible.

PCS:

The mean hydrodynamic diameter and polydispersity index were determined by PCS to characterize the original and the sheared solution. The original solution was sheared by pumping with RPP 3 at a minimal speed of 0.5. The total volume in the system in this pre-run was 43 ml. 100 piston strokes were applied; the dosage volume was 300. The results are listed in Table D.3.1.

Table D.3.1: PCS results: pre-run

Solution	Z average (nm)	Polydispersity index
original solution	12.0±0.1	0.091±0.031
sheared solution (100 strokes)	14.0±1.2	0.142±0.079
blank solution	not detectable	not detectable

The blank solution, which had exactly the same composition as the original rituximab solution without rituximab did not deliver a detectable signal during PCS analysis. No detectable particles were present in the blank solution. This confirmed that the mean hydrodynamic diameter and polydispersity index measured in the original solution refer to rituximab protein particles. The hydrodynamic diameter of rituximab in this solution was determined to be 12.0 nm. The increase of the mean hydrodynamic diameter in the sheared solution showed that larger particles had been generated during shearing. The increased polydispersity index indicated that the size distribution in the sheared solution had broadened. However, it was still a narrow distribution.

Rituximab was identified with this pre-run as shear-sensitive protein suitable for the following work. Furthermore, PCS was found to be a potential analytical method to detect even slight changes in the composition of sheared solutions.

D.3.3 Transmission Electron Microscopy

Principle:

Transmission electron microscopy (TEM) is an imaging method where photographs of the sample are obtained indirectly. It was used to identify protein agglomerations.

Procedure:

Samples have been used directly or centrifuged at 14000 g. The sample solution was spread on a grid, which had a diameter of 3 mm and was coated with a 50 nm synthetic film. Particles were stained with uranylacetat before taking the TEM micrograph.

D.3.4 Photon Correlation Spectroscopy

Principle:

PCS was used to detect aggregated protein in the sample solutions. The method delivers with the measured changes of intensities of scattered light a size distribution of the particles in the solution as well as the mean hydrodynamic diameter and the polydispersity index, which is a measure for the width of the distribution, see theoretical part C.1.8.2. The method is very sensitive to large particles in the solution, which made it suitable to detect protein aggregates at very low concentrations.

Instrumentation:

The instrument used for the measurements was a Zetasizer 1000 HS_A (Malvern Instruments Ltd., Malvern, United Kingdom) equipped with an autocorrelator 8 type 7032CN. Data analysis was done with Zetasizer software Version 1.61 Rev. 1. Measurements were performed at a scattering angle of 90° at 633 nm. As light source a Helium-Neon-Laser is integrated in the Zetasizer 1000 HS_A.

Optimization:

In optimization runs the method was improved and adapted for the measurement of the original and sheared rituximab solution. To pass the quality check which is integrated into the system the following measure parameters were established:

The initial count rate was too low as small particle of a size of approximately 12 nm had to be detected; to achieve a count rate between 100 and 200 K counts, the detection aperture 200 was used. The duration of a measurement was set to 300 sec. Automatic selection of the attenuator and size range was used. The correlator was configured in parallel mode. Measuring temperature was set to 25 °C. The analysis selected for result processing was contin. Further parameters are listed in Table D.3.2.

Table D.3.2: Parameters set for PCS measurements

Refractive index dispersant	1.330	Real refractive index	1.590
Viscosity (cP)	0.890	Core real refractive index	1.600
Analysis: Dilation	1.20	Delay between measurements	10 sec
Analysis: Weighting	quadric	Point selection	auto

Procedure:

The samples were measured in a square quartz cell of uniform wall thickness, which was cleaned between every sample with tap water followed by 3 rinses with freshly distilled water. The distilled water was checked for the absence of particles by a PCS measurement before use. One final rinse with the sample solution was performed just before introducing the undiluted sample solution. The outside of the cell was dried using a paper tissue. Every sample was measured in triplicate.

Data analysis and interpretation:

Characterization of monodisperse samples was done by analysis of PI and z average resulting form the cumulants method. The mean of the 3 measurements for one sample was taken. The following indications were respected for the interpretation of PI results:

0.03 – 0.06: monodisperse distribution

0.10 – 0.20: narrow distribution

0.25 – 0.50: broad distribution

 > 0.50: not evaluable as it concerns a broad distribution of undefined shape.

Polydisperse samples, for which the interpretation of the data is considerably more difficult, were characterized by PI and z average from the cumulants analysis. Although, it has to be noted that if the PI is greater than 0.25, the z average size

should be used in a relative sense. Additionally, the result from the contin analysis was taken into consideration in terms of mean and width at half peak height and particularly the number of detected peaks.

D.3.5   Size-Exclusion HPLC

Principle:

SEC-HPLC was employed to quantify the loss of rituximab monomers due to the exposed shear during the test runs over 3 hours. The sample is separated by passing the column according to the molecular weight of the proteins in solution. Precipitates were centrifuged to eliminate protein particles with very high molecular weight. The area of the rituximab peak in the original solution was set to 100% monomers. The loss of monomers in % was calculated using the area of the rituximab peak.

Procedure:

Rituximab samples were left at 5-8°C for 3-5 days so that the precipitate could settle and then centrifuged in a centrifuge type 5415C (Eppendorf, Germany) for 30 min at 14000 min^{-1}. The supernatant was transferred into HPLC glass vials (Agilent, USA) and crimped. 20 µl was injected into a Tosoh TSK-GEL G3000SW XL column; size 7.8 mm i.d. x 30.0 cm length; particle size 5 µm. The mobile phase consisted of 15.6 mg/ml NaH_2PO_4 x 2 H_2O (Fluka Chemie GmbH, Buchs, Switzerland), 14.2 mg/ml Na_2SO_4 (Merck, Darmstadt, Germany) and 0.502 mg/ml NaN_3 (Fluka Chemie GmbH, Buchs, Switzerland) in double distilled water, pH adjusted to 6.7, pumped at a flow rate of 1 ml/min. The instrument used was a Hewlett Packard series 1050 pump (Hewlett Packard, Waldbronn, Germany) and a Hewlett Packard series 1050 auto sampler (Hewlett Packard, Waldbronn, Germany). The detection was performed at a wavelength of 280 nm using a Hewlett Packard series 1050 UV-detector model 79835A (Hewlett Packard, Waldbronn, Germany).

D.3.6   Visual Inspection

Principle:

A visual inspection of the sheared solution at the end of each shear experiment was performed. The aim of this examination was to detect precipitates which formed under the applied shear stress. The turbidity of the solution increases with increasing formation of protein aggregates.

The storage of the sheared solution at 5-8°C for several days served to allow eventual precipitation to settle. With this procedure even a very light precipitation could be detected by eye. If precipitates were present, they moved upwards forming a white cloud when shaking the vial as described below.

Procedure:

The remaining test solution in the test system was emptied at the end of a shear experiment into a 50 ml glass vial, hydrolytic glass type I and closed with a grey stopper and parafilm. Glass vials and stoppers were the reused primary packaging from the original rituximab solution. The vials and stoppers were washed and finally rinsed with distilled water.

The turbidity of the test solution at the end of the shear experiment was visually inspected by comparing the sheared solution with a vial containing the original rituximab solution in front of a dark background. A second visual inspection was performed after storing the vial with the sheared solution at refrigerated temperature for 5-7 days. The vial was taken out and left at room temperature till the solution had adapted to room temperature to avoid formation of condensate on the external of the vial during the visual inspection. The vial was then moved with one quick horizontal circular shake. It was verified if an upward moving cloud was detected. A classification of the intensity and size of this cloud was done into 3 categories according to Table D.3.3:

Table D.3.3: Type and intensity of precipitation for visual inspection

Type and intensity of cloud	Description
fine cloud	a very fine upward moving line is observed
medium cloud	a small to medium sized upward moving cloud can clearly be seen in the middle of the vial
large cloud	white precipitation can be clearly seen on the bottom of the vial before shaking. A large upward moving cloud can be detected when shaking the vial

E RESULTS AND DISCUSSION

E.1   Influence of shear on a β-galactosidase solution

The suitability of lactase (= β-galactosidase) in solution for use as a model protein to examine the impact of shear caused by dosing systems was evaluated. Therefore the lactase solution was circulated in the test system using the rotary piston pump size 1, see section C.2. 20.0 ml of solution was introduced into the test system and pumped by applying in total 180 strokes with a dosing volume of 1.12 ml per stroke at maximum pumping speed. This corresponds to 10 cycles to which the solution was submitted. No significant loss of activity was observed during the shear experiment. Figure E.1.1 shows the results obtained in a plot of enzyme activity over the number of strokes.
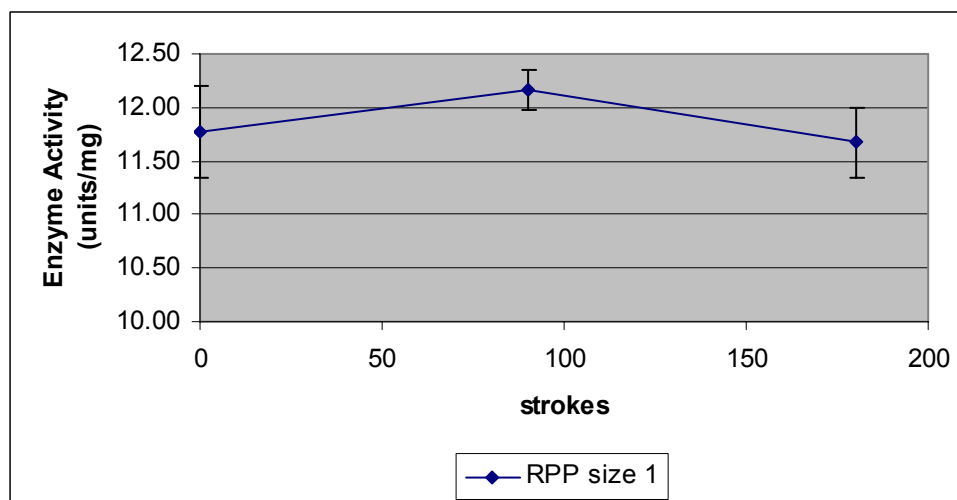
Figure E.1.1: Influence of circulation of a lactase solution on the enzyme activity

No physical degradation, which could potentially have been generated by the shear stress caused by RPP 1, was observed by measuring the enzyme activity.

Conclusion:

As no impact of the exerted shear on lactase was detected, this enzyme was not suitable for performing the shear experiments for the evaluation of the impact of shear caused by different dosing equipment and dosing parameters. The absence of loss of activity can be explained with the fact that either lactase is not sensitive to

shear as caused by the test system used for the present work or by a not sufficient sensitivity of the analytical method.

E.2 Characterization of rituximab solution

The original rituximab solution was analysed. The results of the characterization are presented in this chapter.

Table E.2.1: Results of analysis of rituximab original solution

Parameter	Result
UV maximum	280 nm
pH	6.52
osmolality	300 mOsm
aspect	clear, colourless solution; no precipitation
z average (PCS)	11.9 ± 0.0 nm
polydispersity index (PCS)	0.066 ± 0.008
width at half peak height (PCS)	7.4 ± 1.7 nm
mean (PCS)	12.6 ± 0.1 nm
retention time (SEC-HPLC)	8.144 ± 0.001 min
peak area (SEC-HPLC)	19277.5 ± 4.9 mAU*s
% rituximab monomers (SEC-HPLC)	97.45 ± 0.01 %

The polydispersity index result from the PCS measurements showed that the original rituximab solution has a strictly monodisperse distribution with an average hydrodynamic diameter of the protein monomers of 11.9 nm. The contin analysis of the distribution confirmed these results with a width of the distribution at half peak height of 7.4 nm. The intensity mean of 12.6 nm, which represents the distribution mean, was found to be a little higher than from the cumulants analysis. A percentage of 97.45 rituximab monomers from the SEC-HPLC revealed that approximately 2.5 % protein of higher or lower molecular size was present; 0.7 % larger particles and 1.8 % smaller particles.

Transmission electron microscopy pictures were in agreement to the SEC-HPLC result concerning the presence of larger molecules, whereas smaller molecules were too small to be seen in the pictures (Figure E.2.1and Figure E.2.2).
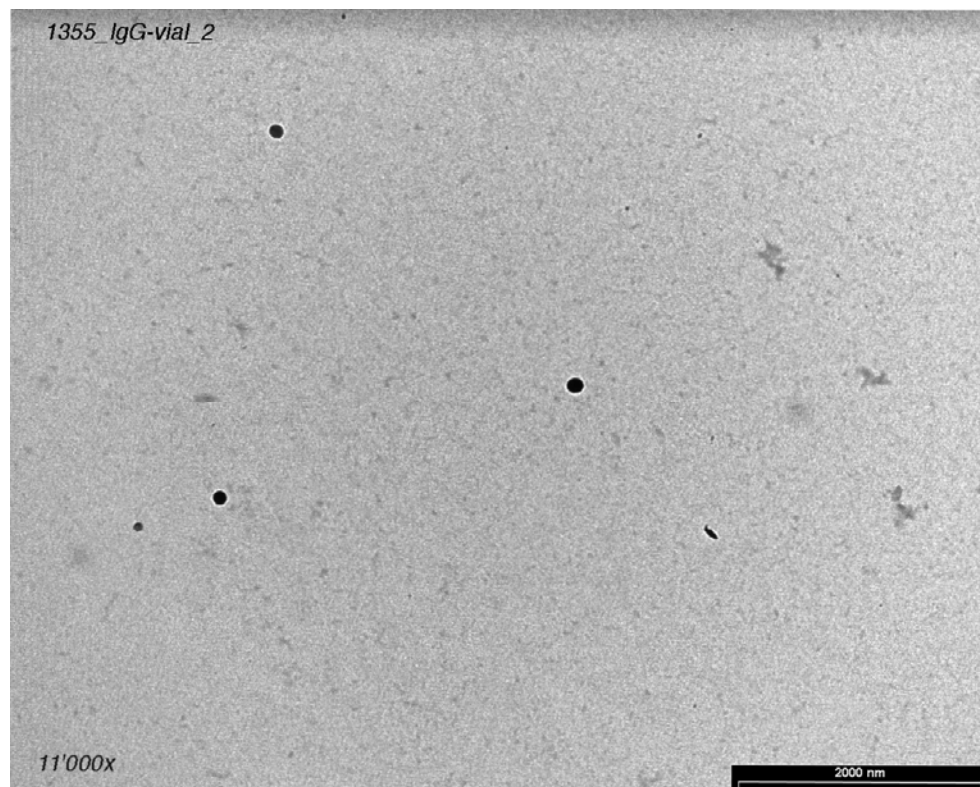
Figure E.2.1: TEM picture without centrifugation of original rituximab solution

The TEM pictures show the presence of larger particles in the rituximab solution. For the picture in Figure E.2.2 the particles were concentrated by previous centrifugation of the solution. The large unstructured agglomerations probably represent protein aggregates. The black round spots in Figure E.2.1 have eventually been introduced accidentally during preparation of the samples and are not present in the original solution.
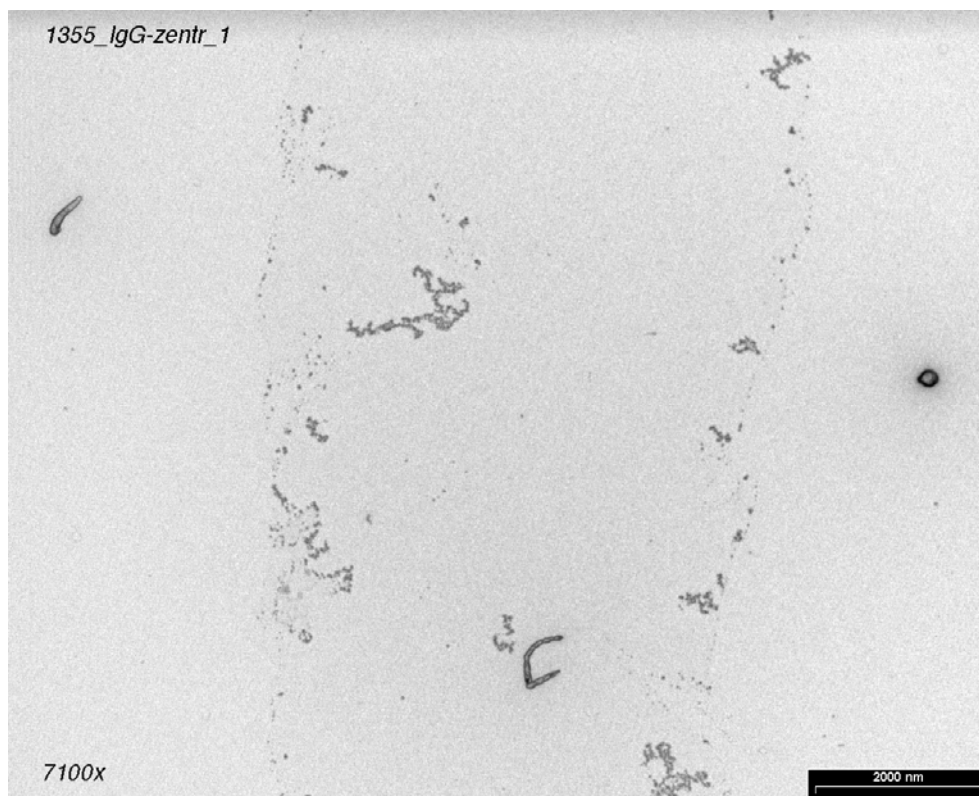
Figure E.2.2: TEM picture with previous centrifugation of original rituximab solution

E.3 Evaluation of quality of PCS data

In this chapter considerations in respect of the quality of data obtained from PCS measurements are made. The quality of the data is essential for the estimation how well the analysis algorithms will perform. For the evaluation of the data quality the stability of the count rate from repeat measurements, the repeatability of the z average diameter, the result of the quality factor and the precision of the method was observed.

E.3.1 Quality factor

For every single measurement the system delivers a quality factor. The quality factor was considered for evaluating PCS data. If results are within predetermined limits the quality factor obtained is a PASS. If one or more of the limits are exceeded a CHECK message for the parameter which failed is displayed. The limits are listed in Table E.3.1.

Table E.3.1: Result quality check criteria

Check criteria	Check error message
Count rate < 10K or > 500K	check count rate
Merit < 10% or > 99%	check merit
Polydispersity > 0.7	check poly index
Fit error > 0.005	Check fit
In Range < 80%	check baseline
Z average diameter < 1 or > 5000nm	check z-average mean range
Polydispersity < 0.1 and Fit error >0.01	check fit
duration of data used in analysis < 101s	check duration

In preliminary test runs the PCS measure parameters were fixed as described in chapter D.3.4 and the experimental conditions e.g. the number of cycles with the respective pump were adapted with the aim that the taken samples could fulfil above mentioned quality criteria. Every measurement was checked for the quality factor. It was found that for nearly all measurements performed the quality factor was a PASS. In a few cases, the samples which were taken at the end of the shear experiment (sample P3) with RPP 2 and 1, a CHECK parameter was indicated. In these cases the result was examined for the failed quality criterion. The reason for the failure was the presence of large aggregated protein particles which on the other hand was the phenomenon to be measured. Therefore even these measurements were accepted.

The evaluation of the resulting quality factor indicates that the quality of the data obtained from measuring unstressed or slightly stressed rituximab solutions is good. Increasing shear gives rise to the formation of aggregates and to a deterioration of the quality of PCS data.

E.3.2 Stability of count rate

The count rate of 3 – 5 repeat measurements should be within a few percent of one another (Zetasizer, 2000). This parameter was evaluated for the measurements of the original solution and for the solutions after cycling in the test system with RPP 1 - 4 with DV 180. The last sample (P3) was analysed. The results are in Table E.3.2. It was seen that the relative standard deviation of the count rate for 3 repeat measurements is in the range of 1 - 2% for the original solution and for the solutions

circulated with RPP 4 and 3. It was increasing when circulated with RPP 2 and 1. As well the count rate itself increased, as aggregation of the protein molecules took place. For RPP 1, which was found to stress the protein most, the relative standard deviation of the count rate was approximately 5.5%. In respect of the count rate the quality of the PCS data obtained was considered to be excellent for the original solution and less stressed solution and was still good for stressed solutions. With increasing formation of aggregates the data quality was found to decrease, as large particles perturb the measurements.

Table E.3.2: Comparison of count rates and relative standard deviation of PCS measurements

Solution	original solution	DV 180, speed 9.25, sample P3, RPP 4	DV 180, speed 9.25, sample P3, RPP 3	DV 180, speed 9.25, sample P3, RPP 2	DV 180, speed 9.25, sample P3, RPP 1
count rate Mean ± SD$_{rel}$	251.0 (± 1.7%)	282.8 (± 1.2%)	280.5 (± 1.9%)	289.3 (± 2.6%)	196.3 (± 5.6%)
Attenuator:	x1	x1	x1	x1	x2

E.3.3   Precision of the PCS method

The precision of the PCS method is given by the relative standard deviation SD$_{rel}$ in percent:

$$SD_{rel} = \frac{SD}{M} \cdot 100 \qquad\qquad \textbf{Equation E.3.1}$$

where SD is standard deviation and M is mean value.

For the present evaluation 5 determinations of the original solution were performed on the same day and the relative standard deviation was calculated. The same was performed on 2 further days. The relative standard deviation was calculated from the 15 measurement. Furthermore the average mean was calculated from the 5 determinations per day and the relative standard deviation was calculated from the 3 averaged values.

The same procedure was performed for a solution submitted to shear stress with the following conditions. The pump RPP 1 was used with a dosage volume of 300 (1.12 ml) at a pumping speed 2 (5.7 s/stroke). The total volume was cycled 6 times under these experimental conditions in the test system described under D.2.1.

Precision of the cumulants analysis

The results obtained from the PCS analysis using the cumulants analysis are presented in Table E.3.3 and Table E.3.4.

Table E.3.3: Precision Cumulants Analysis - z average

Solution	M ± SD (nm)	SD$_{rel}$ (%)	M ± SD (nm)	SD$_{rel}$ (%)	M ± SD (nm)	SD$_{rel}$ (%)
	precision on one day (n=5)		precision on 3 days (n=15)		precision on 3 days (n=3) calculated with the mean of 5 measurements per day	
original solution	11.9 ± 0.0	0.38	11.9 ± 0.1	0.43	11.9 ± 0.0	0.26
sheared solution	20.6 ± 2.5	12.14	19.7 ± 1.81	9.19	19.8 ± 0.7	3.54

The determination of z average obtained from the cumulants analysis for the original, unsheared solution showed an extremely low relative standard deviation below 0.5%, whereas the relative standard deviation for the sheared solution was considerably higher at approximately 10%. If the experiment was performed 3 times and the 3 mean values of 5 repeat measurements were considered to calculate the precision, a relative standard deviation of approximately 4% was obtained.

Table E.3.4: Precision Cumulants Analysis – Polydispersity index

Solution	M ± SD (nm)	SD$_{rel}$ (%)	M ± SD (nm)	SD$_{rel}$ (%)	M ± SD (nm)	SD$_{rel}$ (%)
Precision	precision on one day (n=5)		precision on 3 days (n=15)		precision on 3 days (n=3) calculated with the mean of 5 measurements per day	
original solution	0.052 ± 0.008	15.89	0.052 ± 0.010	18.15	0.052 ± 0.002	3.24
sheared solution	0.578 ± 0.074	12.80	0.554 ± 0.056	10.09	0.553 ± 0.022	3.93

The precision of the determinations of the polydispersity index was approximately the same for the original and the sheared solution. The relative standard deviation was

between 10-20%. The precision on 3 days calculated with the mean of 5 determinations was found to be in an acceptable range of 4%.

Precision of the contin analysis

The precision for the contin analysis was investigated for the sheared solution. Unlike the original solution, the sheared solution showed a size distribution with different particle sizes. The mean values of the different peaks and the width at half peak height were considered for the present evaluation. Results are displayed in Table E.3.5 for the mean values and in Table E.3.6 for the width values.

Table E.3.5: Precision Contin Analysis – Mean: sheared solution

	Peak 1 (nm)	M ± SD (nm)	Peak 2 (nm)	M ± SD (nm)	Peak 3 (nm)	M ± SD (nm)
M1-Day1	11.5		409.0		--	
M2-Day1	11.5	11.6 ± 0.3	519.0	554.2±138.1	--	
M3-Day1	11.5	(SD_{rel}=2.7%)	593.2	(SD_{rel}=24.9%)	--	n/a
M4-Day1	12.2		479.2		1816.7	
M5-Day1	11.5		770.5		--	
M1-Day2	11.4		574.9		--	
M2-Day2	11.7	11.5±0.2	853.4	770.9±170.5	--	
M3-Day2	11.4	(SD_{rel}=1.3%)	--	(SD_{rel}=22.1%)	--	n/a
M4-Day2	11.5		--		--	
M5-Day2	11.3		884.5		--	
M1-Day3	11.4		--		1594.6	
M2-Day3	11.4	11.5 ± 0.1	--		--	
M3-Day3	11.5	(SD_{rel}=0.7%)	--	n/a	--	n/a
M4-Day3	11.6		669.2		--	
M5-Day3	11.5		--		--	
M±SD (nm) SD_{rel}	11.5±0.2 1.8%	11.5±0.1 0.5%	639.2±167.1 26.1%	662.6±153.2 23.1%	1705.7±157.0 9.2%	n/a

Table E.3.6: Precision Contin Analysis – Width: sheared solution

	Peak 1 (nm)	M ± SD (nm)	Peak 2 (nm)	M ± SD (nm)	Peak 3 (nm)	M ± SD (nm)
M1-Day1	5.0		260.7		--	
M2-Day1	5.0		285.1		--	
M3-Day1	5.4	5.5 ± 0.5 (SD$_{rel}$=9.9%)	253.6	272.0±25.9 (SD$_{rel}$=9.5%)	--	n/a
M4-Day1	6.3		249.4		1106.9	
M5-Day1	5.7		311.2		--	
M1-Day2	5.1		236.8		--	
M2-Day2	5.3		382.8		--	
M3-Day2	5.0	5.1±0.2 (SD$_{rel}$=3.0%)	--	328.8±80.1 (SD$_{rel}$=24.4%)	--	n/a
M4-Day2	5.3		--		--	
M5-Day2	5.0		366.8		--	
M1-Day3	5.0		--		904.8	
M2-Day3	5.1		--		--	
M3-Day3	7.8	5.6 ± 1.2 (SD$_{rel}$=21.4%)	--	n/a	--	n/a
M4-Day3	5.2		377.8		--	
M5-Day3	5.1		--		--	
M±SD (nm) SD$_{rel}$	5.4±0.7 13.8%	5.4±0.3 4.9%	302.7±59.1 19.5%	300.4±40.2 13.2%	1005.9±142.9 14.2%	n/a

The size distribution calculated with the contin algorithm showed that the first peak at 11.5 nm was reliably detected. The relative standard deviation of the mean of 1.8% or 0.5%, depending on the way of calculation, stands for a high precision. The relative standard deviation for the width was found to be a little bit higher at 13.8% or 4.9%. The second and third peak was not detected in every measurement. The second peak was seen in 9 determinations out of 15; the third in 2 out of 15. The mean and width values were calculated from these 9 and 2 available values; the fact that in the other determinations the peaks were not detected was not considered for the calculation. The precision of the contin analysis was therefore relatively low. However, it still gave a good indication if more than one particle size was present in the solution.

It can be concluded that the precision of the PCS data was very high for the original solution and decreased with the presence of large particles, which were created through the applied shear stress. The method of cumulants worked extremely well for monodisperse samples like the original rituximab solution and delivered still very

acceptable results for the sheared solutions in this work. The precision of the contin analysis had to be considered low, but was in the present work in addition to the cumulants analysis a good indicator for the size distribution.

E.3.4   Influence of excipients on PCS data

An evaluation of the influence of added excipients to the original rituximab solution on the PCS measurements was performed. Z average was measured for the original solution and the solutions with added excipients. The obtained values were compared. It was found that the z average values of the solutions containing excipients differed from the original rituximab solution in the range of up to 1 nm. This can be explained with a change in viscosity of the solution when adding excipients. The viscosity introduced into the Zetasizer software for the original rituximab solution was 0.89 cP; this is the theoretical value indicated in the manual for aqueous solutions. Another explanation for the change of the mean hydrodynamic diameter of the protein in solution is the direct influence of the added excipients on the size of the molecule. The hydrodynamic diameter differs from the diameter of the dry particle because of a layer of solvent molecules around charged particles or attached surfactant molecules (Weiner, 1984). Excipients may influence this layer. In the case of very small sizes to be measured, which was true for the present determinations, these layers add to the diameter (Weiner, 1984). Furthermore, excipients that stabilize proteins against aggregation via the preferential exclusion mechanism drive the protein into a more compact conformation. The more compact conformation can lead to a smaller mean hydrodynamic diameter of the molecules.

As for the present work the change of the mean hydrodynamic diameter with the circulation time in the test system was of higher relevance compared to the absolute value, the following procedure was developed to achieve a starting z average of 12.0 nm ± 0.2 nm for all solutions. A viscosity value was empirically established by measuring the solutions and adapting the viscosity values till the measured z average showed 12.0 nm ± 0.2 nm. The acquired viscosity values are shown in Table E.3.7. These viscosity values were introduced into the program when measurements of the respective solutions were performed.

Table E.3.7: Viscosity values used for PCS measurements

solution	Viscosity (cP)
orig. solution	0.89
PEG 0.1% + Treh. 1%	0.92
PEG 0.5% + Treh. 5%	1.04
Treh. 5%	0.95
PEG 0.5 %	0.95
Tween 80 1.3%	0.95

The quality of the obtained PCS data was not influenced by the added excipients.

E.4 Comparison of WMP and RPP

The peristaltic pump and the rotary piston pumps were compared in 2 aspects: filling precision and exerted shear stress on the protein solution.

E.4.1   Filling precision

The precision for different filling weights was calculated using Equation E.3.1. The WMP, RPP 2 and RPP 3 were compared. 5 consecutive dosing operations were performed. Every single dose was immediately weighed on an analytical balance (type AG204 Delta Range, Mettler Toledo Schweiz GmbH, Greifensee). Results are shown in Table G.5.1. It was found that at a filling weight at approximately 5 g, the WMP filling precision was circa 1 %, RPP 3 was circa 0.5 % and RPP 2 showed the best precision of 0.06 %. As expected the precision increased with increasing filling weight, e.g. 0.25 % for a fill weight of 11g with WMP. RPP 2 still showed a very high precision of 0.2 % for a lower fill weight around 2 g.

E.4.2   Shear stress

The results from the shear experiments with the WMP and the RPP 3 were compared and are illustrated in the graphs in Figure E.4.1 and Figure E.4.2. The test conditions corresponded to the description in D.2.3 I. For RPP 3 the dosage volume was 180, corresponding to 5.55 ml. The dosage volume used for the WMP of 4.3 ml was approximately in the same range. The speed applied in the shear experiment for

RPP 3 corresponded to 9.25 (=1.8 sec/stroke) resulting in a flow rate of approximately 185 ml/ min. The flow rate of the WMP was 200 ml/min.
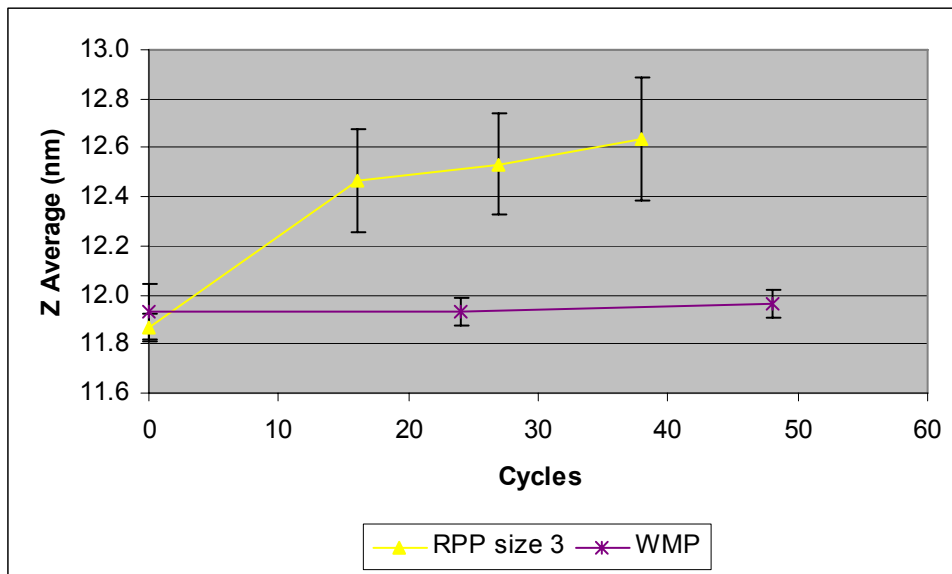
Figure E.4.1: Developing of z average with increasing circulation in the test system

Figure E.4.1 shows the effect of shear stress caused by the two different dosing systems on the developing of the mean hydrodynamic diameter (z average) of rituximab. In the shear experiment with RPP 3 the mean hydrodynamic diameter increased with increasing circulation of the protein solution in the test system. This was not the case when the WMP was used as dosing system. No effect on the mean hydrodynamic diameter was seen during cycling of the test solution with the WMP.
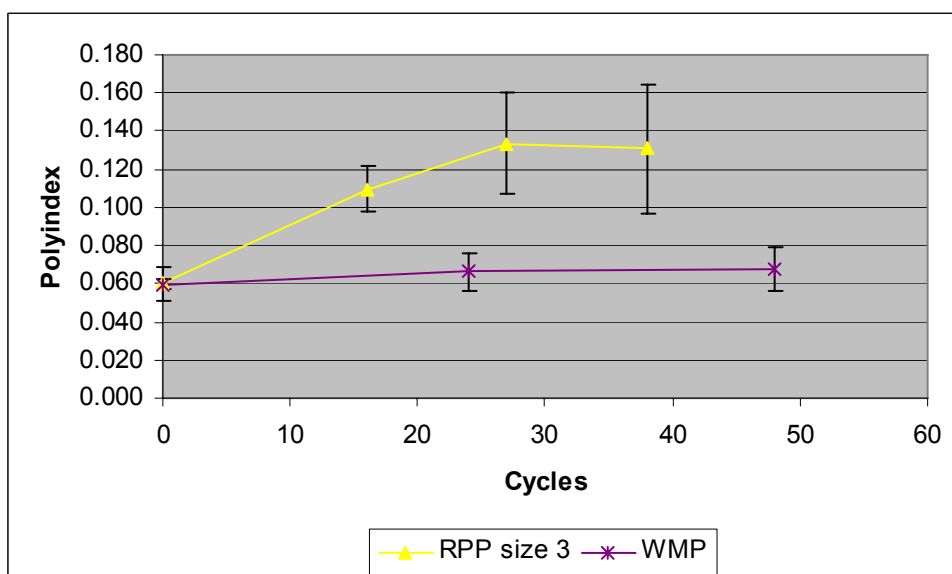
Figure E.4.2: Developing of PI with increasing circulation in the test system

Furthermore, it was observed that as well the polydispersity index increased when circulating the rituximab solution with RPP 3. It increased only marginally and not significantly when cycling with the WMP as shown in Figure E.4.2. Under the shear influence of the RPP 3 a development from a very narrow size distribution with a polydispersity index below 0.1 towards a broader size distribution could be observed.

However, the evaluation of the visual aspect of the circulated solutions did not show any difference between solutions circulated with RPP 3 and WMP. All solutions remained clear without any visible precipitation throughout the shear experiments. Even the visual inspection after storing the solutions at 5 - 8°C for 5 - 7 days did not show any precipitation or cloud.

The contin analysis method showed a slight increase of the width from 6.3 nm to 8.8 nm at the end of the shear experiment with RPP 3. The size distribution always consisted of one peak.

Conclusion:

The shear stress which resulted from circulating the protein solution with the use of RPP 3 generated damage to the protein. This damage resulted in the formation of aggregated protein and could be seen in an increasing z average and a broadening of the size distribution indicated by a rising value for the polydispersity index. In comparison the WMP did not cause shear stress on the protein in solution. No damage of the protein in solution was indicated by the PCS results. However, the extent of shear and damage caused by RPP 3 was very limited. The polydispersity index after 10 cycles with RPP 3 was still below 0.1 which accounts for a monodisperse distribution. The contin analysis of the PCS measurements, which is good in finding contaminants like larger particles, did not show the appearance of a second peak. The width at half peak height gained only by 2.5 nm after 38 cycles.

It is known that the selection of the appropriate processing equipment is a critical point in protein formulation (Wang et al., 2007). Factors which can influence the stability are contact surfaces (Tzannis et al., 1996) as well as shear stress exerted by the equipment. The reason for the slight increase in z average and PI due to circulation with RPP 3 in comparison to the WMP is suggested to lie in the different

geometry of the 2 pumps and the different flow of the solution. In the WMP the solution is driven by a peristaltic movement and the hydrodynamic shear stress can be calculated according to Equation C.4.3. In a cylindrical tube the shear stress for a laminar flow is 0 in the centre and maximal towards the inner surface. Evidently this maximum shear stress did not cause aggregation of the model protein. Due to the fact that the tubing had the same diameter, approximately the same length and the flow rate was in a comparable range for the 2 different pumps used, the hydrodynamic shear stress which occurred in the cylindrical tube was in a comparable range as well. For RPP 3 additional shear stress which might occur in the pump, predominantly originating from the rotary and vertical movement of the piston has to be considered. It is suggested that the shear stress which occurred in the gap between the cylinder and piston during the movements of the piston led to protein damage. This is in agreement with findings in literature. Maa and Hsu (1996) observed that during shear experiments using a concentric-cylinder shear device consisting of two concentric cylinders, where the inner cylinder can be rotated, a rhGH solution was slightly opalescent and the amount of soluble aggregates increased 2.4 ± 0.3% after 16 hours of shearing. Tirrell and Middleman (1975) studied the effect of shear in a coaxial cylinder viscometer using a urease solution. The rate of urea hydrolysis showed a continuous decrease as a function of shear time at a given shear rate.

E.5 Comparison of different sizes of RPPs

Shear experiments with RPP 1, 2, 3 and 4 were performed according to the conditions described in chapter D.2.3 I. The parameters used in the shear experiments for the comparison of the different rotary piston pumps were a DV of 180 and a maximal pumping speed of 9.25. The aim of the comparison was to evaluate if the shear stress on the test solution is dependent on the pump size of the rotary piston pump.

Figure E.5.1 shows the influence of circulating the solution with RPP 1-4 on the hydrodynamic mean diameter of the protein monomers. As a reference of a pump which was found not to cause any shear stress on the solution, the WMP was added to the graphs in Figure E.5.1 and Figure E.5.2.

Whereas RPP 3 and RPP 4 showed a minor influence on z average, the smallest pump RPP 1 could clearly be identified to very quickly induce the generation of larger particles, i.e. protein aggregates. A sharp increase of z average from originally 12.0 nm to 15.0 nm was observed after circulating the solution twice. However, it has to be taken into account that if the polydispersity index is over 0.25, the z average size should only be used in a relative sense (Zetasizer 1000HS/3000HS, 2000). The solution cycled 38 times with RPP 3 and 4 showed in comparison a slow rise of z average from 11.9 nm up to only 12.6 nm and 12.9 nm respectively. The influence of circulating the solution with RPP 2 on hydrodynamic mean diameter was in-between. Z average showed a moderate rise in respect to the number of cycles performed.
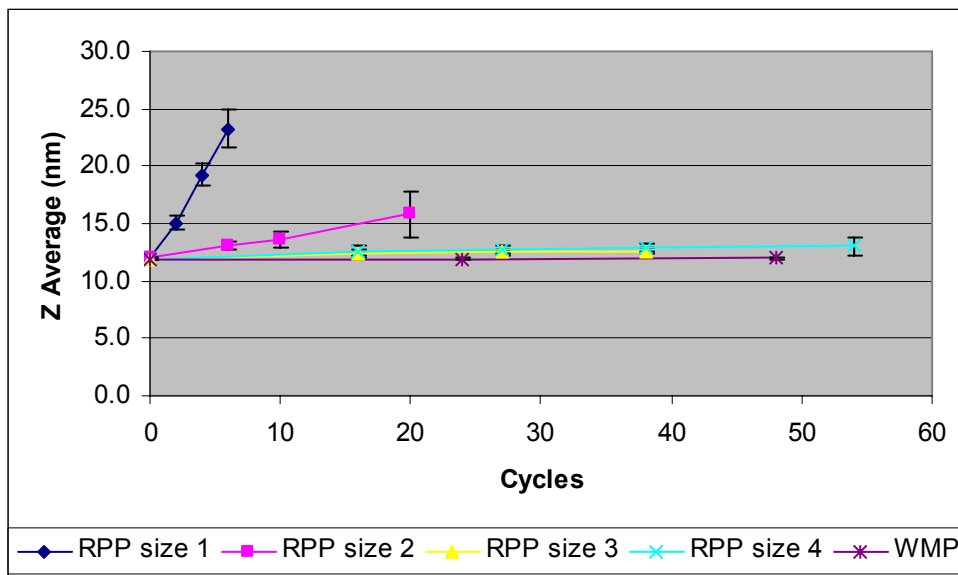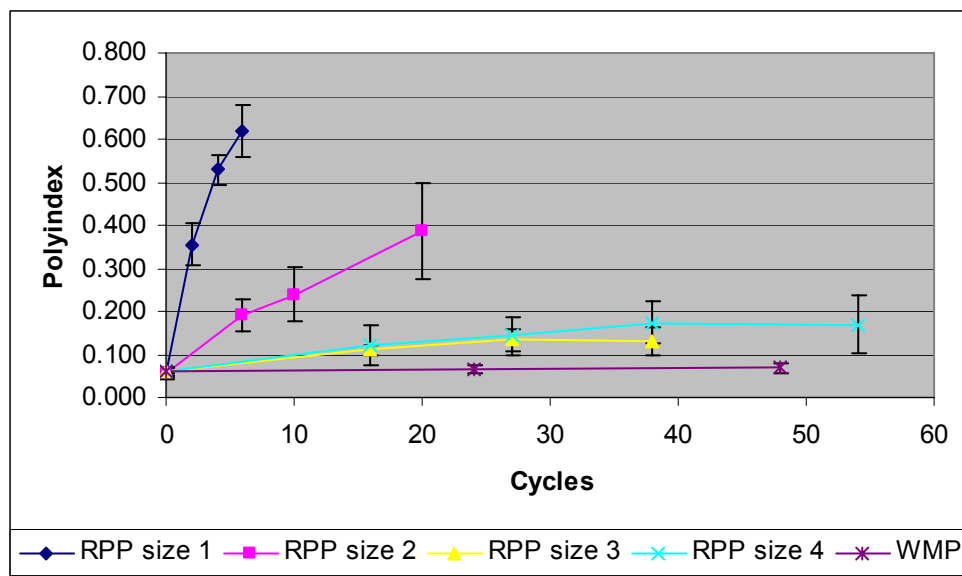

Figure E.5.1: Developing of z average with increasing circulation in the test system

Figure E.5.2: Developing of PI with increasing circulation in the test system

The polydispersity index plotted over the number of cycles shown in Figure E.5.2 indicated as well that RPP 1 affected the protein solution most in comparison to the other sizes of pumps. After 2 cycles with RPP 1 the polydispersity index calculated with the cumulants analysis did not show a monodisperse size distribution any more, which was defined for this work to be below 0.1. The polydispersity index exceeded 0.3 already after 2 cycles. The polydispersity index during pumping with RPP 3 and 4 showed that the distribution of the particle size in the sheared solution gradually became broader during circulating but passed the limit for monomodal distribution of 0.1 only after approximately 10 cycles.

The size distribution calculated by the contin analysis showed during the circulation with RPP 1 a second peak at 200 nm or above. It was detected after 4 cycles. In one case the second peak appeared after 2 cycles already. The intensity of the second peak increased with cycling the solution in the test system. Representative examples for the size distributions in the original solution and after 2, 4 and 6 cycles with RPP 1 are shown in Figure G.3.1 to Figure G.3.4 in the annex. The contin analysis of shear experiments with RPP 3 and 4 did not show a second peak in the size distribution but an increase of the width at half peak height of 2.5 nm and 1.6 nm respectively as shown in Table E.5.1. RPP 2 occasionally showed the appearance of a second peak after 20 cycles; out of 9 measurements obtained from performing the shear experiment 3 times with triplicate determination by PCS per sample, a second peak was detected in 5 measurements.

Table E.5.1: Width from contin analysis

Pump	width at half peak height initial (0 cycles) mean (± SD)	width at half peak height end (38 cycles) mean (± SD)
RPP 3	6.3 nm (± 0.8 nm)	8.8 nm (± 1.0 nm)
RPP 4	5.9 nm (± 0.3 nm)	7.5 nm (± 2.0 nm)

Conclusion:

After 2 -4 cycles with RPP1 and after approximately 20 cycles with RPP 2 the size distributions in the sheared solution represented a multimodal distribution. Large particles had been generated due to the stress caused by the relevant pump and corresponded to protein aggregates. The more the solution was pumped, the more these aggregates dominated the light scattering. When pumping with RPP 3 and 4 the size distribution was found to stay monomodal; just a slight broadening of the distribution was observed.

In terms of shear stress caused by the different pumps, it could be concluded that RPP 1 caused high shear stress which very quickly led to physical degradation of the protein monomers. However, RPP 3 and 4 only marginally affected the protein solution and therefore it could be concluded that the stress caused by these 2 pumps was very limited. Pumping with RPP 2 was seen to create moderate stress. A clear dependency of the induced stress on the pump size could be established: the smaller the pump, the higher the shear stress on the solution. However, for pumps equal to the size of RPP 3 or larger a significant difference was not seen.

E.6 Influence of the friction surface

In this chapter the relationship between the friction surface and the exerted degree of stress on the test solution is examined. In the above chapters it was shown that the degree of stress generated by RPPs was different for the different sizes of pumps. The relation of the friction surface and the dosed volume is one factor which changed with the dimension of a pump. Furthermore, it was assumed that the stress on the solution was generated in the gap between the cylinder and the piston. The size of this gap is the clearance listed in Table D.2.2.

For this evaluation two different approaches were taken into account. First, the friction surface was set equal to the generated friction surface A during one stroke. A has been calculated according to Equation D.2.1 and results are listed in Table D.2.4 (chapter D.2.1). The calculation of the generated friction surface considered the new contact area between the piston and the cylinder at the distance of the clearance, which was generated during one stroke. The generated friction surface has then been divided by the dosage in ml to obtain a comparable value for the different sizes of RPPs. The results are shown in Table E.6.1.

The second approach was to take into account the cumulated friction surface FS as calculated in chapter D.2.1. Results are listed in Table D.2.4. The cumulative friction surface contained the vertical and the rotary movement of the piston. It corresponded to the areas under the curve when plotting the friction surface B over the displacement for the vertical and the rotary movement. The assumption was made that this sum of accumulated friction surface in the course of one stroke is proportional to the amount of stress exerted on the solution. The cumulated friction surface has then been divided by the dosage in ml to obtain a comparable value for the different sizes of RPPs. The results are shown in Table E.6.1.

Table E.6.1: Cumulative friction surface FS and generated friction surface A in relation to the dosage volume DV

Pump size – dosage volume	FS/DV (mm^3/ml)	A/DV (mm^2/ml)
RPP 1- DV 180	117187.28	652.5
RPP 1- DV 300	113190.83	656.4
RPP 2- DV 180	78701.44	312.8
RPP 2- DV 300	64563.08	305.1
RPP 3- DV 180	65936.72	203.7
RPP 3- DV 300	50032.96	199.5
RPP 4- DV 180	53973.00	135.7

The relation of the calculated values in Table E.6.1 show that for the generated friction surface the value for RPP 3 is approximately one third and the value for RPP 2, half compared to the value for RPP 1. The relation of the values regarding the cumulative friction surface is different. Furthermore the values for the same pump for

dosage volume 180 and 300 calculated from the cumulative friction surface vary whereas they are approximately the same when calculated from the generated friction surface.

To evaluate the influence of the friction surface a plot with z average over the friction surface instead of the number of cycles was produced. The plots are shown in Figure E.6.1 and Figure E.6.2.
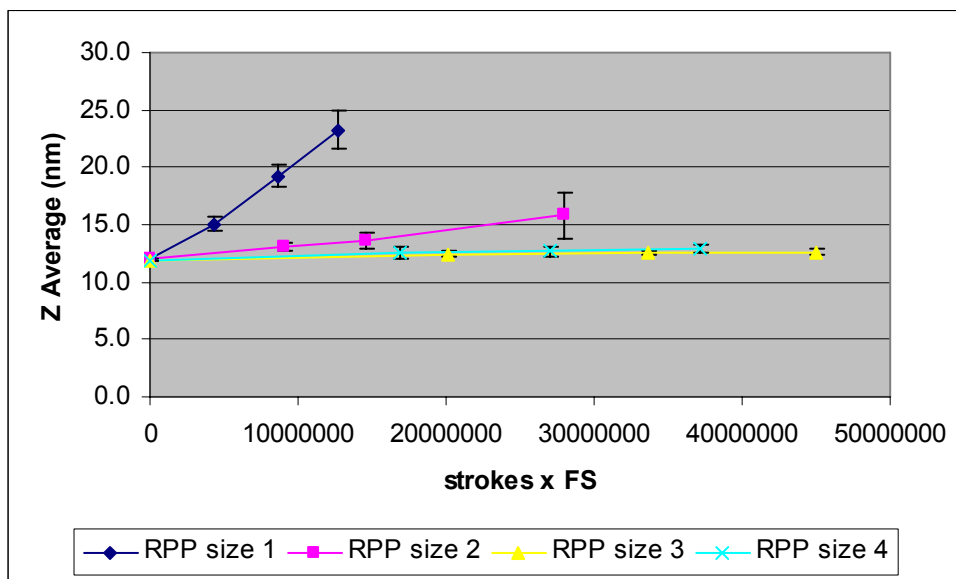

Figure E.6.1: Developing of z average in respect to the cumulative friction surface FS
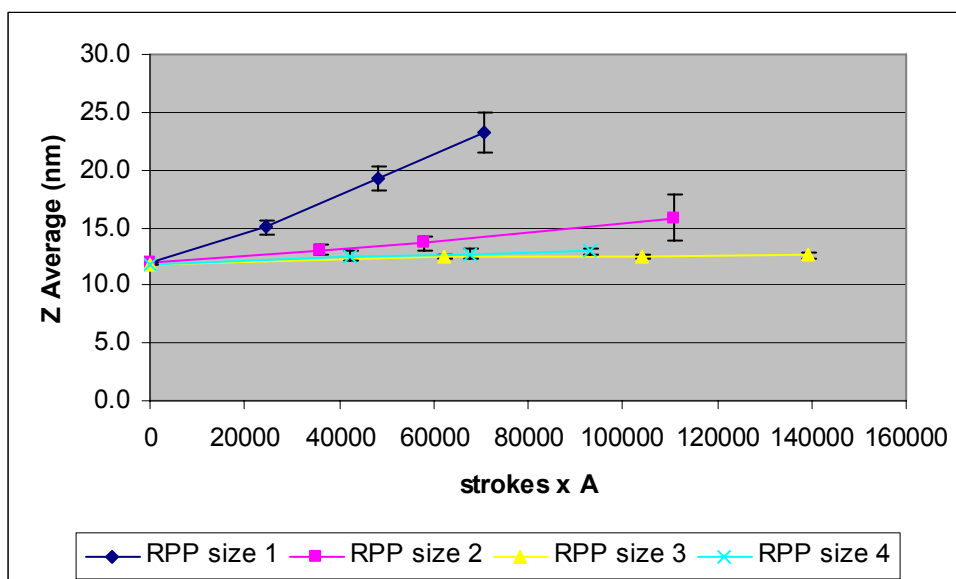

Figure E.6.2: Developing of z average in respect to the generated friction surface A

The curves for RPP 3 and 4 were practically not inclined. Compared to the plot of z average over the number of cycles shown in Figure E.5.1, it was found that the curves for RPP 1 and 2 are more gently inclined relative to the progression of RPP 3 and 4. This effect of approach of the curves when considering the developing of z average over the friction surface was seen to be slightly greater for the plot in Figure E.6.2 (generated friction surface A) than in Figure E.6.1 (cumulative friction surface FS). A correlation of the friction area to which the protein was subjected during the circulation in the test system and the intensity of stress which caused physical protein degradation could be supposed. However, it was evident that the friction surface could not be the only parameter on which the intensity of stress was dependent. Further possible factors which could influence the intensity and which could explain the comparatively high level of protein degradation which occurs during the use of RPP 2 and particularly RPP 1 could be the different clearance between piston and cylinder, the different shear speed in the gap due to the different diameter of the piston, or other parameters which change due to a different ratio in each pump like the flow speed at which the solution is pushed out or drawn inside the pump. Out of these, the clearance seemed to be the most likely one. A detailed experimental evaluation in respect of the influence of the clearance was not performed in the scope of this work. However, in the following chapters further evaluations were performed. As well, a characteristic pump parameter was proposed which considers various factors.

Conclusions: The friction surface is suggested as a parameter which correlates with quantity of stress on the protein solution during circulation in the test system. As the friction surface was not the only parameter, the influence generally as well as the magnitude of the influence could not be proven. Furthermore, it was not possible to evaluate which calculation of the friction surface, i.e. the cumulative friction surface according to Equation D.2.3 or the generated friction surface according to Equation D.2.1, is closer to the reality. Considering the results from the influence of the dosing volume in connection with the calculation of the generated friction surface per ml dosed volume, the generated friction surface seemed to be more appropriate.

E.7 Influence of filling speed

To evaluate the influence of the filling speed on the magnitude of shear stress caused, shear experiments under varying speeds were compared. In Figure E.7.1 and Figure E.7.2 the results of the cycling at different velocities with RPP 3 and RPP 1 respectively are demonstrated.
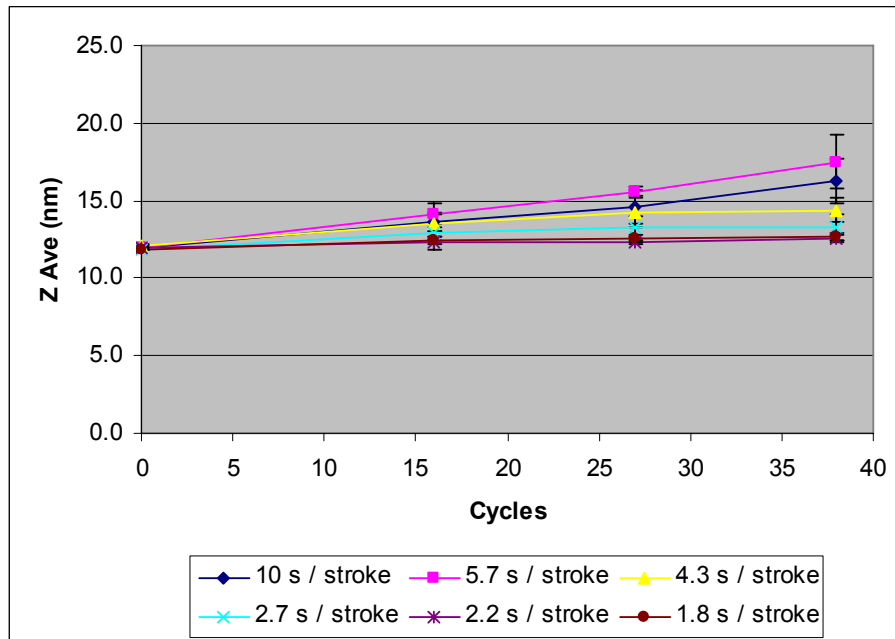

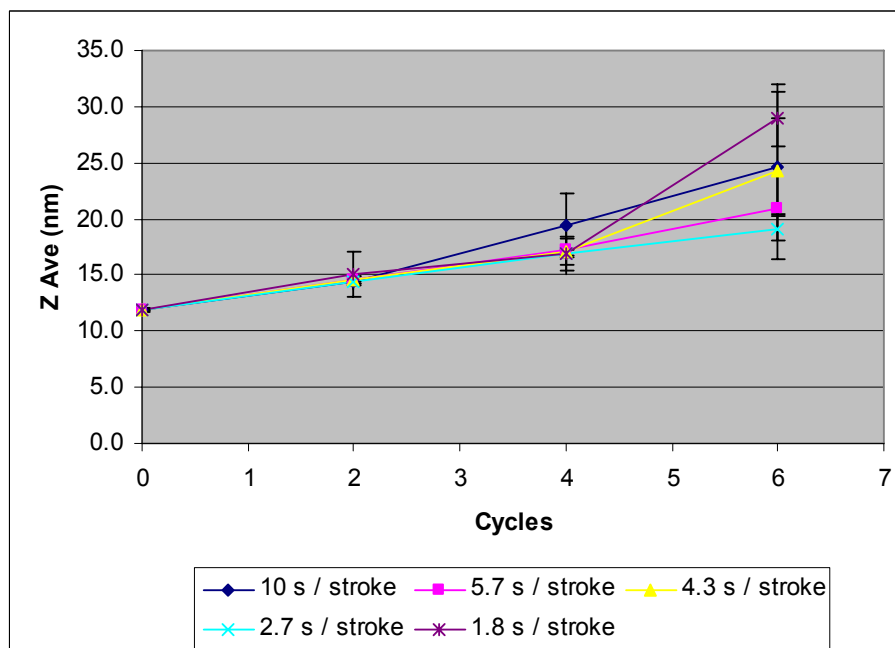
Figure E.7.1: RPP 3, DV 180

Figure E.7.2: RPP 1, DV 300

A quicker increase of z average calculated from the cumulants analysis was seen when circulating the solution with RPP 3 at low speeds. However, this was not consistent for all velocities. Exceptions were the 2 slowest speeds of 10 s/stroke and 5.7 s/stroke. The mean hydrodynamic diameter increased more for the faster velocity of 5.7 s/stroke than that of 10s/stroke.

For RPP 1 the results were less consistent. However, it has to be taken into consideration that circulation with RPP 1 generated large protein aggregates after 2 - 4 cycles, yet. It is fact that the presence of large particles dominates the light scattering in comparison to light scattered by small particles. The relative standard deviation increased for rising z average values. Furthermore the z average value is only valid for monomodal distributions (Eisenring, 1994) and should be used in a relative sense if the polydispersity index is higher than 0.25 (Zetasizer 1000HS/3000HS, 2000). Possibly, protein aggregation occurred too quickly when RPP 1 was used, so that a difference for the pumping velocities was not detectable with PCS.

Conclusion:

In Figure E.7.3 the slopes of the trend lines of the curves out of Figure E.7.1 and Figure E.7.2 calculated by employing least square linear regression have been plotted against the pumping velocities. A tendency to steeper slopes with declining velocities was seen. It can be concluded that higher filling speeds were favourable to low filling speed. The tendency can be explained with a shorter time of residence in the pump in the gap between cylinder and piston resulting in less stress on the test solution. However, it was found that there was no major influence of the filling speed. The contribution of the filling speed to the overall shear stress caused by a specific pump was minor.

The influence of the residence time is in agreement with the calculation of the average shear by Maa and Hsu (1996), which considers the shear rate and the time spent in the shear field. As well, Charm and Wong (1970) found that the level of inactivation of enzymes is dependent on the shear rate and the time of exposure.
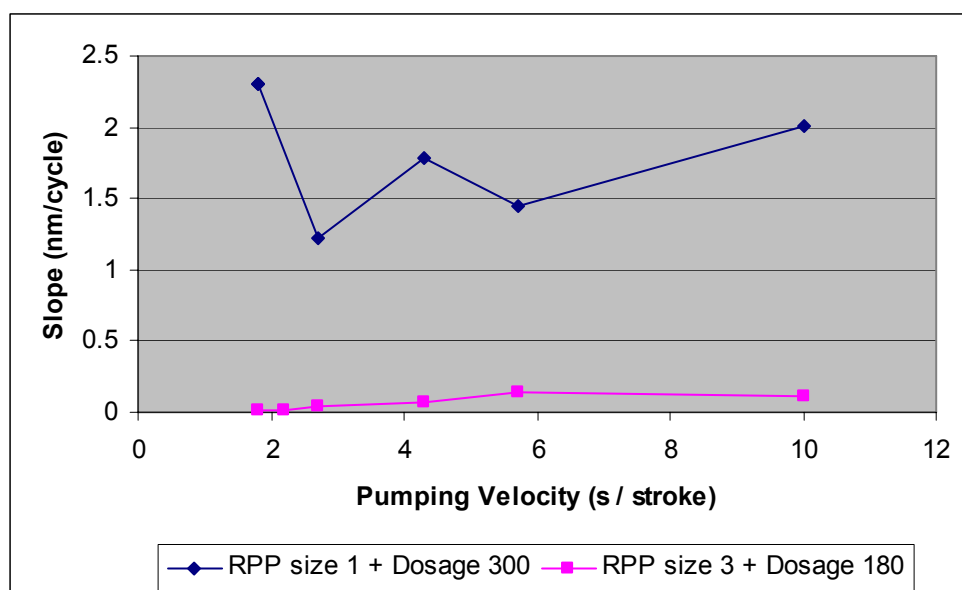
Figure E.7.3: Slopes versus pumping velocity

E.8   Influence of filling volume

The influence of the filling volume on the extent of stress on the circulated solution was evaluated by comparing the development of z average over the number of cycles to which the solution had been subjected. The solutions in this shear experiment were circulated at the maximum pumping speed with RPP 3. The dosage volumes of 300 and 180 were compared with each other. Z average was plotted over the number of cycles and is shown in Figure E.8.1. The same comparisons were done for solutions circulated with RPP1 at the maximum speed and the minimum speed for the 2 different dosage volumes 180 and 300. The graphs are shown in Annex G.4 Figure G.4.1 and Figure G.4.2.

The results from the shear experiments with RPP 3 did not show a difference for the two different dosage volumes. The PI in relation to the number of cycles was coherent with the results of z average measurements. The PI of the starting solution corresponded to a monodisperse distribution. It slightly exceeded 0.1 after 16 cycles and stayed in the range of a narrow distribution till the end of the experiment. This was found for both dosage volumes.
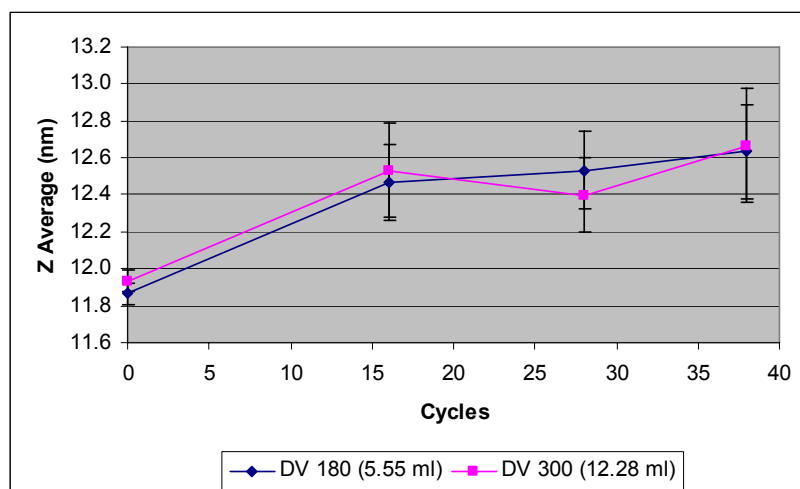
Figure E.8.1: RPP 3, dosing speed of 1.8s / stroke

The two plots in Figure G.4.1 and Figure G.4.2 resulting from the shear experiments with RPP 1 are controversial. The experiment at minimum speed showed a slightly quicker increase of z average with increasing circulation for the small dosage volume of 180, corresponding to 0.52 ml compared to DV 300 equivalent to 1.12 ml. This was particularly true for the end of the experiment after circulating the solution 6 times. However, it can not be neglected that for both dosage volumes the PI of the solution was found to be above 0.25 after 2 cycles, in which case z average should be used in a relative sense only (Zetasizer 1000HS/3000HS, 2000). After circulating the solution 4 times the PI had exceeded 0.5, which means that aggregates of different sizes were formed.

The shear experiment with RPP 1 at maximum speed resulted in a more important rise of z average after 6 cycles of the dosage volume 300. The contrary was found for z average after 4 cycles.

The calculation of the generated surface A in relation to one dosed ml showed that for RPP 1 as well as for RPP 3 these values were in the same range for the dosing volumes of 180 and 300. The results of this calculation are listed in Table E.8.1.

On the other hand, the dosage volume was an important factor taken into account for the calculation of parameter δ in form of the number of strokes needed to pass the volume of 1000 ml once with a specific RPP at a DV of 180. δ was suggested in

chapter E.11 as characteristic pump parameter for rotary piston pumps indicating the risk of causing protein damage.

Table E.8.1: Generated surface in relation to dosed volume

Pump – DV	A/DV (mm^2/ml)
RPP 1 – DV 180	652.5
RPP 1 – DV 300	656.4
RPP 3 – DV 180	203.7
RPP 3 – DV 300	199.5

The influence of the filling volume could not be conclusively evaluated. Within one size of RPP a difference in the amount of stress exerted on the protein solution using different dosage volumes for a fixed number of cycles in the test system could not be confirmed. At low speed of the piston movement a tendency could be observed that large dosing volume is favorable to small one, i.e. number of strokes performed is relevant. At high speed a clear significant difference between large and small dosing volumes was not seen.

No influence of the dosing volume would be coherent to the calculated relation of the generated surface over the dosed volume in ml. However, this would not be in agreement with the established characteristic rotary piston pump parameter δ in chapter E.11.

E.9 Influence of exposed air-liquid interface

In the present chapter an evaluation of the influence of the air-liquid interface was performed to verify if protein aggregation was induced predominantly by the rotary piston pump and not by the accumulation of the protein at the air-liquid interface.

A shear experiment was performed by circulating the protein solution with the filling needle positioned below the liquid level, to avoid the formation of new air-liquid interfaces and keep the size of the interface constant. The results were compared with the shear experiment using the same parameters with exception to the position of the filling needle.

No statistically significant (Student's t-test, p=0.05) difference of the PCS result in respect to z average values after 40 and 80 piston strokes was observed. Results are shown in Table E.9.1.

Table E.9.1: Comparison of the developing of z average for 2 different filling needle positions

Sample	Z average After 0 strokes Mean ± SD (nm)	Z average After 40 strokes Mean ± SD (nm)	Z average After 80 strokes Mean ± SD (nm)
RPP 1, speed 7, DV 300	12.0 ± 0.0	15.2 ± 0.2	19.8 ± 0.7
RPP 1, speed 7, DV 300 Needle below liquid level	11.9 ± 0.1	15.4 ± 0.3	18.5 ± 0.8

It was concluded that protein degradation was not significantly influenced by the increasing air-liquid interfacial area. This is also supported by the fact that pumping with the peristaltic pump did not show an effect on the mean hydrodynamic diameter even though the air-liquid interface renewal during pumping was comparable to that of rotary piston pumps. The exposure to the air-liquid interface during the shear experiments could be excluded as a cause for formation of protein aggregates in this study.

In opposition to this result, literature gives a lot of evidence that physical protein degradation can be caused by the air-liquid interface or by surfaces particularly in combination with shear stress (Tzannis et al., 1996; Maa et al., 1997; Harrison et al., 1998). Depending on the properties of the protein, it can be more or less prone to accumulation and degradation at the air-liquid interface. Maa and Hsu (1997) suggested that recombinant human desoxy-ribonuclease was adsorbed less to the air-liquid interface due to lower surface activity and showed therefore a higher stability. Furthermore, it has to be taken into account that a detergent like polysorbate, which was present in the sheared rituximab solution, is effective in preventing or reducing protein adsorption to interfaces and surfaces and is routinely used in protein formulations (Capelle et al., 2007; Wang et al., 2007, Bam et al., 1998).

E.10 Determination of protein monomer loss

To evaluate the extent of protein damage due to shear stress caused by rotary piston pumps, shear experiments over 3 hours were performed according the conditions described in section D.2.3 III. Loss of protein monomers was determined and is shown in Figure E.10.1. The monomer content decreased linearly with time circulated in the test system. It was found that the monomer content decreased to 97% during 3 hours circulation with RPP 1. When circulating the test solution with RPP 2 the monomer content decreased by approximately 0.5%. With RPP 3 an increase of protein monomers over 3 hours was observed. The increase of monomer content could be explained with the evaporation of water during the 3 hours duration of the shear experiment. When the long term shear experiment was performed the first time an increase of monomer content in the range of 1% was observed for RPP 2 and RPP 3. Therefore the shear experiments were repeated and precautions were taken to reduce evaporation of water during circulation. The system was closed with parafilm. Evaporation could be reduced but not completely eliminated, suggesting that the monomer loss for RPP 2 and 3 was slightly higher.

During the course of the shear experiments with RPP 1 and 2 the test solution became cloudy and the degree of turbidity increased with circulation time due to the formation of protein aggregates. The test solution sheared with RPP 3 stayed clear till the end of the experiment.
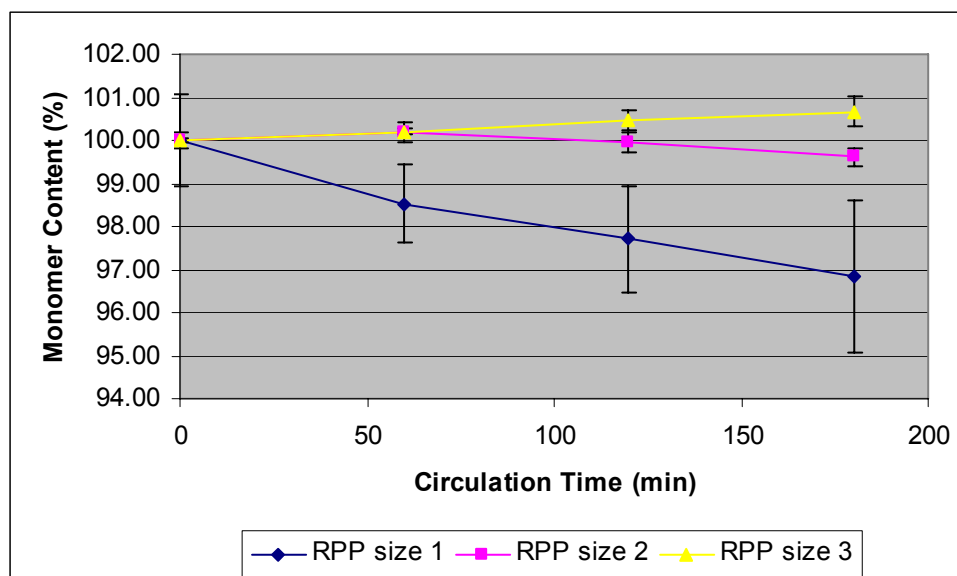
Figure E.10.1: Determination of rituximab monomer loss with SEC-HPLC

Conclusion:

Protein molecules were not damaged by pumping with RPP 3 or the quantity of damaged protein was below the detection limit of the method. Circulation of the solution with RPP 1 clearly caused damage to the protein molecules. The applied shear stress caused by pumping induced protein aggregation and precipitation. The quantity of damaged protein increased linearly with pumping time. As well RPP 2 stressed the protein solution in an extent to cause protein damage with time, even though the shear stress caused by this pump was lower compared to RPP 1.

The results found were consistent with results of the PCS measurements in this work. However, the absolute quantity of protein monomer loss has to be regarded with caution. First, the evaporation of water has to be considered. Second, for the determinations with the SEC-HPLC method it should be taken into account that proteins tend to bind to SEC columns. Gabrielson et al. (2007) found significant antibody losses through the SEC column.

A loss of protein monomer due to applied shear stress and subsequent formation of aggregates was found by Maa et al., (1997) for rhGH solutions. The rhGH solutions as well became cloudy and turbid with increasing shearing time. Further examples can be found in literature where shear stress led to denaturation, e.g. Harrison et al., (1998).

E.11 Characteristic rotary piston pump parameter

To characterise the potential of a rotary piston pump to cause shear during filling and dosing on a protein in solution which subsequently might lead to protein degradation, agglomeration and precipitation, an evaluation to find an applicable characteristic rotary piston pump parameter was performed. In the present chapter such a parameter is proposed and assessed.

The parameter is suggested to be δ and was obtained by dividing the generated friction surface A in mm^2 by the dosage volume DV in ml and by the clearance d between piston and cylinder in mm and by multiplying it with a factor, that was

obtained by dividing 1000 ml by the dosage volume DV in ml. The formula for δ is shown in Equation E.11.1.

$$\delta = \frac{A}{DV \cdot 1000} \cdot \frac{1}{d} \cdot \frac{1000ml}{DV}$$

Equation E.11.1

The dimension of the suggested characteristic pump parameter δ is: $\frac{1}{mm^2}$.

For the calculation of δ the dosage volume and the generated friction area A for dosage 180, which corresponds to a stroke of 18 mm, was considered. The considered dosage had mainly an influence on the above described factor of: 1000 ml/DV, which describes the ratio between cycles and strokes for a specific pump at a specific dosage volume. It is the number of strokes needed to circulate 1000 ml once in the test system with a certain pump at a specific dosage volume. The value for A/DV was only marginally influenced as the obtained values were in a comparable range for a specific pump when calculated e.g. with dosage 180 and 300. The values for the generated friction surface A per dosage volume DV are displayed in Table E.6.1.

Parameter δ was calculated for RPP 1 - 4 and is displayed in Table E.11.1. The lower the value, the less shear stress is exerted by the pump and therefore the lower the risk for a protein to be damaged during the dosing operation. The lowest value was obtained for RPP 4. With decreasing pump size, δ increased. In principal this complied with the results of the shear experiment, which showed that the increase of z average and PI with increasing circulation in the test system was getting more important the smaller the pump size. With exception to RPP 3 and 4, for which the result was less consistent. Although that δ was smaller for RPP 4 than for RPP 3, the shear experiment did not show a significant difference between the 2 pumps. Even a very slight trend was observed that RPP 3 caused marginally less stress in comparison to RPP 4. An explanation for this could be that an impact on the particle size distribution could only be observed if δ exceeded a certain value. If δ was smaller than this limit, the difference in the impact of the pumps would be too small to be detected with PCS. This limit for δ is suggested to be somewhere between 1668.3 mm^{-2}, the value for RPP 3 and 7829.8 mm^{-2}, the value for RPP 2. Furthermore, the

values for δ for RPP 3 and 4 were relatively close to each other and hence, they might be too close to see a difference in the impact on the particle size distribution.

Table E.11.1: Calculation of δ

RPP size	A/DV (mm²/ml)	1000/DV (ml/ml)	d (mm)	δ (1/mm²)
RPP1	652.5	1923.1	0.013	96523.7
RPP2	312.8	425.5	0.017	7829.8
RPP3	203.7	180.2	0.022	1668.3
RPP4	135.7	80.0	0.022	493.5

The course of the curves in Figure E.5.1 was normalized by multiplying the cycles with the characteristic pump parameter δ. The resulting curves are shown in Figure E.11.1 and for a better resolution in Figure E.11.2. without the curve for RPP 1. To compare the course of the curves in Figure E.5.1 and Figure E.11.1 graphs with the slopes of the curves in each Figure in relation to the characteristic δ were plotted and are shown in Figure E.11.3 and Figure E.11.4.

Figure E.11.1 and Figure E.11.2 show that a normalization using the proposed parameter δ led to curves for the different RPP sizes with comparable slopes. Therefore, it seems that δ could compensate the differences in the course of the curves of Figure E.5.1 and hence represented well the influencing factors in an adequate proportion leading to the different slopes of the original curves.
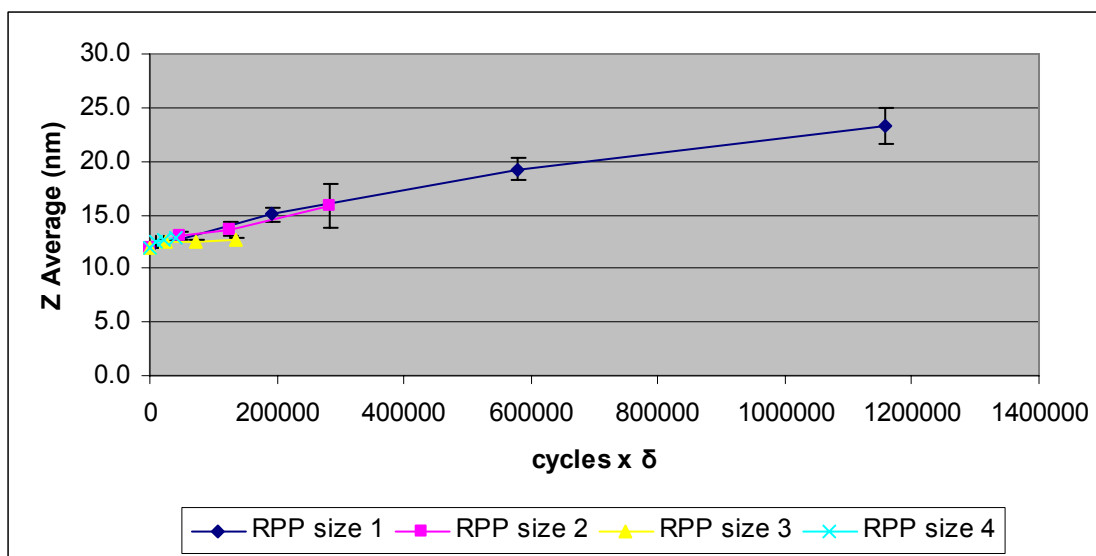
Figure E.11.1: Curves normalized by multiplication of cycles with δ
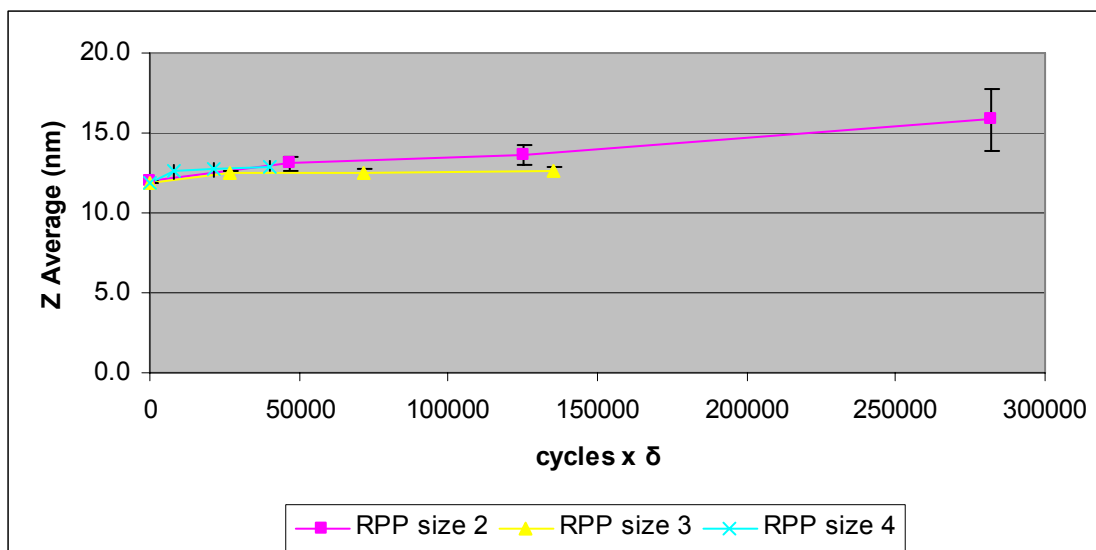
Figure E.11.2: Curves normalized by multiplication of cycles with δ (without curve for RPP 1)

On the basis of the characteristic pump parameter and its calculation, the main factors to explain the difference of the pumps in terms of protein damage are suggested to be first, the clearance between piston and cylinder. The smaller the gap between them, the more stress was exerted. This relation is also represented by Equation C.4.2., used by Maa and Hsu (1996) to calculate the average shear in a concentric-cylinder device. The average shear increases with a decreasing gap. The second important factor influencing the amount of stress was the dosage volume. This work suggests that per stroke a specific amount of stress was exerted. This influencing factor was expressed in the equation for δ as the term 1000/DV, the ratio between cycles and strokes. Therefore, contrary to the results presented in chapter E.8, that no significant influence of the dosage volume on the developing of z average and PI during circulation in the test system at high speed could be demonstrated, smaller dosage volumes would be less favourable, as more strokes are necessary to pass a defined volume. The same is applicable for smaller pump sizes. The third influencing factor is suggested to be the friction surface in proportion to the dosed volume. This ratio was seen to be higher and hence, less favourable for smaller pumps. It was found to be independent of the dosing volume.
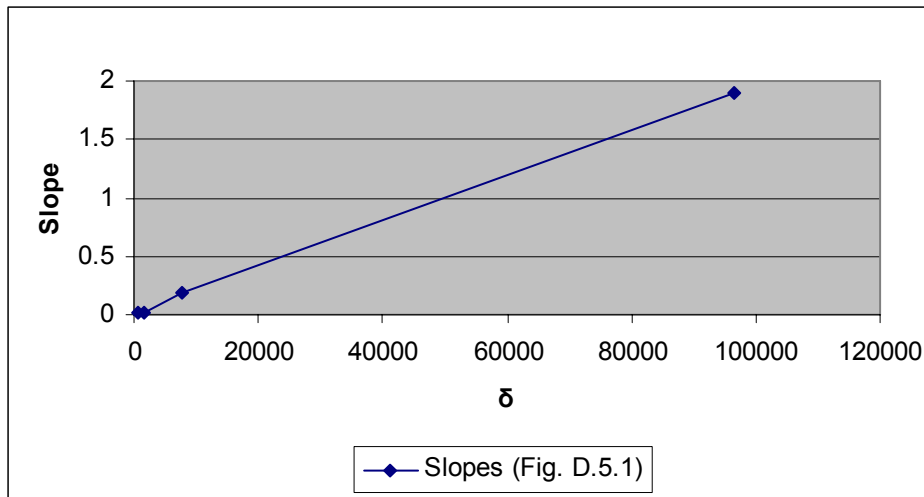
Figure E.11.3: Slopes of the curves in Fig. D.5.1
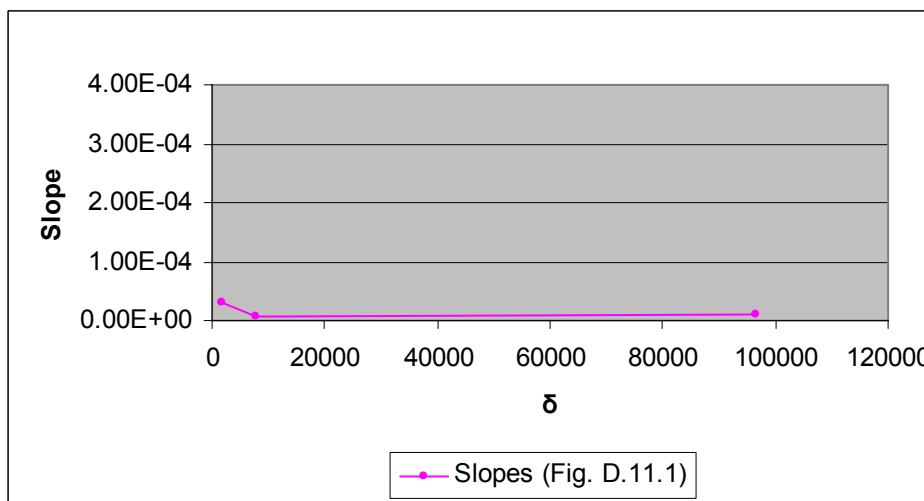
Figure E.11.4: Slopes of the curves in Fig. D.11.1

A correlation between the slopes of the original curves in Figure E.5.1 with the characteristic pump parameter δ was examined and a linear regression was found with a correlation function according to Equation E.11.2 and a coefficient of determination R^2 of 0.9995.

$$f(x) = 2 \cdot 10^{-5} x + 0.01 \qquad\qquad \textbf{Equation E.11.2}$$

Conclusion:

With δ a parameter was created, which seems to adequately reflect the amount of physical stress applied by a specific rotary piston pump. A linear correlation was found between δ and the degree of increase of z average with circulation of a protein solution using a rotary piston pump.

E.12 Evaluation of protective effect of excipients

The protective effect of excipients was determined by circulating solutions containing different excipients and combinations of excipients in the test system using RPP 1 and a pumping speed of 9.25. The mean hydrodynamic diameter and polydispersity index were measured in samples after 0, 2 and 4 cycles. The graph in Figure E.12.1 shows the development of the mean hydrodynamic diameter of the different solutions compared with the original solution. An increase of z average was observed for all solutions. The total of 5 solutions with different combinations of excipients stayed below the measured z average of the original solution after 4 cycles. The smallest increase of z average after 4 cycles was measured for the solution containing 0.5 % PEG 6000 and 5% Trehalose dihydrate.
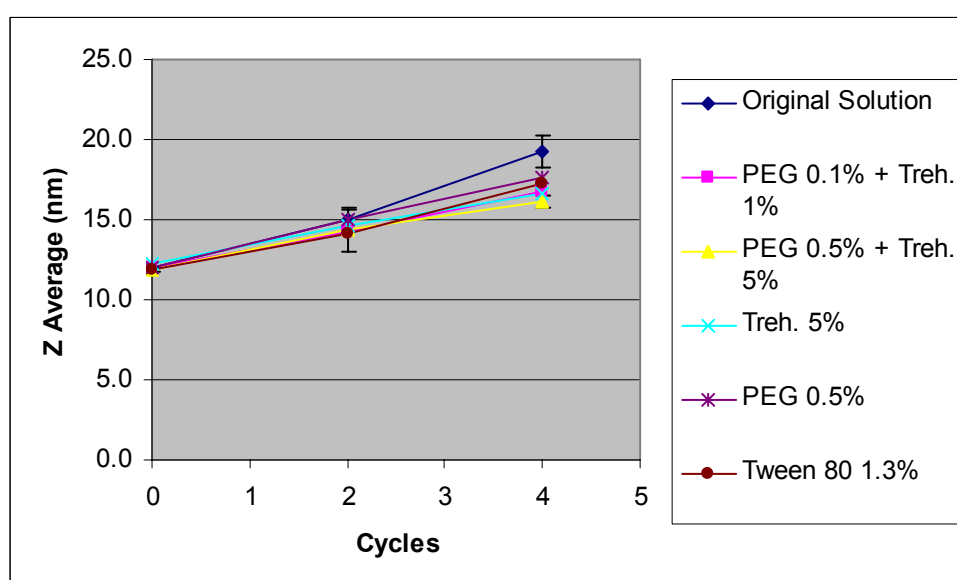
Figure E.12.1: Developing of z average with increasing circulation of the solutions in the test system

The results form the polydispersity index measurements of the unsheared and circulated solutions are summarized in Figure E.12.2. For the original rituximab solution the lowest polydispersity index was measured. The excipients seemed to influence the polydispersity index of the solutions before they were circulated in the test system. An explanation for this could be slight impurities of the excipients. The slopes of the linear regression line of the curves in Figure E.12.2 were considered to evaluate the influence of the excipients on the polydispersity index and are shown in Table E.12.1. It was observed that the unsheared rituximab solution showed the

narrowest size distribution with a polydispersity index of 0.057 ± 0.011. After circulation in the test system the solution developed the highest value for the polydispersity index of 0.529 ± 0.035. The linear regression line of the solution with 0.5% PEG and 5% Trehalose dihydrate showed the lowest slope of 0.0737; the starting polydispersity index for this solution was measured to be 0.161 ± 0.004 and increased to 0.455 ± 0.017 after 4 cycles.
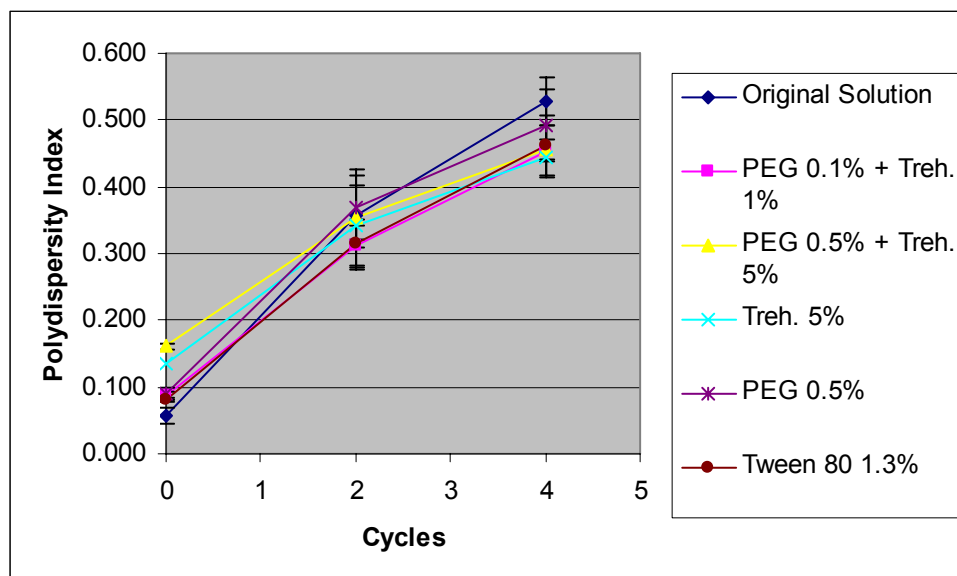
Figure E.12.2: Developing of the PI with increasing circulation of the solutions in the test system with RPP 1

Table E.12.1: Slopes of the Polydispersity index curves in Figure E.12.2

solution	orig. solution	PEG 0.1% + Treh. 1%	PEG 0.5% + Treh. 5%	Treh. 5%	PEG 0.5%	Tween 80 1.3%
slope	0.1179	0.0914	0.0737	0.0774	0.1005	0.0948

The trend that the combination of 0.5 % PEG 6000 and 5% Trehalose dihydrate stabilised the protein complies with findings in literature. Xie and Timasheff (1997) showed that trehalose stabilizes ribonuclease A via preferential exclusion from the protein surface. Bhat and Timasheff (1992) confirmed that polyethylene glycols stabilize proteins by preferential hydration of the protein. Preferential hydration increases with increasing PEG size. The polyethylene glycols are excluded from the proteins surface due to steric reasons.

E.13 Comparison of PCS, SEC-HPLC and TEM

For the test runs performed with a rituximab model solution, different analytical techniques were employed to evaluate the solutions after being subjected to shear by circulation in the test system. The analytical methods, chosen out of a wide range of available methods, were photon correlation spectroscopy, size-exclusion chromatography, and transmission electron microscopy. The aim of the methods was to qualitatively and quantitatively determine the potential damage to the protein caused by a dosing system. The parameter to estimate this damage was chosen to be the formation of aggregates. In the present chapter a comparison of these methods and their suitability for aggregation analysis is evaluated.

PCS was the method which has been predominantly used for this work. By measuring the mean hydrodynamic diameter z average and the polydispersity index, it was possible to detect with this method even very slight changes in the composition of the solution in terms of present particle sizes. Such slight changes were seen for example during the shear experiments with RPP 3 and RPP 4. Z average increased during circulation with RPP 3 from 11.9 nm to 12.5 nm by only 0.6 nm after 16 cycles. A great advantage for the detection of these minimal changes was the fact that no sample preparation or sample dilution was necessary. The samples drawn could be measured directly by introducing them into the measuring quartz cell. Dilution, for example, can lead to dissociation of reversible aggregates (Harn et al., 2007). Furthermore, varying solution conditions like ionic strength, salt type and pH affect protein aggregation (Chi et al., 2003b). Thus, any influence on the aggregation level in the sample during sample preparation or the measurement itself due to changes in solution conditions could be excluded. Particulate contamination of the sample, which would perturb the PCS measurement, was controlled by applying the precautions described in chapter D.2. However, the PCS method as applied in this work, encountered its limitations when the aggregation level in the sample increased. Large aggregates, as occurred e.g. during the circulation with RPP 1, very much perturbed the measurement, as the scattered light was much more intense. Depending on what particle passed the laser beam in the moment of measurement, the result for z average and the polydispersity index varied accordingly. The resulting z average and polydispersity index had to be interpreted carefully and in a relative sense. Even

though the contin analysis displays a size distribution, the concentration of aggregates in the sample could not be determined with this method. Examples of size distributions are shown in chapter G.3. A previous separation by size would be necessary to perform quantification and a determination of size (Demeule et al., 2007).

Size-exclusion HPLC was employed with the purpose to determine the amount of aggregation generated by shear stress from the dosing system, as this determination was a limitation of PCS. A shear experiment with RPP 1 at a pumping speed of 9.25 and a dosing of 300 was performed to have a comparison of the PCS analysis and SEC-HPLC. Samples were drawn after 2, 6, 12, 18, 24, 30 and 42 cycles and analysed with SEC-HPLC. Results are shown in Figure G.8.1 in the annex. A monomer loss was observed between 0 and 2 cycles, however in the following no further loss was seen up to 42 cycles. The loss of protein monomers after performing 2 cycles does not correspond to a loss due to aggregation. It can be explained with the fact that the sample at 0 cycles corresponded to the original rituximab solution and the sample taken after 2 cycles was taken from the test system. A dilution effect of the test solution occurred after the first cycle as the test system was not completely dry; some residual water rested after cleaning. When comparing these results with the results from PCS measurements, it was evident that the sensitivity of SEC-HPLC is much lower to detect aggregation in the test solution. To obtain a result in respect of a quantification of the lost native protein, the circulation in the test system had to be increased. Therefore samples were taken after 60, 120 and 180 min circulation in the test system, which corresponds to approximately 45 cycles per hour for RPP 1 at a pumping speed of 9.0, a dosage volume of 0.52 ml and a total volume in the system of 23.0 ml. A loss of protein monomers in this long-term experiment over 3 hours with RPP 1 of 1.5% (±0.9%) after 60 min., 2.3% (±1.2%) after 120 min. and 3.2% (±1.8%) after 180 min. was observed. In comparison examples of graphs from PCS measurements of similar test conditions after 0, 2, 4 and 6 cycles are shown in chapter G.3. A loss of protein monomers of 1.5% corresponds to a loss of 0.15 mg per ml. As 60 min. circulating corresponds to approximately 45 cycles, it can be calculated as a rough estimation that a loss of 0.007 mg protein monomers resulting in protein aggregates per ml was detected qualitatively with PCS in the sample taken after 2 cycles.

The limits of detection (LOD) and quantification (LOQ) were calculated to be 0.03 mg/ml and 0.09 mg/ml respectively for the SEC-HPLC method. The calculation was performed with the equations in chapter G.7 in the annex.

TEM was used as a method to visualise the aggregates in the solution. It was used to confirm aggregation in the test solutions. A quantification of aggregates with TEM was seen to be rather difficult, as a large range of sizes was observed. In Figure E.13.1 and Figure E.13.2 pictures of TEM measurements of a sheared solution are shown.
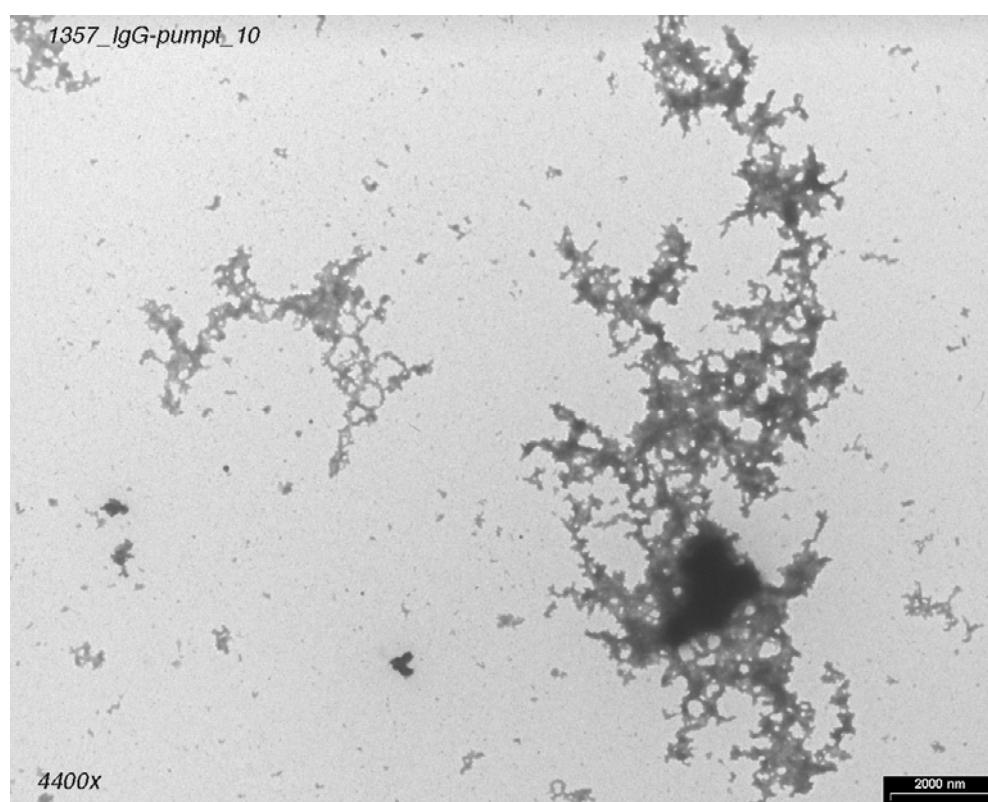
Figure E.13.1: TEM picture of a sheared rituximab solution
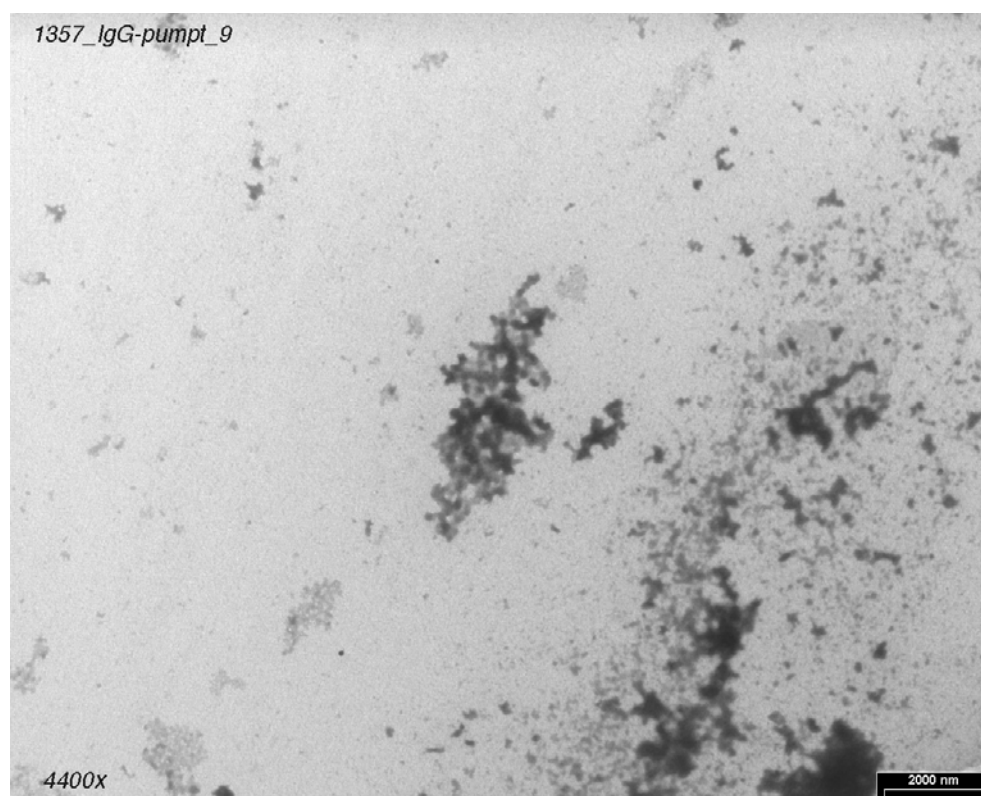
Figure E.13.2: TEM picture of a sheared rituximab solution

In both pictures particles of the size of a few nm up to a few µm are seen. Furthermore particles of different density were observed, ranging from clear grey loose agglomerates to almost black more firm aggregates. Compared to the pictures in Figure E.2.1 and Figure E.2.2 of the unsheared solution, it is evident that the number of aggregates increased remarkably.

Conclusion:

With PCS a very sensitive method to changes due to the formation of protein aggregates in the shared test solution was at disposition. For the determination of the amount of aggregated protein, SEC-HPLC was a suitable method, even though it was found that the sensitivity was much lower than for PCS. Additionally, it was found to be a useful complement for the two methods, to confirm the formation of aggregates by visualization with TEM.

The low sensitivity found for the SEC-HPLC method can be derived from the fact that proteins tend to bind to columns. Gabrielson et al. (2007) examined the aggregation level in a monoclonal antibody formulation using SEC-HPLC, assymetrical flow field flow fractionation and sedimentation velocity and found statistically significant

(p<0.01) antibody loss through the size exclusion column. Arakawa et al. (2006a) observed that larger aggregates of monoclonal antibodies tend to stick to SEC columns and the addition of arginine HCl to the mobile phase leads to a higher recovery of the aggregates. Such binding can lead to abnormal chromatograms, protein loss, column damage and an abnormal separation profile inducing an inaccurate determination of protein molecular weight data and incorrect analysis of protein interactions (Ejima et al., 2005).

F CONCLUSIONS

F.1 Shear Forces during filling processes

In the present study dosing and filling equipment was examined in respect to the effect of physical stress which possibly occurs during filling and dosing processes on protein solutions. A negative effect on protein solutions due to shear stress was confirmed for certain dosing equipment.

β-galactosidase did not show any loss of activity after having been circulated with a rotary piston pump. Rituximab aggregated under the physical stress caused by a rotary piston pump. The reason for this could be a different sensitivity of each protein to shear stress due to the difference in primary, secondary and tertiary structure which leads to different instabilities. To confirm this, additional experiments with other proteins would be required. Another possible reason could be the different sensitivity of the applied analytical methods in respect to detect aggregation. As well possible is a combination of both proposed causes. Before filling protein solutions the sensitivity to shear should be assessed.

The comparison of a peristaltic pump and 4 different sizes of rotary piston pumps showed that the peristaltic pump did not cause any physical stress. The rotary piston pumps delivered different results depending on their size. Rotary piston pump size 2 and particularly size 1 caused aggregation and precipitation of rituximab. Whereas circulating with rotary piston pumps size 3 and 4 did not induce precipitation. A very low level of protein aggregation after extended circulation with RPP 3 and 4 in the test system was seen when analysing with photon correlation spectroscopy. However, it should be kept in mind that during a filling operation within the manufacturing of the final dosage form of a pharmaceutical solution the liquid product is not circulated but passes the dosing equipment one single time. On the other hand even minimal formation of visible or sub visible particles present in the final drug product is unacceptable and leads to low yield and refused batches. Therefore precautions for the filling of shear sensitive proteins should be taken in terms of choosing the appropriate dosing equipment. In this respect peristaltic pumps can be

considered to be suitable for the filling of these kinds of products. Furthermore no negative effect is expected when using rotary piston pumps of size 3 and 4. Rotary piston pumps size 1 and 2 should be avoided for shear sensitive products.

On the basis of the evaluated parameters it was demonstrated that apart from the size of the rotary piston pump, the filling speed had an influence on the aggregation level in the model protein solution. High filling speed was found to be slightly more favourable than slow filling speed. This tendency could be explained with the residence time of the protein in the gap between cylinder and piston. Therefore special attention should be given to slow filling speeds during a filling operation when rotary piston pumps are used. These particularly can occur whenever an intervention which imposes a machine stop happens during manufacturing. The last vials before the stop and the first ones after restarting the machine should very critically be monitored and investigated. Machine stops should be as far as possible avoided.

The relationship between the friction surface and the exerted physical stress during filling with a rotary piston pump could not be definitely clarified to allow for an overall conclusion. A contribution to the physical stress is possible but not stringent. Certainly, at least one further factor significantly influenced the extent of physical stress, which has found to be unequal for the different sizes. The clearance between the piston and the cylinder was suggested as a factor. This would be coherent with the results from the shear experiments. Pump sizes 3 and 4, which have the same clearance, exhibited comparable extent of stress, whereas with diminishing clearance the amount of exerted stress, resulting in protein aggregation, increased. This is as well coherent with the calculation of the shear rate by Maa et al. (1996) as in chapter B4, which implies that the shear rate and therefore shear stress and average shear increase by narrowing the gap between cylinder and piston. Further investigations with identical pumps which differ only in their clearance would be necessary to evidence this implication.

The calculation of the friction surface was performed as the cumulative friction surface and the generated friction surface. The cumulative friction surface takes into account the complete friction surface which accumulated during one stroke. The generated friction surface was defined as the surface which corresponds to the inner

surface of the cylinder in the height of the stroke. This was as well the area which was definitely flushed during every stroke with new solution. It did not consider the complete cylinder area which is covered by the piston throughout the movements. The generated friction surface per ml of dosed solution was characteristic for each pump and independent of the dosing volume. This would be coherent with the results of the shear experiment with different dosing volumes at high filling speed, where a difference for varying dosing volumes within the same pump could not be proven. However, it should be noted that the influence of the dosing volume could not be conclusively analyzed. At low speed of the piston movement a tendency could be observed that large dosing volume is favorable to small, i.e. number of strokes performed is relevant. At high speed a clear significant difference between large and small dosing volumes was not seen.

A characteristic rotary piston pump parameter δ was suggested, which indicates the potential of the respective RPP to cause damage to a protein due to the exerted shear stress during filling. Apart from the 2 above mentioned factors, the clearance between cylinder and piston and the generated friction surface per ml, a third factor, the ratio between cycle and stroke, was taken into account in the equation used for the calculation of δ. This suggested a third important influencing factor to the amount of stress caused by a RPP, which is the dosing volume. It was assumed that every pumping stroke causes a certain amount of stress, independent of RPP size and dosing volume. This implied that smaller dosing volumes are less favorable as the stress per dosed ml is higher than for large dosing volumes. It was found that the calculated values for δ represented well the potential to cause damage for the different pump sizes and therefore seemed to be an adequate characteristic pump parameter for RPPs.

With different combinations of excipients, which were added to the original rituximab solution, the aggregation level caused by rotary piston pump 1 was slightly reduced. The combination of 0.5% polyethylene glycol 6000 and 5% trehalose dihydrate was the most effective protection.

F.2 Suitability of analytical methods for the evaluation of shear sensitivity

Photon correlation spectroscopy was predominantly used for the present work. It was found that it represents a very sensitive method to detect changes in the particle size distribution of the rituximab solution after circulating it in the test system. It was calculated that 0.007 mg aggregated protein per ml could be detected, whereas the limit of detection for the SEC-HPLC method was found to be 0.03 mg/ml. Even very slight changes in the solution were detected with PCS as for example the changes caused by circulating the solution with RPP 3. These changes were not detectable with SEC-HPLC.

SEC-HPLC was used to quantify the aggregated protein. The loss of protein monomers was determined. A direct quantification of aggregates with SEC-HPLC was not chosen, as in some of the sheared solutions aggregated protein precipitated and the solution became turbid. To avoid that precipitated protein entered the column, the solutions were stored and centrifuged before SEC-HPLC analysis. Furthermore, SEC-HPLC is often put into question due to the fact that proteins, particularly in the form of soluble aggregates, tend to bind non-specifically to columns and are therefore lost for quantification (Stulik et al., 2003).

Transmission electron microscopy was found to be suitable imaging method to prove that changes in the particle size distribution detected with PCS came from the formation of protein aggregates. A quantification of the aggregates was not possible with this method.

G ANNEX

G.1 Therapeutic Proteins

Table G.1.1:   List of recombinant therapeutic proteins approved in the European Union till 2004 (ISB, 2004)

| Recombinant enzymes, hormones and cytokines; Recombinant antibodies; recombinant vaccines			
Drug	**Main indication**	**Applicant**	**First approval in EU**
Insulin, human	Diabetes mellitus type 1	Lilly, Novo Nordisk, Hoechst	12/1987
Interleukin-2, IL-2 (Aldesleukin)	Hypernephrom (for T-cell activation)	Chiron	12/1989
Somatotropin (human growth hormone)	Dwarfism	Lilly, Pharmacia, Serono, Novo Nordisk, Ferring	02/1991
Glucagon	Hypoglycemic reaction	Novo Nordisk	03/1992
Erythropoietin beta (Epoetin beta)	Renal anemia	Boehringer Mannheim	05/1992
Interferon gamma 1b	Chronic granulomatosis	Boehringer Ingelheim	1992
Interferon alfa-2b	Hairy cell leukemia, carcinomas Papilloma induced genital warts	Essex Pharma	03/1993 02/2000
Erythropoietin alpha (Epoetin alpha)	Renal anemia	Janssen-Cilag	04/1993
GM-CSF (Molgramostim)	Neutropenia	Essex Pharma Sandoz	04/1993
Interferon alpha-2a	Hairy cell leukemia, carcinomas, Papilloma induced genital warts	Roche	04/1993
Faktor VIII	Hemophilia A	Bayer AG, Baxter, Armour Pharma	07/1993
G – CSF, glycosylated	Neutropenia	Rhône – Poulenc Rorer, Chugai Rhône – Poulenc	10/1993
Tissu plasminogen activator, t-PA	Coronary thrombosis, thrombosis	Dr. Karl Thomae	04/1994
Glucocerebrosidase	Morbus Gaucher	Genzyme B.V.	06/1994
G – CSF	Neutropenia	Hoffmann-La Roche, Kohl Pharma	08/1994
Hum. DNAse	Mucoviscidosis	Hoffmann-La Roche	09/1994
Follitropin alpha	Ovaries stimulation, IVF	Serono Laboratories	10/1995
Interferon beta – 1b	Multiple sclerosis	Schering	11/1995
Factor VII	Bleeding with hemophilia A and B	Novo Nordisk	02/1996
Insulin, Lispro	Diabetes mellitus type 1	Lilly Deutschland	05/1996
Follitropin beta	Ovaries stimulation, IVF	Organon	10/1996
Gewebe - Plasminogen-Activator, r-PA	Coronary thrombosis, thrombosis	Boehringer Mannheim	11/1996
Faktor IX	Hemophilia B	Genetics Institute of Europe	08/1997
Interferon beta-1a	Multiple sclerosis	Biogen France, Ares-Serono	03/1997
Hirudine	Treatment of heparinassociated thrombocytopenia	Behringwerke	03/1997
Desirudine	Prevention of thrombosis during surgery	Ciba Europharm Ltd	03/1997
Calcitonin	Osteoporosis, Paget's disease; hypercalcaemia	Unigene UK	01/1999
Interferon alfacon-1	Hepatitis C	Yamanouchi	02/1999
Platelet cells derived growth factor, r-hPDGF	Treatment of ulceritis of diabetes patients	Janssen-Cilag N.V.	03/1999
Tumor necrosis factor alfa-1a	Palliative therapy of sarcomas; adjuvant therapy after surgery of tumor patients	Boehringer Ingelheim	04/1999
Moroctocog alpha	Preparation for surgery of hemophilia patients	Genetics Institute	04/1999

Thyrotropin alfa	Scintigraphy of thyroid gland with radioactive iodine	Genzyme B.V.	07/1999
Insulin aspart	Diabetes mellitus type 1	Novo Nordisk A/S	09/1999
Peginterferon alfa-2b	Hepatits C	Schering Plough Europe	05/2000
Insulin glargin	Diabetes mellitus	HMR Deutschland/Aventis	06/2000
Etanercept	Rheumatoid arthritis	Wyeth-Lederle	02/2000
Rasburicase	Tumor induced hyperuricaemia	Sanofi	02/2001
Tenecteplase	Coronary thrombosis, thrombosis	Boehringer Ingelheim	02/2001
Choriogonadotropin alpha	Ovaries stimulation IVF	Areos Serono	02/2001
Lutropin alpha	Maturation of follicles, IVF	Ares Serono	02/2001
Darbepoetin alfa	Renal anemia	Amgen Europe	06/2001
Agalsidase alfa	Therapy of Fabry disease	TKT Europe-5S AB	08/2001
Agalsidase beta	Therapy of Fabry disease	Genzyme B.V.	08/2001
Anakinra	Rheumatoid arthritis	Amgen	03/2002
Dynepo	Renal anaemia	Aventis	02/2002
Pegfilgrastim	Neutropenia	Amgen Europe	08/2002
Drotrecogin alfa	Severe sepsis with multiple organ failure	Eli Lilly	08/2002
Dibotermin alfa	Treatment of acute tibia fractures in adults	Genetics Institute Europe B.V.	09/2002
Aldurazyme	Mucopolysaccharidosis	Genzyme Europe	06/2003
Abciximab	Anti coagulant for treatment of myocard infarcts	Centocor Europ B.V.	05/1995
Votumumab	Detection of colon carcinomas	Organon Teknika	11/1996
Rituximab	Treatment of CD20 positive B-cell lymphomas	Roche	1998
Basiliximab	Prevention of transplant rejection	Novartis	10/1998
Daclizumab	Prevention of transplant rejection	Roche Registration	02/1999
Palivizumab	Monoclonal antibody against Respiratory Syncytial Virus (RSV) subtypes A and B	Abbott Laboratories	05/1999
Infliximab	Anti TNF alphaantobody for treatment of immune and inflammatory diseases	Centocor	08/1999
Trastuzumab	Breastcancer; HER2 receptor found with 30% of all cases	Roche	09/2000
Alemtuzumab	Anti CD52 antibody for therapy of chronic lymphocytic leukemia when alkylating cytostatics fail	Millenium & Ilex UK	03/2001
Adalimumab	Anti TNF alpha antibody for therapy of rheumatoid arthritis	Abbott	03/2003
Cetuximab	Chimeric IgG antibody against epidermal	Imclone, Merck	02/2004
Hepatitis-B antigen	Hepatitis B prevention	SmithKline	09/1989
Hepatitis-B vaccine combinations	Hepatitis B prevention additional vaccination against hepatitis A, tetanus, pertussis or/and diphtheria	SmithKline Beecham Biologicals MSD Pasteur Mérieux	07/1996 09/1996 02/1997 07/1997 05/1998
Triacelluvax® three recombinant B pertussis toxins	Vaccination against tetanus, pertussis, and diphtheria	Chiron	01/1999
Hepatitis B antigens S, pre-S1, pre-S2	Hepatitis B prevention	Medeva Pharma	03/2000
Glycosylated recombinant diphetria toxin CRM197	Prevention of Pneumococcus infections with children	Wyeth – Lederle	02/2001
Lyme disease vaccine	Prevention of infections	Wyeth – Lederle	02/2001

G.2 Overview Shear Experiment Test Runs

Ex. No.:	Total Vol.	Pump	DV	Speed	sampling	strokes	analysis	model substance
1	20.0 ml	RPP 1	300	0.5	0,2,4,6 cyc.	0+35+32+30	PCS	rituximab
2	20.0 ml	RPP 1	300	2.0	0,2,4,6 cyc	0+35+32+30	PCS	rituximab
3	20.0 ml	RPP 1	300	3.0	0,2,4,6 cyc	0+35+32+30	PCS	rituximab
4	20.0 ml	RPP 1	300	5.5	0,2,4,6 cyc	0+35+32+30	PCS	rituximab
5	20.0 ml	RPP 1	300	9.25	0,2,4,6 cyc	0+35+32+30	PCS	rituximab
6	20.0 ml	RPP 1	180	0.5	0,2,4,6 cyc	0+72+70+66	PCS	rituximab
7	20.0 ml	RPP 1	180	9.25	0,2,4,6 cyc	0+72+70+66	PCS	rituximab
9	23.0 ml	RPP 2	180	9.25	0,6,10,20 cyc	0+56+36+85	PCS	rituximab
10	20.0 ml	RPP 3	180	0.5	0,16,28,38 cyc	0+55+37+31	PCS	rituximab
11	20.0 ml	RPP 3	180	2.0	0,16,28,38 cyc	0+55+37+31	PCS	rituximab
12	20.0 ml	RPP 3	180	3.0	0,16,28,38 cyc	0+55+37+31	PCS	rituximab
13	20.0 ml	RPP 3	180	5.5	0,16,28,38 cyc	0+55+37+31	PCS	rituximab
14	20.0 ml	RPP 3	180	8.0	0,16,28,38 cyc	0+55+37+31	PCS	rituximab
15	20.0 ml	RPP 3	180	9.25	0,16,28,38 cyc	0+55+37+31	PCS	rituximab
16	30.0 ml	RPP 3	300	9.25	0,16,28,38 cyc	0+38+28+22	PCS	rituximab
17	35.0 ml	RPP 4	180	9.25	0,16,27,38 cyc	0+44+29+28	PCS	rituximab
18 Compare-ison to 19	30.0 ml	RPP 3	300	7.0	n/a	0+40+40	PCS	rituximab
19 below liq. level	30.0 ml	RPP 3	300	7.0	n/a	0+40+40	PCS	rituximab
20	23.0 ml	WMP	4.36	200	0,24,48 cyc.	0+121+116	PCS	rituximab
LT 10	23.0 ml	RPP 1	180	9.0	0,60,120,180 min	n/a	SE-HPLC	rituximab
LT 20	23.0 ml	RPP 2	180	9.0	0,60,120,180 min	n/a	SE-HPLC	rituximab
LT 30	30.0 ml	RPP 3	180	9.0	0,60,120,180 min	n/a	SE-HPLC	rituximab
Excipients 1	20.0 ml	RPP 1	180	9.25	0, 2, 4 cyc.	0+72+70	PCS	rituximab
Excipients 2	20.0 ml	RPP 1	180	9.25	0, 2, 4 cyc.	0+72+70	PCS	rituximab
Excipients 3	20.0 ml	RPP 1	180	9.25	0, 2, 4 cyc.	0+72+70	PCS	rituximab
Excipients 4	20.0 ml	RPP 1	180	9.25	0, 2, 4 cyc.	0+72+70	PCS	rituximab
Excipients 5	20.0 ml	RPP 1	180	9.25	0, 2, 4 cyc.	0+72+70	PCS	rituximab
Excipients 6	20.0 ml	RPP 1	180	9.25	0, 2, 4 cyc.	0+72+70	PCS	rituximab
lactase	20.0 ml	RPP 1	300	9.25	5, 10	90, 180	assay	lactase

G.3 Size distributions from PCS measurements

Run	Angle	KCps.	ZAve	Poly	Fit	Time
1	90.0	258.8	12.0	0.042	0.000198	14:17:49
2	90.0	258.8	11.9	0.047	0.000276	14:24:19
3	90.0	259.6	12.0	0.041	0.000231	14:29:58
Average		259.1	12.0	0.044		
+/-		0.4	0.0	0.003		
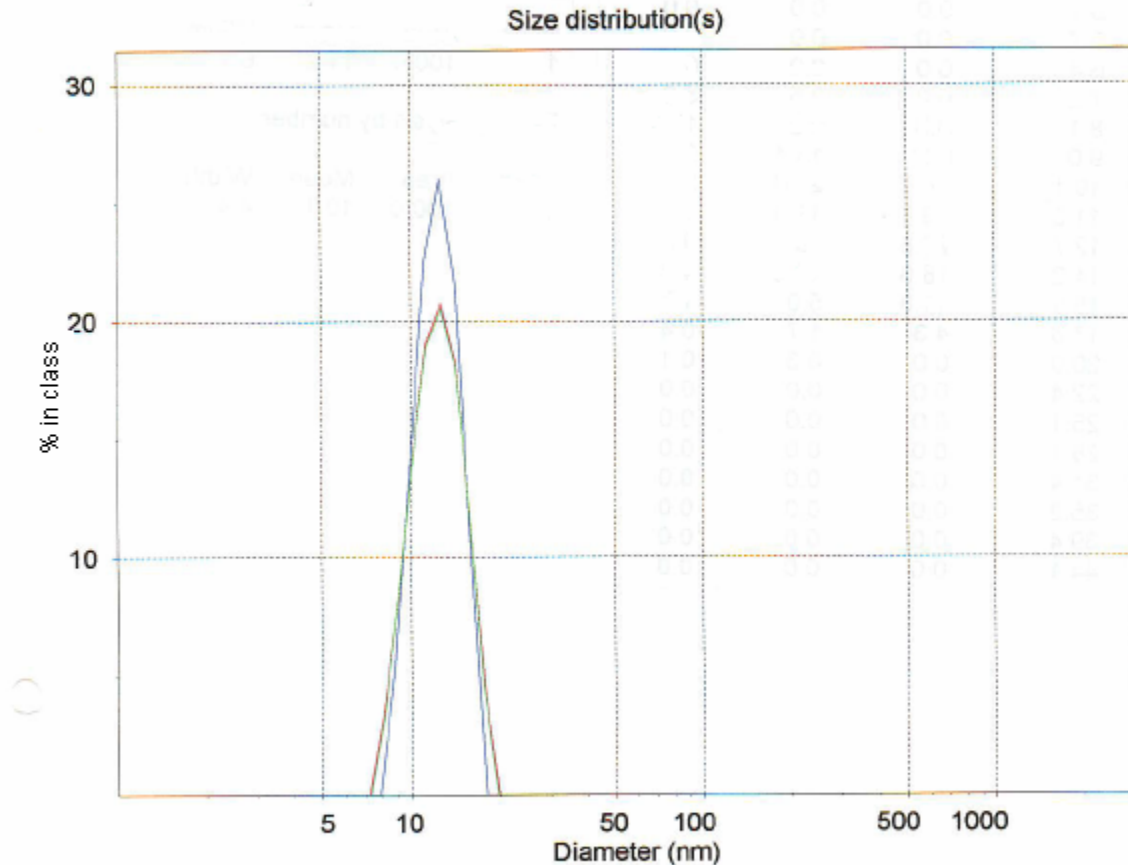
Rec	Angle	KCounts	ZAve(nm)	Poly.Index	Quality	Error	Analysis
1	90.0	258.8	11.993	0.0424	Pass	1.98e-004	Contin
2	90.0	258.8	11.937	0.0473	Pass	2.76e-004	Contin
3	90.0	259.6	11.997	0.0409	Pass	2.31e-004	Contin

Figure G.3.1: Size distribution plot after 0 cycles with RPP1, DV 180, speed 9.25 (P0)

Run	Angle	KCps.	ZAve	Poly	Fit	Time
1	90.0	324.0	15.9	0.417	0.000329	15:48:22
2	90.0	313.4	15.4	0.381	0.000287	15:53:59
3	90.0	307.8	14.9	0.345	0.000272	15:59:37
Average		315.0	15.4	0.381		
+/-		8.2	0.5	0.036		
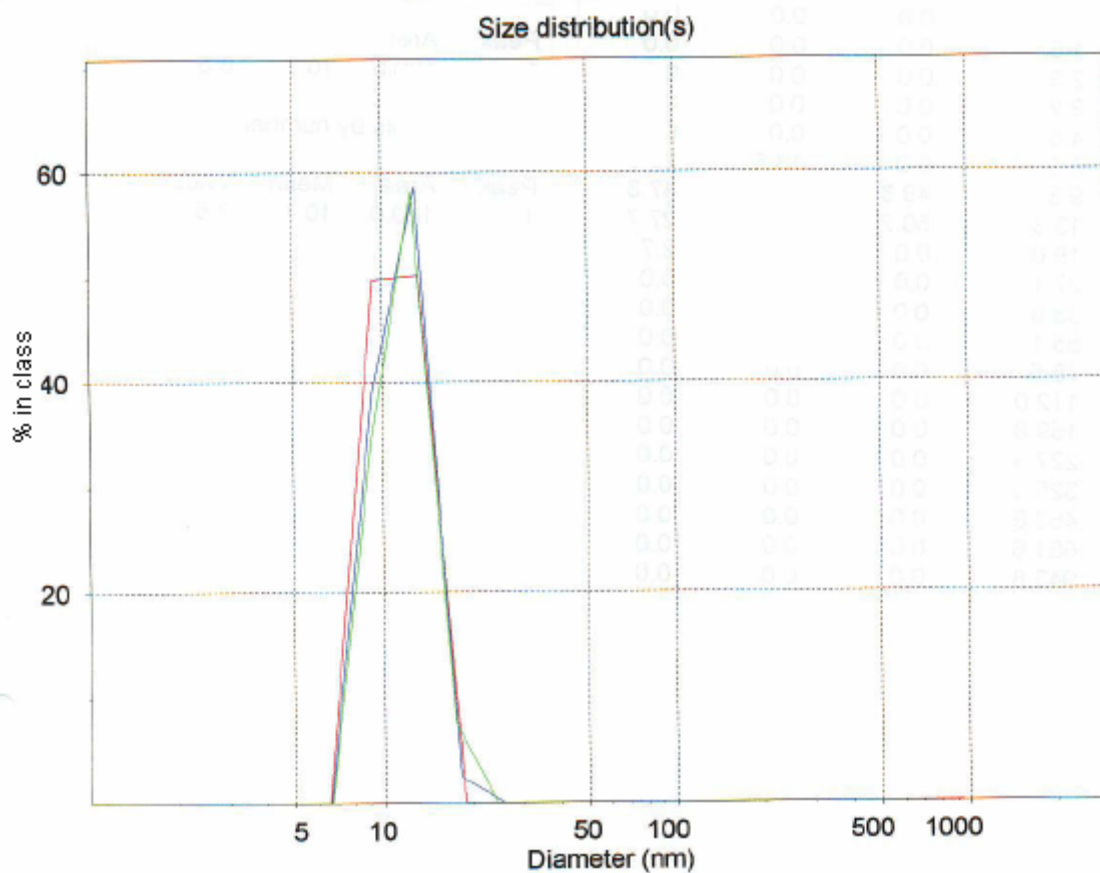
Rec	Angle	KCounts	ZAve(nm)	Poly.Index	Quality	Error	Analysis
4	90.0	324.0	15.9	0.417	Pass	3.29e-004	Contin
5	90.0	313.4	15.4	0.381	Pass	2.87e-004	Contin
6	90.0	307.8	14.895	0.345	Pass	2.72e-004	Contin

Figure G.3.2: Size distribution plot after 2 cycles with RPP1, DV 180, speed 9.25 (P1)

Run	Angle	KCps.	ZAve	Poly	Fit	Time
1	90.0	369.5	18.8	0.518	0.000274	13:38:32
2	90.0	382.9	19.8	0.550	0.000287	13:45:24
3	90.0	393.1	21.0	0.591	0.000303	13:51:33
Average		381.8	19.9	0.553		
+/-		11.8	1.1	0.037		

Size distribution(s)

RecAngle		KCounts	ZAve(nm)	Poly.Index	Quality	Error	Analysis
7	90.0	369.5	18.8	0.518	Pass	2.74e-004	Contin
8	90.0	382.9	19.8	0.550	Pass	2.87e-004	Contin
9	90.0	393.1	21.0	0.591	Pass	3.03e-004	Contin

Figure G.3.3: Size distribution plot after 4 cycles with RPP1, DV 180, speed 9.25 (P2)

Run	Angle	KCps.	ZAve	Poly	Fit	Time
1	90.0	208.8	24.9	0.698	0.000328	15:11:13
2	90.0	191.3	25.9	0.413	0.000241	15:17:11
3	90.0	188.8	21.4	0.602	0.000535	15:23:09
Average		196.3	24.1	0.571		
+/-		10.9	2.3	0.145		

Size distribution(s)
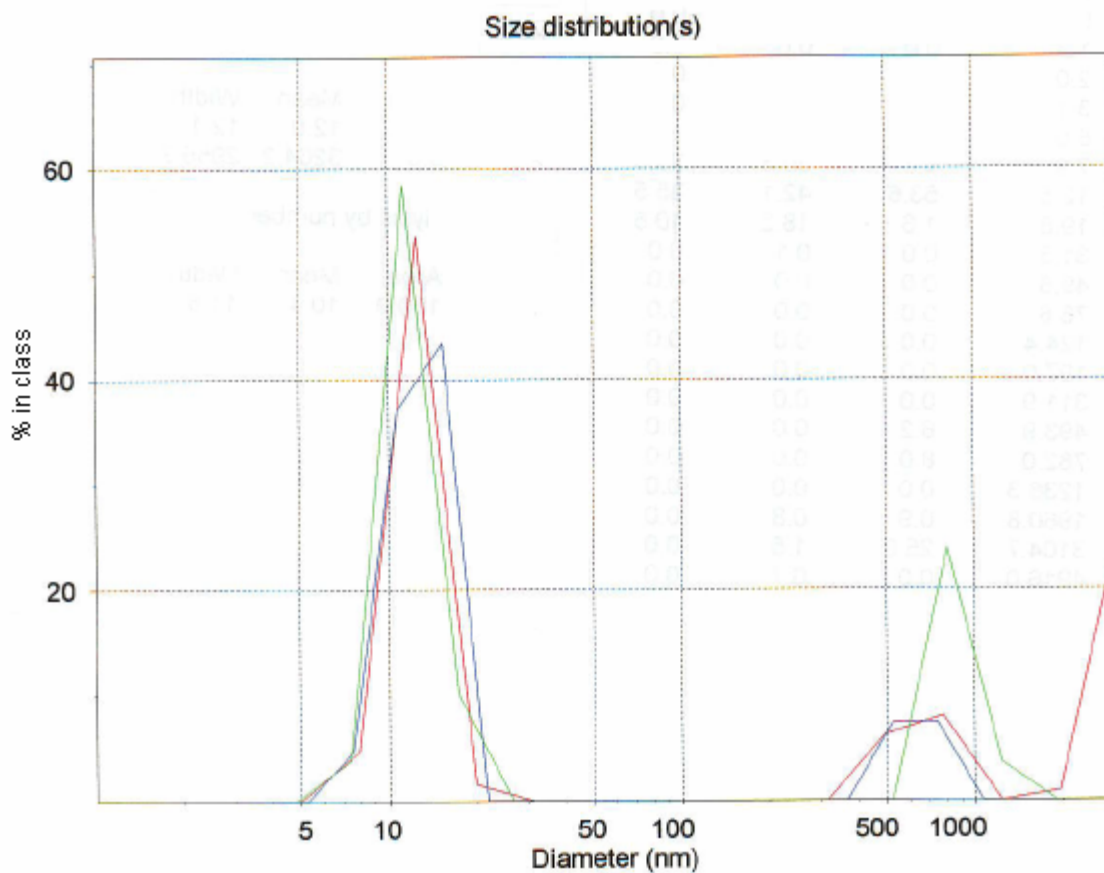
Rec	Angle	KCounts	ZAve(nm)	Poly.Index	Quality	Error	Analysis
10	90.0	208.8	24.9	0.698	Pass	3.28e-004	Contin
11	90.0	191.3	25.9	0.413	Pass	2.41e-004	Contin
12	90.0	188.8	21.4	0.602	Pass	5.35e-004	Contin

Figure G.3.4: Size distribution plot after 6 cycles with RPP1, DV 180, speed 9.25 (P3)
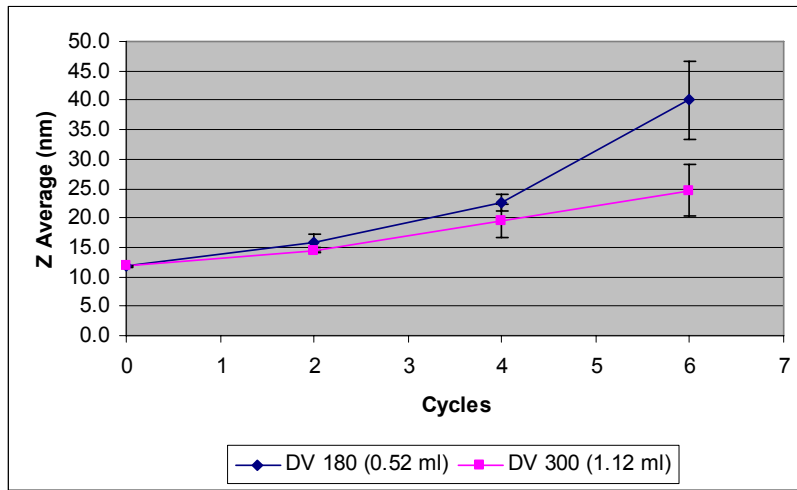
G.4 Influence of filling volume

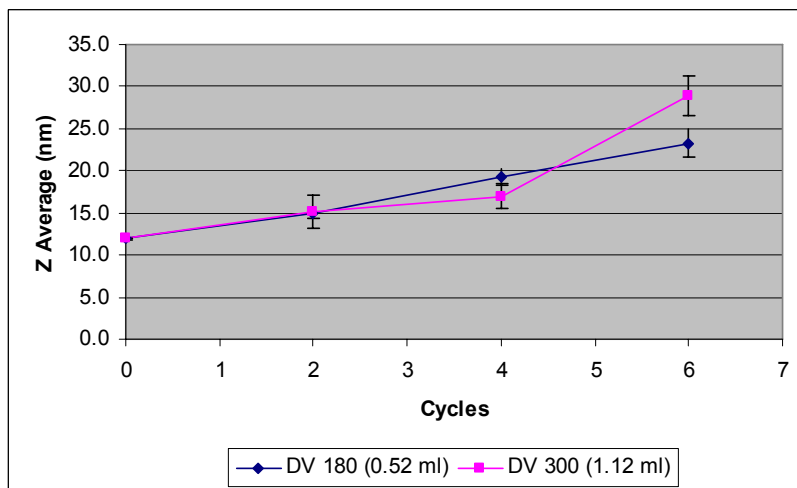**Figure G.4.1: RPP 1, dosing speed of 10s / stroke**

Figure G.4.2: RPP 1, dosing speed of 1.8s / stroke

G.5 Filling precision

Table G.5.1: Comparison of filling precision of WMP and RPPs

	WMP Dosing	WMP Dosing	RPP 2 Dosing	RPP 2 Dosing	RPP 3 Dosing
Dosing 1	4.3318 g	11.1204 g	5.2227 g	2.3467 g	5.5554 g
Dosing 2	4.3228 g	11.1387 g	5.2188 g	2.3567 g	5.5545 g
Dosing 3	4.4110 g	11.1442 g	5.2156 g	2.3432 g	5.5859 g
Dosing 4	4.3223 g	11.1835 g	5.2212 g	2.3443 g	5.5260 g
Dosing 5	4.3916 g	11.1815 g	5.2162 g	2.3467 g	5.5191 g
Mean	4.3559 g	11.1537 g	5.2189 g	2.3475 g	5.5482 g
SD	0.0422	0.0278	0.0031	0.0054	0.0267
SD_{rel}	**0.97 %**	**0.25 %**	**0.06 %**	**0.23 %**	**0.48 %**

G.6 Linearity of SEC-HPLC method

The original rituximab solution at 10 mg/ml was for the purpose of a dilution series diluted with mobile phase to obtain standard solutions in the range from 0.3125 mg/ml – 10 mg/ml. The concentration was correlated with the rituximab peak area by using linear regression. The linear regression function and the determination coefficient are shown in Figure G.6.1.
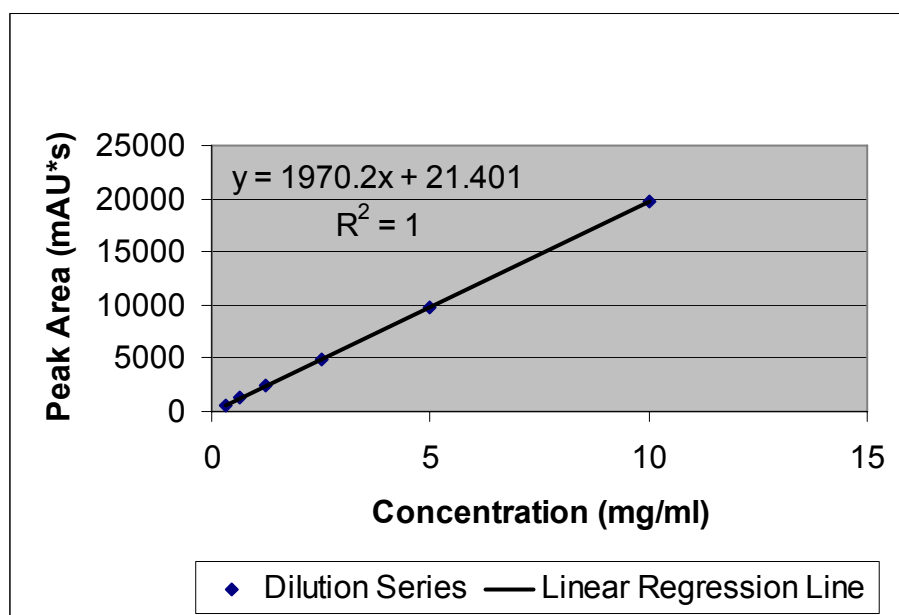

Figure G.6.1: Correlation of rituximab concentration with peak area

G.7 Calculation of LOD and LOQ

Calculation used to determine Limits of detection (LOD) and quantification (LOQ) using linear regression analysis:

Having generated appropriate data, a graph of response (y-axis) against concentration (x axis) is plotted and linear regression, using least squares fit, is performed.

This yields a line of best fit with an equation of

$$y = a + b \cdot x \qquad\qquad (1)$$

where y is response, x is the concentration, b the slope of the line of regression and a is the intercept on y axis at x = 0.

Let y'= response at the limit of detection (or quantification)

then x'= corresponding concentration at the limit of detection (or quantification)

Hence $y' = a + b \cdot x'$ (2)

Accepting the IUPAC convention of estimating LOD/LOQ as

$$\text{LOD or LOQ} = y_b + K \cdot S_b \qquad (3)$$

where y_b= blank signal, S_b= standard deviation of the blank signal and K= 3 for LOD, 10 for LOQ

then $y' = y_b + K \cdot S_b$ (4)

Assuming that the intercept, a, may be used as an estimate of y_b and the statistic $S_{y/x}$ may be used as an estimate of S_b

Then equation (4) transposes to

$$y' = a + K \cdot S_{y/x} \qquad (5)$$

where
$$S_{y/x} = \left[\frac{\sum_i (y_i - \hat{y}_i)^2}{(n-2)} \right]^{\frac{1}{2}} \qquad (6)$$

y_i= response at concentration x_i

$\hat{y}_i$= the fitted response at concentration x_i

n= the number of data points used

and $y_i - \hat{y}_i$= y residual at concentration x_i

Hence substituting and transposing (2) and (5)

$$b \cdot x' = K \cdot S_{y/x} \quad\quad\quad (7)$$

$$x' = \frac{K \cdot S_{y/x}}{b} \quad\quad\quad (8)$$

Where x' is LOD for K=3, or LOQ for K=10, calculated using the slope of the linear regression analysis.

Now, as a worst case estimate for LOD or LOQ, the lower 95% confidence value for the slope (b'') may be used instead of the slope of the linear regression line in equation (8).

The lower 95% confidence limit for the slope may be calculated as follows:

Using $S_{y/x}$ as in equation (6), the standard deviation of the slope SD_b may be calculated as

$$SD_b = \frac{S_{y/x}}{\left[\sum_i (xi - \overline{x})^2\right]^{\frac{1}{2}}} \qu\quad\quad (9)$$

where $\overline{x} = x$ coordinate of the centroid of the points.

Therefore the lower of 95% confidence value for the slope (b'') is given by

$$b'' = b - t \cdot SD_b \quad\quad\quad (10)$$

where t is the t-statistic for (n-2) degrees of freedom at the 95% confidence level.

Hence $\quad\quad$ $\mathrm{LOD\ or\ LOQ} = \frac{K \cdot S_{y/x}}{b''} \quad\quad\quad (11)$

where K=3 for LOD and K=10 for LOQ.

(Miller and Miller, 1988)
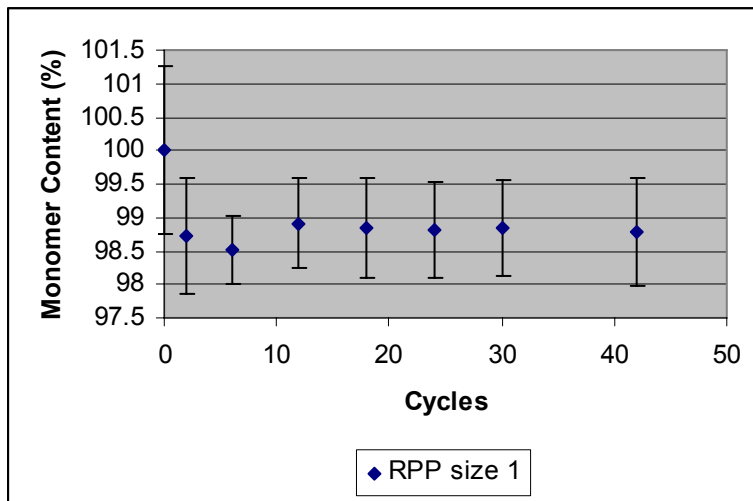
G.8 Monomer content analysed by SEC-HPLC

Figure G.8.1: Monomer content in the sheared rituximab solution after 2, 6, 12, 18, 24, 30 and 42 cycles with RPP1, DV 300, speed 9.25

G.9 Calculation of the average shear rate <γ>

The average shear rate in a concentric cylinder shear device, where the solution is introduced into the gap between two cylinders with the inner cylinder rotating, can be calculated according to Maa et al (1996) with equation (1)

$$\langle \gamma \rangle = \frac{4 \cdot \kappa^2 \cdot \omega \cdot \ln\left(\frac{1}{\kappa}\right)}{\left(1 - \kappa^2\right)^2} \qquad \text{equation (1)}$$

where ω is the angular velocity of the rotating piston calculated as in equation (3);

$$\omega = \frac{\varphi}{t} \qquad \text{equation (3)}$$

where φ is the angle in radian measure, which is rotated in the time t; φ is calculated according to equation (4);

$$\varphi = \frac{s}{r} = \frac{d \cdot \pi}{r} \qquad \text{equation (4)}$$

where s is the length of the arc of the circle and r is the radius; d is the diameter of the piston;

and κ in equation (1) is the ratio between the radii of the inner (ri) and outer (ro) cylinder, calculated according to equation (5)

$$\kappa = \frac{r_i}{r_o} = \frac{r_o - c}{r_o}$$ equation (5)

where c is the clearance between the inner (piston) and outer cylinder.

H REFERENCES

Akasaki, M., Suzuki, M., Funakoshi, I., Yamashina, I., 1976. Characterization of β-galactosidase from a special strain of *Aspergillus oryzae.* J. Biochem. 80, 1195-1200.

Arakawa, T., Timasheff, S. N., 1982. Stabilization of protein structure by sugars. Biochem. 21, 6536-6544.

Arakawa, T., Timasheff, S. N., 1983. Preferential interaction of proteins with solvent components in aqueous amino acid solutions. Arch. Biochem. Biophys. 224, 169-177.

Arakawa, T., Timasheff, S. N., 1984a. Mechanism of protein salting in and salting out by divalent cation salts: balance between hydration and salt binding. Biochem. 23, 5912-5923.

Arakawa, T., Timasheff, S. N., 1984b. Protein stabilization and destabilization by guanidinium salts. Biochem. 23, 5924-5929.

Arakawa, T., Timasheff, S. N., 1985. The stabilization of proteins by osmolytes. Biophys. J. 47, 411-414.

Arakawa, T., Bhat, R., Timasheff, S. N., 1990. Why preferential hydration does not always stabilize the native structure of globular proteins. Biochem. 29, 1924-1931.

Arakawa, T., Prestrelski, S. J., Kenney, W. C., Carpenter, J. F., 2001. Factors affecting short-term and long-term stabilities of proteins. Adv. Drug Deliv. Rev. 46, 307-326.

Arakawa, T., Li, T., Narhi, L.O., 2002. Surfactant-Protein Interactions. In: Carpenter, J. F., Manning, M. C., editors. Rational design of stable protein formulations. Theory and practice. Pharmaceutical Biotechnology Vol. 13. New York: Kluwer Academic / Plenum Publishers. pp 27-60.

Arakawa, T., Dix, D. B., Chang, B. S., 2003. The effect of protein stabilizers on aggregation induced by multiple-stresses. Yakugaku Zasshi 123, 957-961.

Arakawa, T., Philo, J. S., Ejima, D., Tsumoto, K., Arisaka, F., 2006a. Aggregation analysis of therapeutic proteins, part 1. General aspects and techniques for assessment. BioProcess International,Vol. 4, No. 10, 32-42.

Arakawa, T., Ejima, D., Tsumoto, K., Ishibashi, M., Tokunaga, M., 2006b. Improved performance of column chromatography by arginine: dye-affinity chromatography. Protein Expr. Purif. In Press.

Arakawa, T., Ejima, D., Tsumoto, K., Obeyama, N., Tanaka, Y., Kita, Y., Timasheff, S. N., 2007. Suppression of protein interactions by arginine: A proposed mechanism of the arginine effects. Biophys. Chemist. 127, 1-8.

Arzneimittelkompendium der Schweiz, 2001. Deutsche Ausgabe, 22. Auflage. Morant, J., editor. Documed AG, Basel, Switzerland.

Bam, N. B., Cleland, J. L., Yang, J., Manning, M. C., Carpenter, J. F., Kelley, R. F., Randolph, T. W., 1998. Tween protects recombinant human growth hormone against agitation-induced damage via hydrophobic interactions. J. Pharm. Sci. 87, 1554-1559.

Bausch Advanced Technology Group, 2007. Presentation on Dosing Systems. Editor: Base Europe GmbH, D-07607 Hainspitz, Germany.

Bhat, R., Timasheff S. N., 1992. Steric exclusion is the principal source of the preferential hydration of proteins in the presence of polyethylene glycols. Protein Sci. 1, 1133-1143.

Brüggemeier, M., 2005. Biotechnologie – neue Wege in der Medizin. Editor: F. Hoffmann – La Roche AG, Corporate Communications, CH 4070 Basel, Switzerland.

Capelle, M. A. H., Gurny, R., Arvinte, T., 2007. High throughput screening of protein formulation stability: Practical considerations. Eur. J. Pharm. Biopharm. 65, 131-148.

Charm, S. E., Wong, B. L., 1970. Enzyme inactivation with shearing. Biotechnol. Bioeng. XII, 1103-1109.

Chi, E. Y., Krishnan, S., Kendrick, B. S., Chang, B. S., Carpenter, J. F., Randolph, T. W., 2003a. Roles of conformational stability and colloidal stability in the aggregation of recombinant human granulocyte colony-stimulating factor. Protein Sci. 12, 903-913.

Chi, E. Y., Krishnan, S., Randolph, T. W., Carpenter, J. F., 2003b. Physical stability of proteins in aqueous solution: mechanism and driving forces in nonnative protein aggregation. Pharm. Res. 20, 1325-1336.

Chi, E. Y., Weickmann, J., Carpenter, J. F., Manning, M. C., Randolph, T. W., 2005. Heterogeneous nucleation-controlled particulate formation of recombinant human platelet-activating factor acetylhydrolase in pharmaceutical formulation. J. Pharm. Sci. 94, 256-274.

Cleland, J. L., Powell, M. F., Shire, S. J., 1993. The development of stable protein formulations: a close look at protein aggregation, deamidation, and oxidation. [published erratum in Crit Rev Ther Drug Carrier Syst 1994; 11(1):60]. Crit. Rev. Ther. Drug. Carrier Syst. 10, 307-377.

Cross, R. T., Schirch, V., 1991. Effect of amino acid sequence, buffers, and ionic strength on the rate and mechanism of deamidation of asparagine residues in small peptides. J. Biol. Chem. 266, 22549-22556.

Daniel, R. M., Dines, M., Petach, H. H., 1996. The denaturation and degradation of stable enzymes at high temperature. Biochem. J. 317, 1-11.

Demeule, B., Gurny, R., Arvinte, T., 2006. Where disease pathogenesis meets protein formulation: Renal deposition of immunoglobulin aggregates. Eur. J. Pharm. Biopharm. 62, 121-130.

Demeule, B., Lawrence, M. J., Drake, A. F., Gurny, R., Arvinte, T., 2007. Characterization of protein aggregation: The case of a therapeutic immunoglobulin. Biochim. Biophys. Acta Protein Struct. Molec. Enzym 1774, 146-153.

Dill, K. A., 1990. Dominant forces in protein folding. Biochemistry 29, 7133-7155.

Doonan S., 2002. Peptides and Proteins. Tutorial chemistry texts Vol. 15. Cambridge: The Royal Society of Chemistry. pp

Eisenring, R., Perschke, N., Amado, R., Pfenniger, H., 1994. Messung der Partikel- bzw. Kolloidgrössenverteilung in Bier mittels Photonenkorrelationsspektroskopie. Brauerei- und Getränke-Rundschau 6, 101-108.

Ejima, D., Yumioka, R., Arakawa, T., Tsumoto, K., 2005. Arginine as an effective additive in gel permeation chromatography. J. Chromatogr. A 1094, 49-55.

Ejima, D., Tsumoto, K., Fukada, H., Yumioka, R., Nagase, K., Arakawa, T., Philo, J. S., 2006. Effects of acid exposure on the conformation, stability, and aggregation of monoclonal antibodies. Proteins: Structure, Function and Bioinformatics. In press.

Elias, C. B., Joshi, J. B., 1998. Role of hydrodynamic shear on activity and structure of proteins. Adv. Biochem. Eng. 59, 47-71.

European Pharmacopoeia, 2006a. 5. Edition 5.05. Parenteral Preparations. EDQM Council of Europe, Strasbourg (France).

European Pharmacopoeia, 2006b. 5. Edition 5.05. 2.9.20. Particulate contamination: Visible particles. EDQM Council of Europe, Strasbourg (France).

European Pharmacopoeia, 2006c. 5. Edition 5.05. 2.9.19. Particulate contamination: sub-visible particles. EDQM Council of Europe, Strasbourg (France).

Gabrielson, J. P., Brader M. L., Pekar, A. H., Mathis, K. B., Winter, G., Carpenter, J. F., Randolph, T. W., 2007. Quantification of aggregate levels in a recombinant humanized monoclonal antibody formulation by size-exclusion chromatography, asymmetrical flow field flow fractionation, and sedimentation velocity. J. Pharm. Sci. 96, 268-279.

Gekko, K., Timasheff, S. N., 1981a. Mechnism of protein stabilization by glycerol: Preferential hydration in glycerol-water mixtures. Biochemistry 20, 4667-4676.

Gekko, K., Timasheff, S. N., 1981b. Thermodynamic and kinetic examination of protein stabilization by glycerol. Biochemistry 20, 4677-4686.

Gupta, S., Kaisheva, E., 2003. Development of a multidose formulation for a humanized monoclonal antibody using experimental design techniques. AAPS Pharm. Sci. 5 (2), Article 8, pp 1-9.

Halbeisen, Susanne, 1993. Untersuchungen zur Stabilisierung des Pharmaproteins Superoxid-Dismutase in flüssigen Formulierungen. Inauguraldisseratation, Basel.

Harn, N., Allan, C., Oliver, C., Middaugh, C. R., 2007. Highly concentrated monoclonal antibody solutions: Direct analysis of physical structure and thermal stability. J. Pharm. Sci. 96, 532-546.

Harris, R. J., Shire, S. J., Winter, C., 2004. Commercial manufacturing scale formulation and analytical characterization of therapeutic recombinant antibodies. Drug Dev. Res. 61, 137-154.

Harrison, J. S., Gill, M., Hoare, M., 1998. Stability of a single-chain Fv Antibody Fragment when exposed to a high shear environment combined with air-liquid interfaces. Biotechnol. Bioeng. 59, 517-519.

Idusogie, E. E., Presta, L. G., Gazzano-Santoro, H., Totpal, K., Wong, P. Y., Ultsch, M., Meng, Y. G., Mulkerrin, M. G., 2000. Mapping of the C1q binding site on rituxan, a chimeric antibody with a human IgG1 Fc. J. Immunol. 164, 4178-4184.

ISB, 2004. InfoService Biotechnology Dechema dated 11. August 2004 on http://www.i-s-b.org/business/rec_drugs.htm.

Janmey, P. A., 1993. Applications of dynamic light scattering to biological systems. In: Brown, W., editor. Dynamic light scattering: the method and some applications. Oxford: Clarendon Press. pp 611-621.

Juers, D. H., Jacobson, R. H., Wigley, D., Zhang, X., Huber, R. E., Tronrud, D. E., Matthews, B. W., 2000. High resolution refinement of β-galactosidase in a new crystal form reveals multiple metal-binding sites and provides a structural basis for α-complementation. Protein Science 9, 1685-1699.

Kendrick, B. S., Chang, B. S., Arakawa, T., Peterson, B., Randolph, T. W., Manning, M. C., Carpenter, J. F., 1997. Preferential exclusion of sucrose from recombinant interleukin-1 receptor antagonist: Role in restricted conformational mobility and compaction of native state. Proc. Natl. Acad. Sci. USA 94, 11917-11922.

Kendrick, B. S., Cleland, J. L., Lam, X., Nguyen, T., Randolph, T. W., Manning, M. C., Carpenter, J. F., 1998a. Aggregation of recombinant human interferon gamma: Kinetics and structural transitions. J. Pharm. Sci. 87, 1069-1076.

Kendrick, B. S., Carpenter, J. F., Cleland, J. L., Randolph, T. W., 1998b. A transient expansion of the native state precedes aggregation of recombinant human interferon-γ. Proc. Natl. Acad. Sci. USA 95, 14142-14146.

Kendrick, B. S., Li, T., Chang, B. S., 2002. Physical stabilization of proteins in aqueous solution. In: Carpenter, J. F., Manning, M. C., editors. Rational design of stable protein formulations. Theory and practice. Pharmaceutical Biotechnology Vol. 13. New York: Kluwer Academic / Plenum Publishers. pp 61-84.

Kim, Y.-S., Jones, L. S., Dong, A., Kendrick, B. S., Chang, B. S., Manning, M. C., Randolph, T. W., Carpenter, J. F., 2003. Effects of sucrose on the conformational

equilibria and fluctuations within the native-state ensemble of proteins. Protein Sci. 12, 1252-1261.

Kita, Y., Arakawa, T., Lin T. Y., Timasheff, S. N., 1994. Contribution of the surface free energy perturbation to protein-solvent interactions. Biochem. 33, 15178-15189.

Lee, J. C., Timasheff, S. N., 1974. Partial specific volumes and interactions with solvent components of proteins in guanidine hydrochloride. Biochem. 13, 257-265.

Lee, J. C., Timasheff, S. N., 1981. The Stabilization of Proteins by Sucrose. J. Biol. Chem. 256, 7193-7201.

Lumry, R., Eyring , H., 1954. Conformation changes of proteins. J. Phys. Chem. 58, 110-120.

Maa, Y.-F., Hsu, C. C., 1996. Effect of high shear on proteins. Biotechnol. Bioeng. 51, 458-465.

Maa, Y.-F., Hsu, C. C., 1997. Protein denaturation by combined effect of shear and air-liquid interface. Biotechnol. Bioeng. 54, 503-512.

Manning M. C., Patel K., Borchardt R. T., 1989. Stability of protein pharmaceuticals. Pharm. Res. 6, 903-918.

Meyer, J. D., Ho, B., Manning, M. C., 2002. Effects of conformation on the chemical stability of pharmaceutical relevant polypeptides. In: Carpenter, J. F., Manning, M. C., editors. Rational design of stable protein formulations. Theory and practice. Pharmaceutical Biotechnology Vol. 13. New York: Kluwer Academic / Plenum Publishers. pp 85-107.

Miller, J. C., Miller, J. N., 1988. Statistics for analytical chemistry. 2nd edition. Chichester: Ellis Horwood. p109ff.

Müller, R. H., Schuhmann, R., 1997. Teilchengrössenmessung in der Laborpraxis. Photonenkorrelationsspektroskopie. Wissenschaftliche Verlagsgesellschaft mbH Stuttgart, APV paperback 38, pp 23-53.

Nayar, R., Manning, M. C., 2002. High throughput formulation: strategies for rapid development of stable protein products. In: Carpenter, J. F., Manning, M. C., editors. Rational design of stable protein formulations. Theory and practice. Pharmaceutical Biotechnology Vol. 13. New York: Kluwer Academic / Plenum Publishers. pp 177-198.

Otto, M., 2000. Analytische Chemie. Zweite, vollständig überarbeitete Auflage. Choromatographie. Wiley-VCH Verlag GmbH, Weinheim (Federal Republic of Germany), pp 413-514.

Parkins, D. A., Lashmar, U. T., 2000. The formulation of biopharmaceutical products. Pharm. Sci. Technol. Today 3, 129-137.

PIC-Leitfaden einer Guten Herstellungspraxis für pharmazeutische Produkte mit ergänzender Leitlinie und Empfehlungen zu Validierung sowie zur Validierung aseptischer Prozesse, 2004 a. 3. Auflage. A1 Herstellung steriler pharmazeutischer Produkte. Kantonale Heilmittelkontrolle Zürich, Regionale Fachstelle der Ost- und Zentralschweiz, Zürich, pp 62-75.

PIC-Leitfaden einer Guten Herstellungspraxis für pharmazeutische Produkte mit ergänzender Leitlinie und Empfehlungen zu Validierung sowie zur Validierung aseptischer Prozesse, 2004 b. 3. Auflage. E2 Validierung aseptischer Prozesse. Kantonale Heilmittelkontrolle Zürich, Regionale Fachstelle der Ost- und Zentralschweiz, Zürich, pp 217-231.

Powell, M. F., Nguyen, T., Baloian, L., 1998. Compendium of excipients for parenteral formulations. PDA J. Pharm. Sci. Technol. 52, 238-311.

Randolph, T. W., Jones, L. S., 2002. Surfactant-Protein Interactions. In: Carpenter, J. F., Manning, M. C., editors. Rational design of stable protein formulations. Theory and practice. Pharmaceutical Biotechnology Vol. 13. New York: Kluwer Academic / Plenum Publishers. pp 159-175.

Römpp-Lexikon Biotechnologie und Gentechnik, 1999. 2. Edition. Deckwer, W-D., Pühler, A., Schmid, R. D., editors. Georg Thieme Verlag, Stuttgart.

Schmid, R. D., 2002. Taschenatlas der Biotechnologie und Gentechnik. Medizinische Biotechnologie. Wiley-VCH Verlag GmbH, Weinheim (Federal Republic of Germany), pp 114-151.

Stellmach, B., 1988. Bestimmungsmethoden Enzyme für Pharmazie, Lebensmittel-chemie, Technik, Biochemie, Biologie, Medizin. Darmstadt: Steinkopff Verlag, pp. 155-161.

Štulík, K., Pacáková, V., Tichá, M., 2003. Some potentialities and drawbacks of contemporary size-exclusion chromatography. J. Biochem. Biophys. Methods 56, 1-13.

Tanaka, Y., Kagamiishi, A., Kiuchi, A., Horiuchi, T., 1975. Purification and properties of beta-galactosidase from *Aspergillus oryzae*. J. Biochem. 77, 241-247.

Tavornvipas, S., Tajiri, S., Hirayama, F., Arima, H., Uekama, K., 2004. Effects of hydrophilic cyclodextrins on aggregation of human growth hormone. Pharm. Res. 21, 2369-2376.

Tavornvipas, S., Hirayama, F., Takeda, S., Arima, H., Uekama, K., 2006. Effect on chemically and thermally induced unfolding and aggregation of lysozyme and basic fibroblast growth factor. J. Pharm. Sci. 95, 2722-2729.

Timansheff, S. N., 1998. Control of protein stability and reactions by weakly interacting cosolvents: The simplicity of the complicated. Adv. Protein Chem. 51, 355-432.

Tirrell, M., Middleman, S., 1975. Shear modification of enzyme kinetics. Biotechnol. Bioeng. XVII, 299-303.

Tsumoto, K., Ejima, D., Senczuk, A. M., Kita, Y., Arakawa, T., 2007. Effects of salts on protein-surface interactions: applications for column chromatography. J. Pharm. Sci. published online ahead of print in January.

Tzannis, S. T., Hrushesky, W. J. M., Wood, P. A., Przybycien, T. M., 1996. Irreversible inactivation of interleukin 2 in a pump-based delivery environment. Proc. Natl. Acad. Sci. USA 93, 5460-5465.

Vidanovic, D., Askrabic, J. M., Stankovic, M., Poprzen, V., 2003. Effects of nonionic surfactants on the physical stability of immunoglobulin G in aqueous solution during mechanical agitation. Pharmazie 58, 399-404.

Wallenfels, K., Weil, R., 1972. β-Galactosidase. In: Boyer, P. D., editor. The enzymes. Third edition. New York and London: Academic Press Inc. 7 (20), pp 618-663.

Wang, W., 1999. Instability, stabilization and formulation of liquid protein pharmaceuticals. Int. J. Pharm. 185, 129-188.

Wang, W., Singh, S., Zeng, D. L., King, K., Nema, S., 2007. Antibody structure, instability, and formulation. J. Pharm. Sci. 96, 1-26.

Weiner, B. B., 1984. Particle sizing using photon correlation spectroscopy. In: Barth, H. G., editor. Modern methods of particle size analysis. New York: John Wiley & Sons. pp 93-116.

Xie, Guiju, Timasheff S. N., 1997. The thermodynamic mechanism of protein stabilization by trehalose. Biophys. Chem. 64, 25-43.

Zetasizer 1000 / 2000 / 3000, 1996. Principles of operation, Manual Number MAN 0152, Issue 1.1, Malvern Instruments Ltd., Spring Lane South, Malvern, Worcs.WR14 1XZ, UK.

Zetasizer 1000 HS / 3000 HS, 2000. Making Size measurements, Manual Number MAN 0149, Issue 2.0, Malvern Instruments Ltd., Spring Lane South, Malvern, Worcs.WR14 1XZ, UK.